UNIVERSITÀ DI PARMA

DOTTORATO DI RICERCA IN
MEDICINA MOLECOLARE

CICLO XXXII

Synthesis and biological testing of nanowires for tissue regeneration

Coordinatore:
Chiar.ma Prof.ssa Stefania Conti

Tutore:
Chiar.mo Prof. Guido M. Macaluso

Dottoranda: Benedetta Ghezzi

A.A. 2016/2017 – 2018/2019

Ai miei nonni, con tutto il mio amore.

Index

Preface

Nowadays, tissue engineering has been focusing on the development of promising strategies for bone regeneration, which is the fundamental process to consider in order to improve the success of complex clinical cases in the field of oral and maxillo-facial surgery. One of the most common approaches has been the development of micro- and nanotopographies leading to an increase of osteoconductive properties of biomaterials and, in particular, of implantable materials.

It is well known that the importance of biomaterials surfaces micro- and nanotopography has been increased in the last decades. Indeed, nanotopographic disposition of extracellular signals has revealed to be central in the control of cellular adhesion, proliferation and differentiation, all events having a positive impact on tissue regeneration. Although the lack of information about the ideal spatial distribution promoting cellular response, it has been demonstrated that this disposition should be in the dimensional range of its components. Furthermore, it has been underlined the cellular ability to specifically respond to different nanopatterns in order to activate particular topography-dependent signal transduction pathways (for instance conformational changes of the cytoskeleton, cellular motility).

The aim of this project was to improve dental implants osteointegration with the use of nanostructures created *ad hoc* to optimize bone cells adhesion, proliferation and differentiation. Particularly, different categories of nanowires have been developed and characterized on the basis of their physico-chemical and biological properties in presence and in absence of functionalization with 3-mercaptopropyltrimethoxysilane. This kind of functional group has been chosen as the molecule can advance osteoblastic differentiation.

Results of cytocompatibility studies performed on silicon oxycarbide nanowires demonstrated no toxic effects for control nanowires as well as functionalized. It has been shown an increase of cells proliferation after functionalization, probably due to factors as different protein absorption pattern, improved adhesion and expression of genes having a fundamental role in the early stages of osteoblastic differentiation. In addition, titanium dioxide nanowires revealed to have great potential both for osteoblastic differentiation and focal adhesion formation, confirming the idea that nanostructured surfaces can promote cellular response supporting bone regeneration.

In conclusion, silicon oxycarbide nanowires and titanium dioxide nanowires have been confirmed to be promising substrates to improve dental implants osteointegration.

Chapter 1 – Regenerative medicine

During the last century, we have witnessed a radical change of disease spectrum, moving from acute and infective to chronic and degenerative illness. It reflected in the expectation to change the therapeutic approach from rescuing to supporting patients in the long-term. This allowed the advent of regenerative medicine (RM), a multidisciplinary field of health sciences that aims at repairing, regenerating, or replacing disfunctioning cells, tissues or organs using allogenic or autologous cells, supporting scaffolding biomaterials, gene modifications, and molecular cues, alone or in combination. In this arena, RM represents the forefront of health sciences and holds promises for the treatment and, possibly, the cure of a number of challenging conditions[1]. The field of RM has significantly increased in the past decades, and in its advances have involved a multitude of researches, including biomaterials design and processing, surface characterization, and functionalization for improved cell-material interactions[1].

One of the principal technologies characterizing RM is the tissue engineering (TE). TE is basically the modern approach to RM; a first definition of TE was given at the *1st TE symposium*, held in 1988 in California. TE is considered as *"an interdisciplinary field of research that applies the principles of engineering and the life sciences towards the development of biological substitutes that restore, maintain or improve tissue function"*, but the term "tissue engineering" was coined in 1993 by Langer and Vacanti and was conceived to address the most urgent need, at that time, of transplant medicine, the lack of transplantable organs. In a more applicative interpretation, tissue engineering is defined as "a process that affects the structure and architecture of any viable and non-viable tissue with the aim to increase the effectiveness of the construct in biologic environments".

The idea of artificially generate a tissue, an organ or even more complex living systems was throughout the history of mankind a matter of myths and dreams, but during the last decade this vision became feasible and has been recently introduced in clinical medicine and holds the promise of custom-made medical solutions for injured or diseased patients. The first approach to tissue engineering is not new, but there are proofs that during Inca's dominations were developed gold and silver prothesis for cranioplasty and dental implants[2].

TE refers to the field of health sciences that aims at restoring the function of injured tissues using a combination of cells, supporting scaffolding materials, molecular and physical cues that, harnessed together, will eventually recreate the damaged and functionally impaired tissues. It is fundamentally based on the use of a structure, called scaffold, projected to be the biological substitute of the lost tissue that aims to act as a support surface thus

creating a favourable environment that can restore the physiological and histological characteristics of the injured tissue[3]. In particular, the extracellular matrix (ECM) must be resembled as better as possible to replace the damaged tissue or enable tissue regeneration by providing ideal conditions to direct cell behaviour as close as possible to natural tissue before injury. The main achievement of the scaffold is to mimic the stromal component of an organ or a tissue, in order to allow cells to adhere, proliferate, differentiate and produce new ECM; the ECM coats the scaffold's structure and leads to the development of the new tissue, while the biomaterial is progressively resorbed. Scaffolds can be employed by TE in two different ways, which consent the distinction of TE in *in vitro* and *in vivo.* The first approach is based on the use of autologous cells seeded within specific growth factors on the scaffold lading to new tissue generation *ex vivo*; the obtained tissue will subsequently be grafted. *In vivo* TE instead, is based on the idea of creating a scaffold to be implanted directly in the anatomical site where the lesion occurred.

The goal of TE is to reach the production of a complete functional tissue where the natural occurring reparation is a scar, with consequent loss of the functionality of the tissue or organ. In this contest, it becomes clear that scaffold must have many features as shape, capacity to induce adequate cell response, control of cell differentiation and biodegradability. The ideal scaffold for TE emulates the biomechanical properties of the targeted tissue as serves as a host for either endogenous or implanted cells, by supporting cell adhesion, migration and differentiation.

1.1 Biomaterials for tissue engineering

The use of biomaterials can be synthetized as the development and use of materials to replace lost tissues and promote new tissue formation[4]. Biomaterials are currently defined as tissue scaffolds consisting predominantly of structured and modified biological materials such as collagen or decellularized bone, whereas biomimetic materials consist of synthetic polymers, metal or ceramics with surface or bulk modification able to render the material biocompatible and suitable for tissue implant or tissue engineering. Since cells in the natural tissue are surrounded by a biological matrix, called as a whole extracellular matrix (ECM), which comprehends a multitude of different insoluble proteins (e.g. collagen, elastin, etc), glycosaminoglycans, inorganic crystals, cell-signaling motifs, growth factors, it become obvious that the biomaterial has to mimic this composition to guide cellular anchorage, proliferation and differentiation. In particular, their spatial distribution and concentration plays, together with the tissue specific topography and mechanical properties, a pivotal role in providing cells with the correct molecular stimuli to allow the synthesis of ECM products. Moreover, tissue structure at ECM level is

characterized by a tissue-defined micro and nano topographical pattern, whose presence leads cells to behave in different ways.

It is obvious that the structural organization of a tissue is the key for its function, so as a first step in the development of a scaffold is necessary to identify specific cues and characteristics the biomaterial must have to resemble as better as possible the ECM. Moreover, to design the ideal scaffold, it is necessary to accurately characterize this structure in a 3D environment and to understand exactly how its microscopic structure influences important macroscopic properties. In this regard the golden scaffold has a number of requirements it should possess to be suitable for TE: biodegradability, bioactivity, mechanical properties, porosity, topography, chemistry and surface energy.

- Biodegradability

Biodegradability is one of the most desired properties for a TE scaffold, since it is not seen as a permanent implant as it occurs for example for dental implants or orthopaedic prothesis. This property consists in the ability of the material to decompose over the time as consequence of biological processes, such as enzymatic activity. A TE scaffold should be resorbed in a controlled manner during the time, in order to allow resident cells to colonize it and start to regenerate the tissue. Degradation is fundamental because if it does not occur, it can lead to undesired collateral effects due to the filling of pores and consequent lack of oxygen. Moreover, the control of degradation process is fundamental, in order to avoid the release of toxic, inflammatory, mutagens or carcinogens agents.

- Bioactivity

The concept of biocompatibility in tissue engineering is defined as “the ability to perform as a substrate that will support the appropriate cellular activity”[5]; the concept of bioactivity is the capability of the material to establish a dynamic dialogue with its biological surrounding. Seen that, a biocompatible scaffold has to possess within its structure opportune stimuli recognizable by relevant cells for scaffold colonization and thus proper regeneration[5].

The biological activity of the biomaterial may be enhanced by a scaffold enrichment with specific molecules or growth factors acting on cell adhesion, spreading, migration and differentiation. Normally, cell adhesion and spreading is better on polymeric scaffolds, because they already contain biopolymers and protein related binding sites suitable for cell adhesion; however, many efforts have been done to ameliorate protein adsorption on synthetic materials and consequently to enhance the number of present binding sites at the interface[6-8].

Moreover, the scaffold can be supplemented with a gradient of inductive molecules in order to promote cell migration and motility. For example, in bone tissue engineering, bone morphogenetic proteins (BMP-2) or calcium ions are often used to facilitate bone cells recruitment[9, 10]. Many molecules of the ECM have function of regulation for cell proliferation and differentiation and can be introduced into scaffolds to guide cell commitment and new tissue development (e.g. polyaniline and polypyrrole seem to have a fundamental role in osteogenic maturation)[11, 12]. It is obvious that in a biologic microenvironment, proteins play a pivotal role in cell response to the material, since they tend to be adsorbed on the scaffold surface, in a not specific manner, during the first moment of contact between the biological environment and the biomaterial. In accordance with this, the control of amount, composition and conformation of protein at the scaffold interface may be a viable approach to design very specific materials for TE applications, considering two main aspects: the introduction of cues to facilitate scaffold colonization and the surface enrichment with molecular signals that specifically trigger cell fate and function.

- Mechanical properties

During the choice of an effective scaffold for tissue regeneration, is of pivotal importance to analyse its mechanical properties, which should resemble as much as possible those of the native tissue. So, one of the most important characteristics of a scaffold is to be considered as mechanistically biocompatible, in order to maintain both, its integrity and the defect one, from the moment of the insertion to its complete resorption and substitution with regenerate tissue. As during this process, the material has to respond to a number of external forces, it must possess fatigue properties to avoid its breakage when exposed to cyclic loading. The parameters which should be critically studied when a scaffold has to be designed are: elastic modulus (the strain in response to a given tensile or compressive stress along the plane of the applied force), flexural modulus (relationship between a bending stress and the resulting strain after a compressive stress applied perpendicularly), tensile strength (maximum stress a material can withstand before its break) and maximum strain (ductility exhibited by the material before a fracture). In particular, the flow of biological fluids inside and outside the scaffold is very important for the functioning of cellular metabolism and it is strictly related to the scaffold elastic modulus[13].

Moreover, cells are able to sense through mechanotransduction the characteristics of the environment, feeling the stiffness of the surrounding tissues or materials. Cells mechanosensory protein complex are composed by talin, vinculin, tensin, paxillin, Src and focal adhesion kinase (FAK). The kinetics of response events in mechanically loaded cells may entail, in a very brief time after stimulation, a signal response involving many mechanically active channels as Ca^{2+}, Mg^{2+}, K^{+}, H^{+}, IP3, CAMP, PGE2 kinases, G protein, etc., which start transcription and traduction processes, ending in the cytoskeletal protein polymerization and focal adhesion arrangement[14]. According to

mechanobiology, cells can control their adhesion, migration and spreading on a substrate material due to the mechanic characteristics of the substrate and they normally prefer a substrate which presents the same stiffness of the tissue they belong to, or a similar one; in particular, in the human body cells can sense in a wide range of stiffness, from hundreds of Pa (skin/subcutaneous tissue – 57Pa[15]) to GPa (trabecular bone – 100GPa[16]). The manner in that occurs cellular adhesion is of pivotal importance to direct cell proliferation and differentiation within the scaffold, so these parameters have to be precisely analyzed during the planning of the scaffold; in fact, if the substrate does not accomplish the rigidity of the native tissue, cells can alter their migration and adhesion way, a characteristic typical of several pathologic conditions (e.g. cancer metastasis)[17].

Figure 1.1 shows how different cell phenotypes are due to the substrate stiffness.

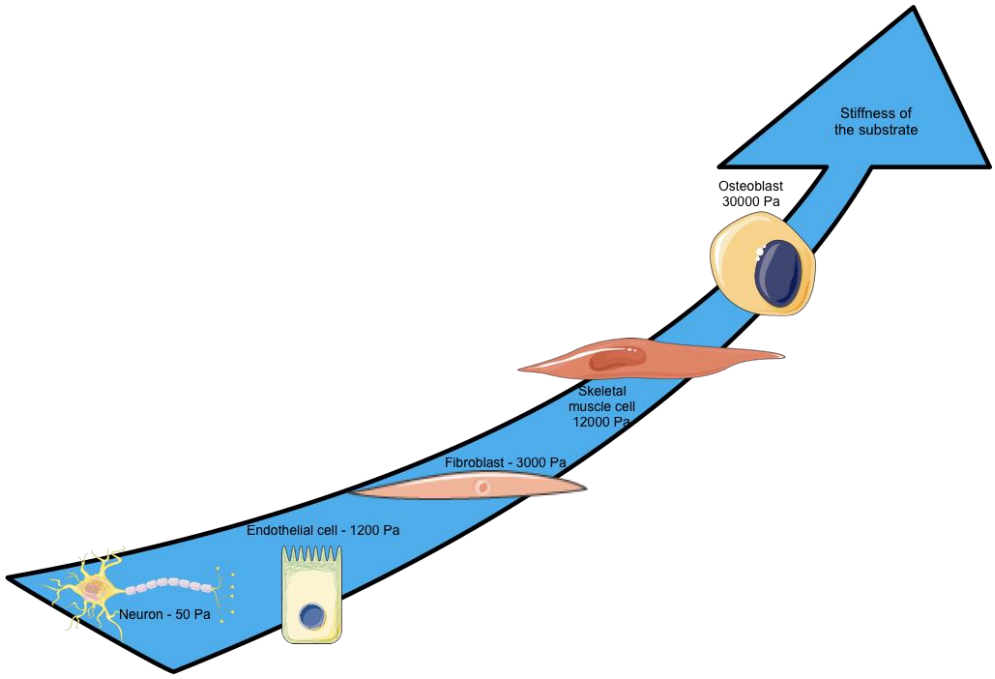

Figure 1.1: Relationship between substrate stiffness (Pa) and cell phenotype. Cell shape depends on the stiffness of the material.

In literature it has been demonstrated that the interaction between cell and material can define cellular morphology, that is a fundamental factor for the start of cell commitment; for example, mesenchymal stem cells tend to undertake to myogenic or adipogenic commitment if the substrate stiffness is soft (around 10kPa), while they commit into osteoblastic lineage if the environment presents a higher rigidity (30-35kPa)[18, 19].

Thus, it becomes obvious that different biomaterials would be employed for different applications (e.g. polysaccharides will be used for soft tissue regeneration, while fibrous proteins will be considered for hard tissue regeneration). Moreover, it has to be underlined that the final mechanical properties of the scaffold are depending

on the manufacturing process and the same material can be molded into different kind of scaffolds with specific characteristics.

- Porosity

For an optimal scaffold construction, porosity is fundamental. In fact, TE scaffold requires a specific and controlled porosity which allows the necessary connectivity for nutrient flow, cellular growth and transport of gasses and waste products. Scaffold porosity, pore size, geometry, distribution and interconnectivity, which affect the mechanical properties, may be controlled by fabrication techniques; a porous network has to be induced during the manufacturing process, in order to strictly resemble the *in vivo* mass transport of nutrients, oxygen, molecules, signals and waste products to and from cells that normally occurs by permeability through blood vessels[20]. The normal scaffold porosity must consider the total porosity, the pore interconnectivity and the pore size; the size of inter-pore connection is the most important parameter for a deep colonization of the material after the implant. In fact, if the pore size is too small, cellular migration is hindered and cells cannot penetrate the material, leading to the formation of a capsule around the edge of the scaffold, which can progress with the development of a necrotic region caused by the limited reach of gasses and nutrients across cell population. On the contrary, if pore dimensions are too big, cell adhesion is insufficient due to the limited area they can feel; obviously, different cell types express preference for adhesion to different pore dimensions within the scaffold[21].

In the complex, it is possible to say that the number of struts and the density of ligand available for cell adhesion is proportional to the dimension of pores and they must be in the proper nanosize, considering the kind of material and the type of resident cells, since it is a key factor able to enhance or impair cell function. Pore size may range from few nanometers to millimeters and it has been shown how different pore sizes may influence different cell processes. Different types of cells require scaffolds with suitable pore size for cell tissue growth, for example, in bone tissue engineering, a pore diameter about 53,6±5,9 µm has been seen to facilitate the penetration of murine osteoblasts, calcium deposition and mineralization, while pore size about 100-150µm, 380-405µm or 290-310µm can support osteoblastic growth, proliferation, migration and new bone formation[22, 23]. According to the requirements, bone tissue needs a scaffold with pore diameter between 100 and 350µm to be resembled; in particular pore diameter of about 100-150µm influence initial cellular adhesion and attachment, while higher level of proliferation were demonstrated with an average pore size of 325µm, which is a dimension essential for the vascularization of the scaffold and consequently bone ingrowth[24-26].

- Topography, chemistry and surface energy

As described in literature, cells are sensitive and responsive to ECM in terms of chemistry, topography and surface energy of the material with whom they come into contact. Surface energy and chemistry may influence protein adsorption and the structural arrangement of protein on the material, because protein adsorption is very different on positively or negatively charged material[27]. Seeing that, chemistry and surface energy seem to be fundamental in the design of an effective scaffold because they alter the primary external response in biological environment; it is known that hydrophilic biomaterials promote the adsorption of proteins involved in cell-material adhesion processes[28]. Moreover, a direct relationship exists between surface energy and topography of the material; it seems that apolar components of surface energy tend to increase significantly in presence of a rough surface[29]. On the other hand, also cell adhesion is linked to the presence of a rough surface. Nowadays many methods are commonly used to mechanically create a rough surface on titanium implants, as chemical etching with acids[30], implementation with Ca^{2+} ions[31] or chemical oxidation with H_2SO_4 and H_2O_2[32], but the interesting thing is that some studied underlined how were the parameters describing the surface organization of roughness, more than the roughness itself, to be able to influence cellular adhesion on the material[33, 34]. Substrate topography is the element that physically allows the adhesion, considering that the mechanical coupling exerted by the ECM to cells, directs cell adhesion. In the last few years a change in the way of thinking the design of biomimetic materials occurred, due to the increased relevance of dimensionality in cell-ECM association and interaction. Indeed, it becomes evident the importance not only of microtopographical organization, but also the nanotopographical disposition of extracellular signals to control cell adhesion, proliferation and differentiation in tissue regeneration[35]. Although exact information about the spatial distribution of cell ligands are not available, due to the intricate architecture of the ECM, it is known that the spacing among them should be in the range of dimensions of the matrix component, otherwise in the nanoscale dimension, and numerous studies focused on this aspect of cellular response, highlighting that cells specifically respond to distinct spatial nanopatterns[36, 37]. In fact, it has been seen that at nanotopographical level, cells respond in a different manner, reacting specifically to the nanopattern and activating specific topography-dependent transduction signaling pathways (e.g. changes in cytoskeletal conformation, cell shape, motility, proliferation, etc.). Analysing better the point, some studies showed that this type of topography-related transduction of the signal is related to the nano-pattern geometry as well as the spacing of adhesive ligands[38-40]. After the comprehension of the nanoscale importance, numerous chemical and physical methods to modify biomaterials surfaces have been developed to generate geometrically defined nanoscale surface patterns suitable for biomedical use in TE.

In conclusion, cell adhesion, spreading, proliferation, cytoskeletal organization, apoptosis, etc., are all based and triggered by the presence of distinct nanopatterning (with particular regard over that spacing in the pattern and to pattern symmetry of the resulting adhesion point) of biomimetic surfaces[37, 41-44]; moreover, cell responses to the specific geometry of the pattern have been reported to be very useful for many cell types in TE[36, 37, 41, 43, 45-49].

The dominant mechanisms occurring during tissue formation are mainly related to time and length scales of biology and they comprehend in chronological order the initial macromolecule adsorption, cell adhesion, cell proliferation, ECM production and biomaterial resorption. Length and time approximations of the biological processes are resumed in Figure 1.2.

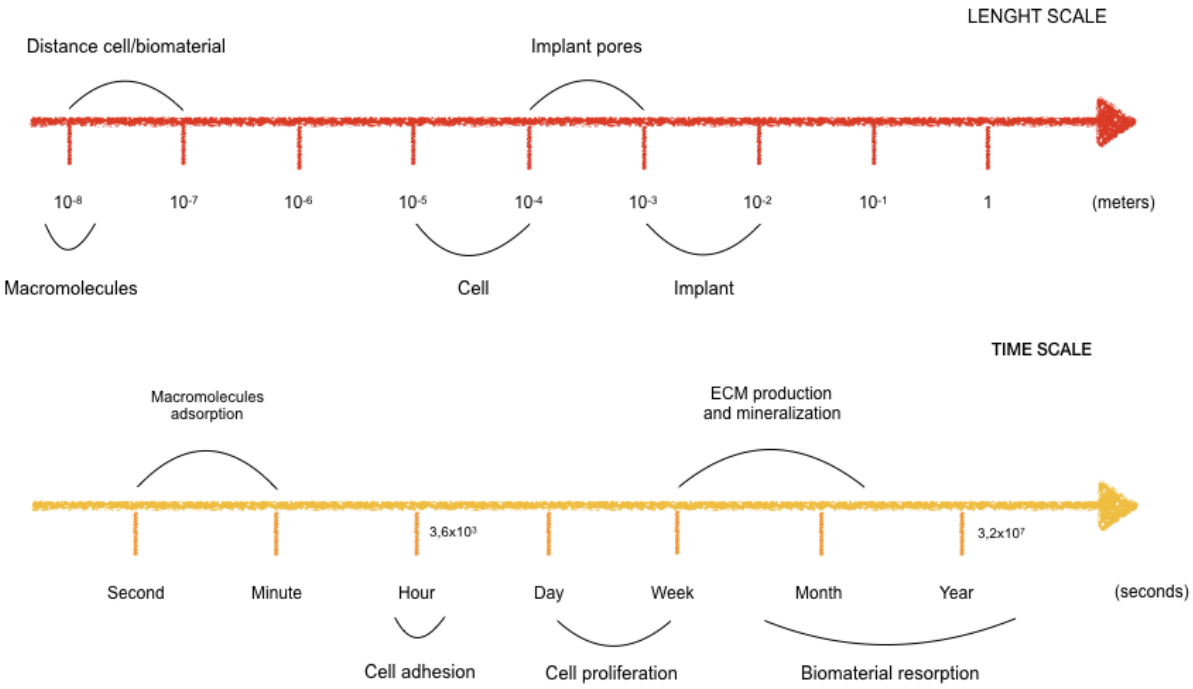

Figure 1.2: Typical length and time scales of biological processes.

1.2 Bone tissue engineering

Generally, bone is a tissue with a great capacity to regenerate itself; nevertheless, in some cases (e.g. big traumas, bone tumour resection, etc.) massive bone defects may need an intervention, and, in these eventualities, the use of bone grafts (autografts, allograft or xenografts) is considered to be the gold standard. The natural regeneration of bone can be negatively affected in case of systemic diseases, infections or insufficient blood and oxygen supply, resulting in an altered or insufficient regeneration[50]. Moreover, biophysical effects as mechanical loading and

electromagnetic signals are important regulators of bone formation, due to bone's capacity to recognize the exact functional environment necessary for the maintenance of a structurally intact tissue; finally, the presence of specific biomolecules, such as the use of osteoinductive factors, is fundamental for bone reconstruction and to promote new bone formation.

In this arena, frequent issues related to the use of auto-, allo- or xenograft (e.g. necessity of a second donor site, immune response, etc.) pushed the tissue engineering research field to develop synthetic scaffolding materials.

Nowadays, bone TE aim to fulfill the many and specific required characteristics of the bone augmentation process, leading to the obtainment of a favorable environment for osteoblastic adhesion, proliferation and differentiation; the main goal of TE is the production of an *ad hoc* scaffold material to perfectly reproduce biological microenvironments for cells and the principal factor impacting on the result is the scaffold customization with biomechanical cues and signaling factors specifically focused on the enhance of osteoinduction and osteogenesis[51]. Since biomaterials for bone TE have as main objective the properly replace of the physicochemical characteristic of the surrounding tissue, a special design must be applied to create the adequate environment. To this purpose, in addition to the characteristics exposed in the previous paragraph, there are many other requirements for the development of an ideal scaffold for bone TE, the most important are osteoinduction (capability of recruiting and stimulating osteoblasts), osteoconduction (ability to allow and support cell adhesion), osteogenesis (formation of new bone) and mechanical stability[52].

A wide range of biomaterials have been developed for bone tissue engineering. For example, ceramics (calcium phosphate and tricalcium phosphate are very useful due to their similar properties to bone tissue), bioactive glass, zirconium oxide, silicon oxide, synthetic and natural polymers represent a viable option for TE approach.

As concerns the oral bone regeneration, the situation is more complicated than that and certain challenges must be overcome, as it occurs for the presence of a biological microenvironment comprehending the exposition to the oral region which includes the presence of a large amount of pathogens. Due to this consideration, the development of a scaffold for oral bone TE must consider several issues about antimicrobial properties, release of bioactive factors and degradation ratio.

In a more clinical view, applications of biologics-based tissue regenerative therapies in the oral and maxillo-facial complex are wide ranging, spacing from the fracture repair, the dentoalveolar augmentation prior to prosthetic reconstruction, to the repair of facial bone defect secondary to trauma or tumor resection, with the ultimate prospect to succeed in regenerating entire teeth and jaws.

1.3 Osseointegration of dental implants

Normally dental implants are titanium-based tooth root substitutes which are surgically placed into alveolar bone to form a new permanent connection with the adjacent tissue, after osteoblast-induced bone ingrowth. The use of dental implants has rapidly increased in the last decades, but their very high clinical success rate is principally linked to their use in an ideal environment. In many patients the optimal placement setting is compromised by previous alveolar bone loss (both quantitatively or qualitatively), lack of mucosa tissue, impaired regenerative capacities or need for early loading protocols and it leads to the lack of osseointegration. Osseointegration has been defined by Branemark, initially as a direct bone-to-implant contact, subsequently as a direct bone-to-implant contact under load, but in its details, it has not been completely defined[53]. In fact, a failure in implant osseointegration can be conceptualized as a failure of the mineralization of the ECM directly attached to the implanted surface, since a mechanically competent implant/bone bond is dependent on an intact mineralized interface structure. Obviously, the microenvironment present at the host site and the interaction occurring with the artificial material are of pivotal importance for the definition of the surrounding tissues structural and functional properties. There is a dynamic interaction between the implant and the surrounding bone and one object affects the other; for example there are anatomical and cellular differences between cortical and spongiosa bone, which reflect in a different interaction with the implanted material, even if the cellular and acellular dynamic processes occurring at a micro- or nanoscale level are not completely understood, as also the early aspects of bone/biomaterial interaction in terms of seconds or minutes in the *in vivo* environment.

To reach the primary stability ensuring the success of a dental implant, it is necessary for the biomaterial to be positioned in an area with sufficient bone density and volume. In the case of a patient who lost a tooth, for esthetic reasons and for the proximity of the implant site with other anatomical structures, the implant tends to be placed approximately in the same position of the natural one, leading to the presence of a tissue with some degree of atrophy and not optimal viability of oral hard tissues, while soft tissues could be compromised by pathological conditions, which may compromise the survival rate of implants. In the last years many modifications have been made to influence implant-specific or bone-specific aspects, such as modifications in implant surface characteristics (material, topography, geometry, chemistry), resulting in a better osteoconduction, bone formation and bone remodeling[54-58]. However, these improvements are not still ideal.

The properties of the bone where implant is inserted are directly related to the features of the mineralized ECM around the implant in two ways:

- the macroscopic and microscopic implant geometry and the insertion approach determine the principal bone/implant relation;

- the properties of bone have a major impact on the load-related characteristics of the microenvironment adjacent to implants.

The presence of different grade of bone mineralization is also a fundamental aspect that enable the implant to remain stable after positioning; bone can be considered as a material composed by soft tissues network that is reinforced by minerals, possessing both rigid and elastic properties. In this contest, cells, matrix and minerals are interconnected in providing bone its unique biophysical and biological properties. The presence of cortical and cancellous bone leads to a different interaction of them towards implants[59]. In fact, they both are able to transfer the loads through the bone with a dynamic cellular feedback between load perception and cellular response, but the cortical layer must provide mechanic strength and protection, while cancellous bone is also involved in metabolic functions (e.g. calcium homeostasis). Both these aspects are closely related to the features of the mineralized ECM at implant/bone interface; for example cortical bone also possesses an elasticity up to 5%, so if the implant insertion does not extend the cortical bone over this threshold, a direct contact between cortical ECM and implant can be assured, but it has been observed that a high bone-to-implant contact is not always related to a higher implant stability, indicative that this parameter must be carefully analysed as a predictive factor of good osseointegration[60, 61]. Because of the complex structure of cortical bone, it becomes very difficult to overcome the technical problems related to implant positioning, as the determination of the force/tissue deformation. The extent of bone deformation under load is perhaps the most important regulating factor, dependent on the physical properties of the bone tissue, the direction and amount of the applied forces and, to a main extent, by the geometry of the used implant[62, 63].

In this arena, novel tools and techniques are being sought to improve the regeneration of bone tissue under compromising situations; some examples are relative to modifications in their surface properties in order to ameliorate the success of osseointegration, as it occurred with surface geometry modifications, addition of layers of calcium phosphate or hydroxyapatite, binding the surface with osteoinductive protein factors or biomimetic compounds, with as main challenges the problem of poor bone quality and acute inflammation at the implant site[64, 65].

Bone tissue possess a unique biology which consent to undergo regeneration to a stage of a repair ad integrum. In the case of dental implants this process occurs between the implant surface and the tissue covering implantation bed due osteoblasts and osteocytes action of recruiting cells, inducing them to proliferate and differentiate adjacent to the positioning site. So, the contribute of bone biology in dental implant osseointegration has to be considered as a highly complex cell-driven process, where biological and biophysical parameters deeply affect the success of remodelling at implant/bone interface. The conditions of the microenvironment are

fundamental to affect cell response during bone regeneration. For instance temperature, oxygen tension, blood supply, loading on bone tissue are factor of special relevance for cell response[66]. Moreover, it has been suggested that proliferation and differentiation of osteoblasts responsible for peri-implant tissue formation are regulated by the local mechanical environment according to the hypothesis of Frost and colleagues about callus formation; the relationship between cell deformation and bone remodelling has been documented in various studies, as the fact that loads regulate bone healing process around the implant[54, 67-76].

Seen what before, it is clear that nowadays materials used in a wide range of tissue engineering applications still require improvements. Since natural tissues and organs have a nanometric hierarchy of cells directly interacting and producing ECM, the biomimetic features and excellent physiochemical properties of the nanomaterials play a pivotal role in stimulating cell growth as well as guided tissue regeneration. In these regards, nanomaterials show such excellent properties and have been extensively investigated in a wide range of biomedical applications gathered together as nanomedicine. Nanotechnology offers a range of new biocompatible coatings for the implants that improve their adhesion, durability and lifespan as well as a big amount of different nanostructures as scaffold. New types of nanomaterials have been evaluated to improve interface properties for tissue replacement and regeneration in various tissues.

References

1. Kobayashi, J.; Akiyama, Y.; Yamato, M.; Shimizu, T.; Okano, T., Design of Temperature-Responsive Cell Culture Surfaces for Cell Sheet-Based Regenerative Therapy and 3D Tissue Fabrication. Adv Exp Med Biol 2018, 1078, 371-393. DOI: 10.1007/978-981-13-0950-2_19.

2. Chim, H.; Schantz, J. T., New frontiers in calvarial reconstruction: integrating computer-assisted design and tissue engineering in cranioplasty. Plast Reconstr Surg 2005, 116 (6), 1726-41.

3. Hatton, J.; Davis, G. R.; Mourad, A. I.; Cherupurakal, N.; Hill, R. G.; Mohsin, S., Fabrication of Porous Bone Scaffolds Using Alginate and Bioactive Glass. J Funct Biomater 2019, 10 (1). DOI: 10.3390/jfb10010015.

4. Burg, K. J.; Holder, W. D., Jr.; Culberson, C. R.; Beiler, R. J.; Greene, K. G.; Loebsack, A. B.; Roland, W. D.; Eiselt, P.; Mooney, D. J.; Halberstadt, C. R., Comparative study of seeding methods for three-dimensional polymeric scaffolds. J Biomed Mater Res 2000, 51 (4), 642-9. DOI: 10.1002/1097-4636(20000915)51:4<642::aid-jbm12>3.0.co;2-l.

5. Williams, D. F., On the mechanisms of biocompatibility. Biomaterials 2008, 29 (20), 2941-53. DOI: 10.1016/j.biomaterials.2008.04.023.

6. Zreiqat, H.; Akin, F. A.; Howlett, C. R.; Markovic, B.; Haynes, D.; Lateef, S.; Hanley, L., Differentiation of human bone-derived cells grown on GRGDSP-peptide bound titanium surfaces. J Biomed Mater Res A 2003, 64 (1), 105-13. DOI: 10.1002/jbm.a.10376.

7. Rezania, A.; Thomas, C. H.; Branger, A. B.; Waters, C. M.; Healy, K. E., The detachment strength and morphology of bone cells contacting materials modified with a peptide sequence found within bone sialoprotein. J Biomed Mater Res 1997, 37 (1), 9-19. DOI: 10.1002/(sici)1097-4636(199710)37:1<9::aid-jbm2>3.0.co;2-w.

8. Dee, K. C.; Anderson, T. T.; Bizios, R., Osteoblast population migration characteristics on substrates modified with immobilized adhesive peptides. Biomaterials 1999, 20 (3), 221-7. DOI: 10.1016/s0142-9612(98)00161-6.

9. Lee, J. H.; Shin, Y. C.; Jin, O. S.; Kang, S. H.; Hwang, Y. S.; Park, J. C.; Hong, S. W.; Han, D. W., Reduced graphene oxide-coated hydroxyapatite composites stimulate spontaneous osteogenic differentiation of human mesenchymal stem cells. Nanoscale 2015, 7 (27), 11642-51. DOI: 10.1039/c5nr01580d.

10. Genge, B. R.; Wu, L. N.; Wuthier, R. E., Mineralization of annexin-5-containing lipid-calcium-phosphate complexes: modulation by varying lipid composition and incubation with cartilage collagens. J Biol Chem 2008, 283 (15), 9737-48. DOI: 10.1074/jbc.M706523200.

11. Lee, J.; Abdeen, A. A.; Zhang, D.; Kilian, K. A., Directing stem cell fate on hydrogel substrates by controlling cell geometry, matrix mechanics and adhesion ligand composition. Biomaterials 2013, 34 (33), 8140-8148. DOI: https://doi.org/10.1016/j.biomaterials.2013.07.074.

12. Kothapalli, C. R.; Kamm, R. D., 3D matrix microenvironment for targeted differentiation of embryonic stem cells into neural and glial lineages. Biomaterials 2013, 34 (25), 5995-6007. DOI: 10.1016/j.biomaterials.2013.04.042.

13. Kreke, M. R.; Huckle, W. R.; Goldstein, A. S., Fluid flow stimulates expression of osteopontin and bone sialoprotein by bone marrow stromal cells in a temporally dependent manner. Bone 2005, 36 (6), 1047-1055. DOI: 10.1016/j.bone.2005.03.008.

14. Banes, A. J.; Tsuzaki, M.; Yamamoto, J.; Fischer, T.; Brigman, B.; Brown, T.; Miller, L., Mechanoreception at the cellular level: the detection, interpretation, and diversity of responses to mechanical signals. Biochem Cell Biol 1995, 73 (7-8), 349-65. DOI: 10.1139/o95-043.

15. Goulet, R. W.; Goldstein, S. A.; Ciarelli, M. J.; Kuhn, J. L.; Brown, M. B.; Feldkamp, L. A., The relationship between the structural and orthogonal compressive properties of trabecular bone. Journal of Biomechanics 1994, 27 (4), 375-389. DOI: https://doi.org/10.1016/0021-9290(94)90014-0.

16. Wu, J. Z.; Cutlip, R. G.; Andrew, M. E.; Dong, R. G., Simultaneous determination of the nonlinear-elastic properties of skin and subcutaneous tissue in unconfined compression tests. Skin research and technology : official journal of International Society for

Bioengineering and the Skin (ISBS) [and] International Society for Digital Imaging of Skin (ISDIS) [and] International Society for Skin Imaging (ISSI) 2007, 13 (1), 34-42. DOI: 10.1111/j.1600-0846.2007.00182.x.

17. Welch, D. R.; Sakamaki, T.; Pioquinto, R.; Leonard, T. O.; Goldberg, S. F.; Hon, Q.; Erikson, R. L.; Rieber, M.; Rieber, M. S.; Hicks, D. J.; Bonventre, J. V.; Alessandrini, A., Transfection of Constitutively Active Mitogen-activated Protein/Extracellular Signal-regulated Kinase Kinase Confers Tumorigenic and Metastatic Potentials to NIH3T3 Cells. Cancer Research 2000, 60 (6), 1552-1556.

18. Mammoto, A.; Mammoto, T.; Ingber, D. E., Mechanosensitive mechanisms in transcriptional regulation. Journal of Cell Science 2012, 125 (13), 3061-3073. DOI: 10.1242/jcs.093005.

19. Engler, A. J.; Sen, S.; Sweeney, H. L.; Discher, D. E., Matrix elasticity directs stem cell lineage specification. Cell 2006, 126 (4), 677-89. DOI: 10.1016/j.cell.2006.06.044.

20. Parisi, L.; Toffoli, A.; Ghiacci, G.; Macaluso, G. M., Tailoring the Interface of Biomaterials to Design Effective Scaffolds. J Funct Biomater 2018, 9 (3). DOI: 10.3390/jfb9030050.

21. Murphy, C. M.; O'Brien, F. J.; Little, D. G.; Schindeler, A., Cell-scaffold interactions in the bone tissue engineering triad. Eur Cell Mater 2013, 26, 120-32.

22. Murphy, C. M.; Haugh, M. G.; O'Brien, F. J., The effect of mean pore size on cell attachment, proliferation and migration in collagen-glycosaminoglycan scaffolds for bone tissue engineering. Biomaterials 2010, 31 (3), 461-6. DOI: 10.1016/j.biomaterials.2009.09.063.

23. Guex, A. G.; Puetzer, J. L.; Armgarth, A.; Littmann, E.; Stavrinidou, E.; Giannelis, E. P.; Malliaras, G. G.; Stevens, M. M., Highly porous scaffolds of PEDOT:PSS for bone tissue engineering. Acta Biomater 2017, 62, 91-101. DOI: 10.1016/j.actbio.2017.08.045.

24. Kuboki, Y.; Jin, Q.; Takita, H., Geometry of carriers controlling phenotypic expression in BMP-induced osteogenesis and chondrogenesis. J Bone Joint Surg Am 2001, 83-A Suppl 1 (Pt 2), S105-15.

25. Tsuruga, E.; Takita, H.; Itoh, H.; Wakisaka, Y.; Kuboki, Y., Pore size of porous hydroxyapatite as the cell-substratum controls BMP-induced osteogenesis. J Biochem 1997, 121 (2), 317-24. DOI: 10.1093/oxfordjournals.jbchem.a021589.

26. Roosa, S. M. M.; Kemppainen, J. M.; Moffitt, E. N.; Krebsbach, P. H.; Hollister, S. J., The pore size of polycaprolactone scaffolds has limited influence on bone regeneration in an in vivo model. Journal of Biomedical Materials Research Part A 2010, 92A (1), 359-368. DOI: 10.1002/jbm.a.32381.

27. Boyan, B. D.; Hummert, T. W.; Dean, D. D.; Schwartz, Z., Role of material surfaces in regulating bone and cartilage cell response. Biomaterials 1996, 17 (2), 137-46. DOI: 10.1016/0142-9612(96)85758-9.

28. Fisher, J. P.; Lalani, Z.; Bossano, C. M.; Brey, E. M.; Demian, N.; Johnston, C. M.; Dean, D.; Jansen, J. A.; Wong, M. E.; Mikos, A. G., Effect of biomaterial properties on bone healing in a rabbit tooth extraction socket model. J Biomed Mater Res A 2004, 68 (3), 428-38. DOI: 10.1002/jbm.a.20073.

29. Lampin, M.; Warocquier, C.; Legris, C.; Degrange, M.; Sigot-Luizard, M. F., Correlation between substratum roughness and wettability, cell adhesion, and cell migration. J Biomed Mater Res 1997, 36 (1), 99-108. DOI: 10.1002/(sici)1097-4636(199707)36:1<99::aid-jbm12>3.0.co;2-e.

30. Knabe, C.; Berger, G.; Gildenhaar, R.; Klar, F.; Zreiqat, H., The modulation of osteogenesis in vitro by calcium titanium phosphate coatings. Biomaterials 2004, 25 (20), 4911-9. DOI: 10.1016/j.biomaterials.2004.01.059.

31. Hanawa, T.; Kamiura, Y.; Yamamoto, S.; Kohgo, T.; Amemiya, A.; Ukai, H.; Murakami, K.; Asaoka, K., Early bone formation around calcium-ion-implanted titanium inserted into rat tibia. J Biomed Mater Res 1997, 36 (1), 131-6. DOI: 10.1002/(sici)1097-4636(199707)36:1<131::aid-jbm16>3.0.co;2-l.

32. de Oliveira, P. T.; Nanci, A., Nanotexturing of titanium-based surfaces upregulates expression of bone sialoprotein and osteopontin by cultured osteogenic cells. Biomaterials 2004, 25 (3), 403-13. DOI: 10.1016/s0142-9612(03)00539-8.

33. Anselme, K.; Bigerelle, M.; Noel, B.; Dufresne, E.; Judas, D.; Iost, A.; Hardouin, P., Qualitative and quantitative study of human osteoblast adhesion on materials with various surface roughnesses. J Biomed Mater Res 2000, 49 (2), 155-66. DOI: 10.1002/(sici)1097-4636(200002)49:2<155::aid-jbm2>3.0.co;2-j.

34. Anselme, K.; Linez, P.; Bigerelle, M.; Le Maguer, D.; Le Maguer, A.; Hardouin, P.; Hildebrand, H. F.; Iost, A.; Leroy, J. M., The relative influence of the topography and chemistry of TiAl6V4 surfaces on osteoblastic cell behaviour. Biomaterials 2000, 21 (15), 1567-77. DOI: 10.1016/s0142-9612(00)00042-9.

35. Cavalcanti-Adam, E. A.; Aydin, D.; Hirschfeld-Warneken, V. C.; Spatz, J. P., Cell adhesion and response to synthetic nanopatterned environments by steering receptor clustering and spatial location. Hfsp j 2008, 2 (5), 276-85. DOI: 10.2976/1.2976662.

36. Dalby, M. J.; McCloy, D.; Robertson, M.; Agheli, H.; Sutherland, D.; Affrossman, S.; Oreffo, R. O., Osteoprogenitor response to semi-ordered and random nanotopographies. Biomaterials 2006, 27 (15), 2980-7. DOI: 10.1016/j.biomaterials.2006.01.010.

37. Park, J.; Bauer, S.; von der Mark, K.; Schmuki, P., Nanosize and vitality: TiO2 nanotube diameter directs cell fate. Nano Lett 2007, 7 (6), 1686-91. DOI: 10.1021/nl070678d.

38. Dalby, M. J.; Riehle, M. O.; Sutherland, D. S.; Agheli, H.; Curtis, A. S., Use of nanotopography to study mechanotransduction in fibroblasts--methods and perspectives. Eur J Cell Biol 2004, 83 (4), 159-69. DOI: 10.1078/0171-9335-00369.

39. Dalby, M. J.; Gadegaard, N.; Curtis, A. S.; Oreffo, R. O., Nanotopographical control of human osteoprogenitor differentiation. Curr Stem Cell Res Ther 2007, 2 (2), 129-38.

40. Arnold, M.; Cavalcanti-Adam, E. A.; Glass, R.; Blummel, J.; Eck, W.; Kantlehner, M.; Kessler, H.; Spatz, J. P., Activation of integrin function by nanopatterned adhesive interfaces. Chemphyschem 2004, 5 (3), 383-8. DOI: 10.1002/cphc.200301014.

41. Park, J.; Bauer, S.; Schlegel, K. A.; Neukam, F. W.; von der Mark, K.; Schmuki, P., TiO2 nanotube surfaces: 15 nm--an optimal length scale of surface topography for cell adhesion and differentiation. Small 2009, 5 (6), 666-71. DOI: 10.1002/smll.200801476.

42. Cavalcanti-Adam, E. A.; Volberg, T.; Micoulet, A.; Kessler, H.; Geiger, B.; Spatz, J. P., Cell spreading and focal adhesion dynamics are regulated by spacing of integrin ligands. Biophys J 2007, 92 (8), 2964-74. DOI: 10.1529/biophysj.106.089730.

43. Brammer, K. S.; Oh, S.; Gallagher, J. O.; Jin, S., Enhanced cellular mobility guided by TiO2 nanotube surfaces. Nano Lett 2008, 8 (3), 786-93. DOI: 10.1021/nl072572o.

44. Massia, S. P.; Hubbell, J. A., An RGD spacing of 440 nm is sufficient for integrin alpha V beta 3-mediated fibroblast spreading and 140 nm for focal contact and stress fiber formation. J Cell Biol 1991, 114 (5), 1089-100. DOI: 10.1083/jcb.114.5.1089.

45. Park, J.; Bauer, S.; Schmuki, P.; von der Mark, K., Narrow window in nanoscale dependent activation of endothelial cell growth and differentiation on TiO2 nanotube surfaces. Nano Lett 2009, 9 (9), 3157-64. DOI: 10.1021/nl9013502.

46. Popat, K. C.; Leoni, L.; Grimes, C. A.; Desai, T. A., Influence of engineered titania nanotubular surfaces on bone cells. Biomaterials 2007, 28 (21), 3188-97. DOI: 10.1016/j.biomaterials.2007.03.020.

47. Peng, L.; Eltgroth, M. L.; LaTempa, T. J.; Grimes, C. A.; Desai, T. A., The effect of TiO2 nanotubes on endothelial function and smooth muscle proliferation. Biomaterials 2009, 30 (7), 1268-72. DOI: 10.1016/j.biomaterials.2008.11.012.

48. Raja, P. M.; Connolley, J.; Ganesan, G. P.; Ci, L.; Ajayan, P. M.; Nalamasu, O.; Thompson, D. M., Impact of carbon nanotube exposure, dosage and aggregation on smooth muscle cells. Toxicol Lett 2007, 169 (1), 51-63. DOI: 10.1016/j.toxlet.2006.12.003.

49. Belyanskaya, L.; Weigel, S.; Hirsch, C.; Tobler, U.; Krug, H. F.; Wick, P., Effects of carbon nanotubes on primary neurons and glial cells. Neurotoxicology 2009, 30 (4), 702-11. DOI: 10.1016/j.neuro.2009.05.005.

50. Oryan, A.; Sahvieh, S., Effectiveness of chitosan scaffold in skin, bone and cartilage healing. Int J Biol Macromol 2017, 104 (Pt A), 1003-1011. DOI: 10.1016/j.ijbiomac.2017.06.124.

51. Moshiri, A.; Shahrezaee, M.; Shekarchi, B.; Oryan, A.; Azma, K., Three-Dimensional Porous Gelapin-Simvastatin Scaffolds Promoted Bone Defect Healing in Rabbits. Calcified tissue international 2015, 96 (6), 552-564. DOI: 10.1007/s00223-015-9981-9.

52. Albrektsson, T.; Branemark, P. I.; Hansson, H. A.; Lindstrom, J., Osseointegrated titanium implants. Requirements for ensuring a long-lasting, direct bone-to-implant anchorage in man. Acta Orthop Scand 1981, 52 (2), 155-70. DOI: 10.3109/17453678108991776.

53. Branemark, P. I.; Adell, R.; Albrektsson, T.; Lekholm, U.; Lundkvist, S.; Rockler, B., Osseointegrated titanium fixtures in the treatment of edentulousness. Biomaterials 1983, 4 (1), 25-8. DOI: 10.1016/0142-9612(83)90065-0.

54. Cooper, L. F., A role for surface topography in creating and maintaining bone at titanium endosseous implants. J Prosthet Dent 2000, 84 (5), 522-34. DOI: 10.1067/mpr.2000.111966.

55. Jayaraman, M.; Meyer, U.; Buhner, M.; Joos, U.; Wiesmann, H. P., Influence of titanium surfaces on attachment of osteoblast-like cells in vitro. Biomaterials 2004, 25 (4), 625-31. DOI: 10.1016/s0142-9612(03)00571-4.

56. Meyer, U.; Buchter, A.; Wiesmann, H. P.; Joos, U.; Jones, D. B., Basic reactions of osteoblasts on structured material surfaces. Eur Cell Mater 2005, 9, 39-49.

57. Hayakawa, T.; Yoshinari, M.; Kiba, H.; Yamamoto, H.; Nemoto, K.; Jansen, J. A., Trabecular bone response to surface roughened and calcium phosphate (Ca-P) coated titanium implants. Biomaterials 2002, 23 (4), 1025-31. DOI: 10.1016/s0142-9612(01)00214-9.

58. Meyer, U.; Wiesmann, H. P.; Fillies, T.; Joos, U., Early tissue reaction at the interface of immediately loaded dental implants. Int J Oral Maxillofac Implants 2003, 18 (4), 489-99.

59. Gorski, J. P., Is all bone the same? Distinctive distributions and properties of non-collagenous matrix proteins in lamellar vs. woven bone imply the existence of different underlying osteogenic mechanisms. Crit Rev Oral Biol Med 1998, 9 (2), 201-23.

60. Schlegel, K. A.; Kloss, F. R.; Kessler, P.; Schultze-Mosgau, S.; Nkenke, E.; Wiltfang, J., Bone conditioning to enhance implant osseointegration: an experimental study in pigs. Int J Oral Maxillofac Implants 2003, 18 (4), 505-11.

61. Buchter, A.; Kleinheinz, J.; Wiesmann, H. P.; Kersken, J.; Nienkemper, M.; Weyhrother, H.; Joos, U.; Meyer, U., Biological and biomechanical evaluation of bone remodelling and implant stability after using an osteotome technique. Clin Oral Implants Res 2005, 16 (1), 1-8. DOI: 10.1111/j.1600-0501.2004.01081.x.

62. Akin-Nergiz, N.; Nergiz, I.; Schulz, A.; Arpak, N.; Niedermeier, W., Reactions of peri-implant tissues to continuous loading of osseointegrated implants. Am J Orthod Dentofacial Orthop 1998, 114 (3), 292-8. DOI: 10.1016/s0889-5406(98)70211-2.

63. Joos, U.; Vollmer, D.; Kleinheinz, J., [Effect of implant geometry on strain distribution in peri-implant bone]. Mund Kiefer Gesichtschir 2000, 4 (3), 143-7. DOI: 10.1007/s100060050186.

64. Liu, Y.; de Groot, K.; Hunziker, E. B., Osteoinductive implants: the mise-en-scene for drug-bearing biomimetic coatings. Ann Biomed Eng 2004, 32 (3), 398-406. DOI: 10.1023/b:abme.0000017536.10767.0f.

65. Jung, R. E.; Cochran, D. L.; Domken, O.; Seibl, R.; Jones, A. A.; Buser, D.; Hammerle, C. H., The effect of matrix bound parathyroid hormone on bone regeneration. Clin Oral Implants Res 2007, 18 (3), 319-25. DOI: 10.1111/j.1600-0501.2007.01342.x.

66. Meyer, U.; Joos, U.; Wiesmann, H. P., Biological and biophysical principles in extracorporal bone tissue engineering. Part III. Int J Oral Maxillofac Surg 2004, 33 (7), 635-41. DOI: 10.1016/j.ijom.2004.04.006.

67. Cheal, E. J.; Mansmann, K. A.; DiGioia, A. M., 3rd; Hayes, W. C.; Perren, S. M., Role of interfragmentary strain in fracture healing: ovine model of a healing osteotomy. J Orthop Res 1991, 9 (1), 131-42. DOI: 10.1002/jor.1100090116.

68. Garces, G. L.; Garcia-Castellano, J. M.; Nogales, J., Longitudinal overgrowth of bone after osteotomy in young rats: influence of bone stability. Calcif Tissue Int 1997, 60 (4), 391-3. DOI: 10.1007/s002239900249.

69. Meyer, U.; Wiesmann, H. P.; Kruse-Losler, B.; Handschel, J.; Stratmann, U.; Joos, U., Strain-related bone remodeling in distraction osteogenesis of the mandible. Plast Reconstr Surg 1999, 103 (3), 800-7. DOI: 10.1097/00006534-199903000-00005.

70. Mosley, J. R.; March, B. M.; Lynch, J.; Lanyon, L. E., Strain magnitude related changes in whole bone architecture in growing rats. Bone 1997, 20 (3), 191-8. DOI: 10.1016/s8756-3282(96)00385-7.

71. Akagawa, Y.; Ichikawa, Y.; Nikai, H.; Tsuru, H., Interface histology of unloaded and early loaded partially stabilized zirconia endosseous implant in initial bone healing. J Prosthet Dent 1993, 69 (6), 599-604. DOI: 10.1016/0022-3913(93)90289-z.

72. Hashimoto, M.; Akagawa, Y.; Nikai, H.; Tsuru, H., Single-crystal sapphire endosseous dental implant loaded with functional stress--clinical and histological evaluation of peri-implant tissues. J Oral Rehabil 1988, 15 (1), 65-76. DOI: 10.1111/j.1365-2842.1988.tb00147.x.

73. Isidor, F., Clinical probing and radiographic assessment in relation to the histologic bone level at oral implants in monkeys. Clin Oral Implants Res 1997, 8 (4), 255-64.

74. Piattelli, A.; Ruggeri, A.; Franchi, M.; Romasco, N.; Trisi, P., An histologic and histomorphometric study of bone reactions to unloaded and loaded non-submerged single implants in monkeys: a pilot study. J Oral Implantol 1993, 19 (4), 314-20.

75. Piattelli, A.; Paolantonio, M.; Corigliano, M.; Scarano, A., Immediate loading of titanium plasma-sprayed screw-shaped implants in man: a clinical and histological report of two cases. J Periodontol 1997, 68 (6), 591-7. DOI: 10.1902/jop.1997.68.6.591.

76. Carr, A. B.; Gerard, D. A.; Larsen, P. E., The response of bone in primates around unloaded dental implants supporting prostheses with different levels of fit. J Prosthet Dent 1996, 76 (5), 500-9. DOI: 10.1016/s0022-3913(96)90008-6.

Chapter 2 – Nanomedicine

2.1 Definition and brief history of nanomedicine

The vision of Richard Feynman to manipulate and control things in the nanoscale dimension allowed the development of nanoscience in 1959. In fact, the history of nanomedicine has a recent advent, the ideal manifesto of this new branch was the Feynman's lecture *There's Plenty of Room at the Bottom*, where he affirmed that "*We can arrange the atoms the way we want; the very atoms, all the way down! What would happen if we could arrange the atoms one by one the way we want them*", where he described the possibility to synthetize nanomaterials through a direct manipulation of atomic matter.

Nanoscience and nanotechnology open new perspective to many fields of study, spacing from optical systems, electronic, chemicals and medicine. In particular, the use of nanoscale materials in the field of medicine enfaces very complex scientific as well as societal and ethical challenges, but allows to argue about solutions for specific diseases, bounded principally to the progressing of age, that have a high socio-economic impact, becoming very promising. Therefore, the US National Nanotechnology Initiative gave the following definition of nanotechnology: "nanotechnology is concerned with materials and systems whose structures and components exhibit novel and significantly improved physical, chemical and biological properties, phenomena and processes due to their nanoscale size". The focal point of the use of nanotechnology is the achievement of new and advantaging characteristics of the material, due to the nanosize, that becomes of the same dimensions of the whole system and its vital component, leading to a better interaction. The idea of ameliorating material-cell interaction become fundamental in order to achieve the goal of tissue regeneration.

The exact term nanotechnology was coined in 1972 by Norio Taniguchi, whose definition "nanotechnology mainly consists of the processing of separation, consolidation and deformation of material by one atom to one molecule" and it is still valid.

In 2011, nanomaterials have been defined from the European Commission as "a natural, or incidental or manufactured material containing particles, in an unbound state or as an aggregate or as an agglomerate and where, for 50% or more of the particles in the number size distribution, one or more external dimensions is in the size range 1nm-100nm". Nevertheless, International Organization for Standardization (ISO), in 2015 presented a more general definition of nanomaterials as "material with any external dimension in the nanoscale or having internal structure in the nanoscale".

The dimensional range of the nanoworld is better understandable in Figure 2.1.

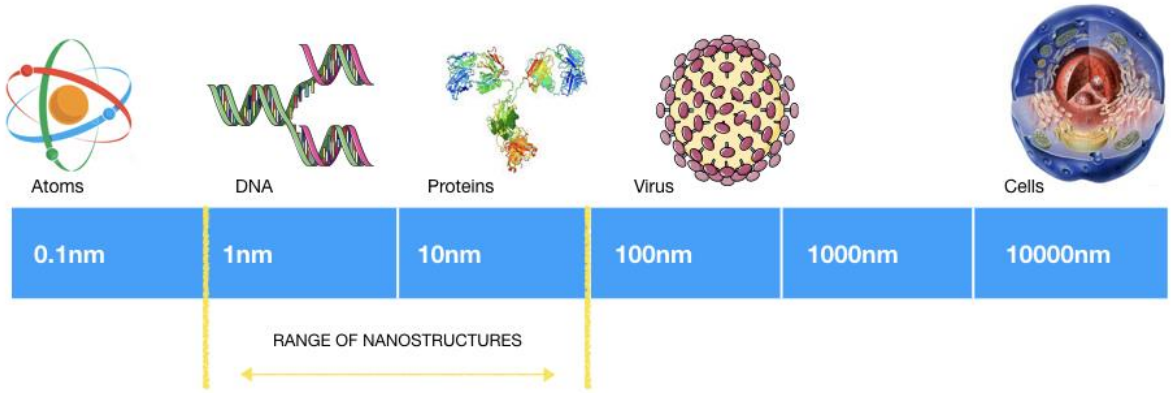

Figure 2.1: Dimensional scale of the nanometric range.

Simplistically, nanomedicine is the possibility to apply nanotechnology to medicine. Sometimes it is defined as a technology that uses molecular tools and knowledge of the human body for medical diagnosis and treatment; others it is defined as a technique that through the take advantages of the physical effects occurring only in nanosized materials and that exist at the interface between the molecular and macroscopic world, where quantum mechanics still reigns. Differently from molecular medicine, which studies biological problems with a more conventional approach, nanomedicine focus on the application of nanotechnology concepts in medicine, promising an alternative with general advantages inherent to the nanometre scale.

At the moment, there is not a universal definition for nanomedicine, but there are severally accepted, the most complete are the following two. Nanomedicine has been defined by the Medical Standing Committee of the European Science Foundation (ESF) as “the science and technology of diagnosing, treating and preventing disease and traumatic injury, of relieving pain, and of preserving and improving human health, using molecular tools and molecular knowledge of the human body”, while for the National Institutes of Health Roadmap for Medical Research, nanomedicine is “an offshoot of nanotechnology, which refers to highly specific medical interventions at the molecular scale for curing disease or repairing damaged tissues, such as bone, muscle or nerve”.

The common point of view of both is the look at nanomedicine as an interdisciplinary science focused on the clinical application of nanotechnology, whose final goal is the improvement ho human health.

The importance of the presence of a nanomaterial becomes clear thinking about the dimensions of the biological systems with the material has to interact with, that is generally less than 100nm. In this arena, the presence of a nano-structured material allows the interaction with the systems of the human body at an atomic, molecular and

macromolecular level. All the efforts have highlighted that nanomaterial exhibit superior cytocompatible, mechanical, electrical, optical, catalytic and magnetic properties compared to conventional (or micro structured) materials. These unique properties have helped to improve various tissue growth over what is achievable today.

The possibility to apply nanotechnology to medicine is also due to the large amount of scientific inventions which made it possible, as the transmission electron microscope, the field ion microscope or the atomic force microscope, that allowed the create nanometric structures through atomic resolution images.

Nowadays, nanotechnology is considered as one of the three major technologies of the twenty-first century and its potential applications in medicine have been deeply researched in the last twenty years. Nanomedicine includes the development of nanoparticles, nanostructured surfaces and nanoanalytical techniques for molecular diagnostics, treatment, follow up and therapy of diseases, as well as integrated medical nanosystems, which, in future, may perform monitoring and complex repairs in the body at the cellular level.

However, in this arena, nanomedicine has the potential to revolutionize medicine and ameliorate all the techniques implied for diagnostic or therapies, becoming the most-promising and potentially impacting application of nanotechnology, it is associated with a number of ethical and social risks that should not be underestimated.

2.2 Applications of nanomedicine

Nanomedicine, as a recent and interdisciplinary science, enters in different fields of medicine and clinical applications, all fundamental for medicine today. In biomedical applications, the nanosize presents many advantages, mainly due to the new features, distinct and excellent performances nanomaterials display, secondly to the ability to reduce the volume and the dimension to enhance the interactions surface between nanomaterial and cell.

The research activity concerning nanomaterials have broad applications in medical field; nanomaterials have been studied for drugs[1], gene carriers[2-4], cancer and gene therapy[5, 6], antibacterial and antiviral agents[7, 8], medical diagnosis[9], medical imaging[1] and tissue engineering[10].

Resuming the main fields that compose nanomedicine can be classified as: drug delivery, imaging, tissue engineering, surgery and theranostics.

- Drug delivery

Targeted drug delivery is one of the most studied techniques to achieve the release of drugs or pharmaceuticals into specific sites of the human body, controlling the rate, the time and the place of release. The focus of drug delivery is to maximise the bioavailability both in a specific site and during the time, purpose potentially reachable through the molecular targeting by nanoengineered carriers. Examples of this application are the liposomal drug carrier in chemotherapy loaded with Doxorubicin or long acting nanoparticulates formulations for insulin release in diabetics[11]. The use of drug delivery systems, with specific targeting for a tissue or an organ, allowed medicine to be more effective and less harmful to the other part of the body. Moreover, drug delivery development consented the development of drugs with increased solubility, thanks to their encapsulation, the limitation of systemic toxicity, the increasing of bioavailability and the improving of cellular up-take. Nowadays, the nanomaterials more studied for drug delivery applications are: nanoparticles[12], dendrimers[13] and liposomes[14].

- Imaging

Imaging is a technique that aims to create a visual representation of a part of the body, to reveal internal structures and bones, as well as to diagnose and treat disease for clinical analysis or medical intervention. In particular, imaging comprehends radiology, endoscopy, elastography, tactile imaging, thermography, medical photography and nuclear medicine functional imaging techniques as positron emission tomography (PET) and Single-photon emission computed tomography (SPECT).

The evolution of nanotechnology and the need for personalized medicine give the drive to foster development of point-of-care diagnostics with higher sensitivity, specificity and reliability[15]. In this regard, some nanomaterials, due to their favorable optical and chemical properties, can be used as non-invasive contrast agents, for biomedical imaging; for example, metal oxide nanoparticles and PEGylated gold nanoparticles are candidates to be used in the marking of biological structure, in order to improve both, the contrast and the biodistribution[16, 17]. The use of magnetic resonance imaging (MRI) to observe the presence of small tumors through the use of magnetic iron oxide nanoparticles is only an example of the impacting applications of nanostructures to medicine; other contrast agent commonly used in *in vivo* diagnostic are dendrimers and quantum dot nanocrystals[18-20].

- Tissue Engineering

Tissue engineering has as pivotal objective the regeneration or the replacement with artificial tissue of damaged tissues and organs. The idea to use biocompatible nanostructured materials for applications in TE becomes

important because of their biologically inspired roughness, increased surface energy, ability to improve interface properties, adhesion, durability and lifespan of the new implanted material.

Nanomaterials have shown much promise to improve many field of TE; some nanopolymers are commonly used in heart surgery to cover implantable devices (mimicking the layered structure of vascular tissue) to prevent the formation of clot when it comes in contact with the blood, to control cell behaviour at the interface, or to create biomedical devices as grafts or catheters etc[21-23]. It has been demonstrated that vascular cell adhesion is greatly improved in presence of nanostructured materials, compared to conventional ones. Moreover, examining the natural structure of some parts of the body, as bone or cartilage, it becomes clear that nanotechnology could lead to the development of new biomaterials mimicking the natural structure of the tissues with limited regenerative properties and ameliorating their regeneration. For example, bone is fundamentally a natural nanocomposite consisting of a protein based soft hydrogel template (e.g. collagen, non-collagenous proteins as laminin, fibronectin, vitronectin) and hard inorganic components (hydroxyapatite). Almost 70% of the bone composition is nanocrystalline hydroxyapatite whose length is typically 20-80nm and thickness is 2-5nm, as it occurs for many components of the ECM[21]. Studies have demonstrated that nanostructured materials that present cell favourable surface properties may promote the enhance of stimulation of bone formation if compared to conventional materials[24-26]. Nanomaterials are also used to help the healing of damaged nerves; in fact, nervous system injuries, diseases and disorders occur far too frequently, and its healing is hard because of the tendency to form a glial scar tissue around the material and the lack of a material with optimal mechanical and electrical properties for nerve regrowth. Nanotechnology could achieve the goal to develop an ideal material for neural TE, thanks to the superior electrical and mechanical properties that materials reach at the nanosize[21, 27-29]. Holmes et al. reported that a self-assembled peptide nanofiber scaffold supported neuronal cell functions, neurite outgrowth and functional synapse[30]. The use of nanomaterials as promising approach to more efficiently improve tissue regenerations is very useful also in bladder TE materials development, due to their ability to mimic the oriented nanostructured bladder ECM, electrospun polymer nanofiber has been widely used[31-33].

- Surgery

The development of nano/microscale machines hold great promise for the advance of medicine also in the field of surgery. In fact, diagnosis and treatment macro-level conventional instruments are going to be substituted with micro and nano-instruments, developed according to the purposes and able to be transported to the site of interest through the blood stream. Minute surgical instruments and nanorobots are nowadays commonly used in operatory rooms to perform high quality and accurate microsurgery, avoiding the damage of other parts of the

body and getting the examination of the target tissue with unprecedent detail. Moreover, nanotechnology-based approaches are of huge help in diagnostic and for the monitoring the medical process during the recovery of patients after surgery or for real time tracking of hematic components as blood glucose level in diabetic[34]. Nanorobots, nanosensors and nanoprobes are the most studied devices to allow the reduction of practical problems faced by doctors during the daily clinical routine.

- Theranostics

Theranostics is a new medical branch, born from the fusion of the words therapy and diagnostics, that aim to combine in the same moment both, diagnosis and therapy. This new emerging treatment strategy allows to follow the progression of the treatment at the same moment of the administration. The possibility to perform *in vivo* diagnostics creates data from the patient and consent both, the follow up of the disease and the control of treatment response. Theranostics includes different subjects of study, including personalized medicine, pharmacogenomics and molecular imaging, in order to create a more efficient and targeted therapy and to better understand the molecular mechanism underlying drug selection and targeted release. Specifically, a theranostics agent provide a rapid and accurate feedback on the performance of a specific drug, since in a single formulation there are both the pharmaceuticals and the imaging agent[16]. For example, it could be monitored in real time how a tumor responses to a therapies through the use of a combination of drug delivery and molecular imaging and with the possibility to develop an image-guided therapy in cancer treatment[35]; hypoxia-active nanoparticles are used for theranostics as noninvasively imaging agents and efficient treatment materials for hypoxic tumors[36], as well as mesoporous silica nanostructures[37].

Currently, the many efforts made by researchers in the field of tissue engineering are the basis of nanomedicine and, in particular, the development of nanomaterials for bone regeneration will be better discussed in Chapters 6, 7, 8 and 9.

2.3 Nanostructures in nanomedicine

As outlined before, nanomedicine can be defined as the clinical application of nanomaterials for the diagnostic or treatment of different diseases in the human body, or for the regeneration of a tissue or an organ. For this reason, nanostructure shape plays a pivotal role in the interaction between the biological system and the biomaterial; the nanosize and the morphology of the material have a large influence on cell adhesion and response, on cell fate and cellular internalization.

The peculiarity of a nanomaterial (material with at least one dimension between 1-100nm) is to behave very differently from the same material in its bulk form does not possess, although they have the same chemical composition. Generally, a microstructured material shares many characteristics with the corresponding bulks, but these properties at the nanometric dimensions are very different. It is known that chemical, thermal, mechanical, electrical, magnetic and optical characteristics at the nanoscale become size dependent.

There are four unique properties of nanomaterials, there are many that need to be discussed: surface to volume ratio, quantum mechanics effects, significant random molecular motion and dominance of electromagnetic forces.

The most important is the surface to volume ratio, which dramatically increases when a material is nanostructured. It is referred to the evidence that the external surface the material could use to create interaction with the biological environment increases when the volume decreases, and this is the key factor to the novel properties. In fact, as a particle decreases in size, a higher portion of the atoms are exposed at the surface compared to the quantity inside, the result is a nanoparticle having a much greater surface area per unit volume compared with larger particles. This allows the material to have freer surface in contact with the surrounding environment and to be much more reactive than the same mass of material made up of larger particles.

Another fundamental characteristic that emerges with the reduction of the material at the nanosized is the appearance of quantum effects, due to the confinement of the movements of atoms and leading to discrete energy levels depending on the size of the structure. When a particle get so small, the quasi-continuous assumption of Fermi-Dirac probability distribution is no longer valid and the energy levels must be considered discrete for the electrons because different mechanisms take precedence and different phenomenon are the results, as oxidation, reduction and catalytic properties change[38]. The classical mechanics explanation for macroscale phenomena obviously collapse at the nanoscale, where predominate the laws of quantum mechanics with the “tunability” of properties. A common effect present in the nanomaterial is the “tunneling”, characterized by the idea that changing the size of the material is possible to optimize its properties; the tunneling is a quantum mechanical phenomenon in which a particle tunnels through a barrier that could not classically overcome. Moreover, the random motion of molecules at the nanoscale is very large if compared to the size of the material. In this contest of nanoscale, the gravitation forces become negligible and the electromagnetic forces become very strong and dominate the gravitational forces.

All the new characteristics obviously strongly influence the thermodynamic properties of the materials, especially if metals, and make them more chemically active than the corresponding bulk materials, enhancing also the catalytic properties. The result is that there might be a direct contact and interaction with biological environment

and cell membranes, because the material in nanodimension is in the same dimensional range of cell receptors and molecules, leading to different responses in biomedical applications.

2.3.1 Classification of nanomaterials

There are many classification methods for nanomaterials, but the most common classifications are the two below. Nanomaterials can be classified from their origin and divided in natural and artificial.

Natural nanomaterials are commonly existing in nature, examples are clays, milk or blood (which are natural colloids), fog, gelatin, mineralized natural materials as shells or corals; artificial nanomaterials are prepared through a mechanical or chemical fabrication process. This last category includes nanowires, nanoparticles, carbon nanotubes, etc.

Otherwise, nanomaterials can be classified through the dimensional classification, that is more detailed and specific. This classification is based on the number of dimensions (x, y, z) which are not limited to the nanoscale range (<100nm).

Nanostructure can be divided in four classes:

- 0-Dimensional nanomaterials (0-D): materials characterized by all the dimensions measured within the nanoscale, otherwise, no dimension exceed 100nm. In this class we can find nanoparticles and fullerenes.
- 1-Dimensional nanomaterials (1-D): materials with two dimensions at the nanoscale (x, y), smaller than 100nm and one dimension (z) that exceed the limit. An example of 1-dimensional material are nanowires, nanorods and carbon tubes.
- 2-Dimensional nanomaterials (2-D): material with one dimension at the nanoscale (x), while the other two (y, z) outside the 100nm. Two-dimensional structures are nanofilms and nanocoating.
- 3-Dimensional nanomaterials (3-D): materials with all the three dimensions outside the nanometer range, in this category there are bulk materials, composite materials containing a dispersion of nanomaterials or nanocomposite thick films.

In Figure 2.2 there is a summary of the dimensional classification of nanomaterials.

CLASSIFICATION	0-D	1-D	2-D	3-D
DIMENSION<100 nm	x,y,z	x,y	x	none
EXAMPLES	Nanoparticles, Fullerenes 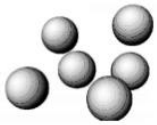	Nanowires, Nanorods, Carbon nanotube 	Nanofilm, Nanocoating 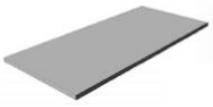	Nanocomposite, Bulk 

Figure 2.2: Schematic representation of the dimensional classification of nanomaterials.

In the field of nanomedicine, the common acceptance extends nanomaterial definition to particles or nanotherapeutics with dimensions up to 1000nm.

2.3.2 Medical applications of nanostructures

The large amount of studies of the last decade underlies the rapid development of nanotechnology in medical fields as diagnostic and therapy; in nanomedicine are commonly used some 0-dimensional and 2-dimensional materials which will be briefly summarized in this paragraph.

- Nanoparticles (NPs)

Nanoparticles are 0-D structures whose synthesis can be done with many materials, in order to obtain different compositions: metal NPs (in particular gold, silver, and other transition metals) magnetic NPs (iron oxide, zincous, cobalt, nitrogen) and polymeric NPs[39, 40].

As previously described, nanoparticles have a various range of applications and they are the most used nanostructure in drug delivery, medical diagnostics and theranostics, and the most nanomedicine products approved for clinical use belong to this category. For example, in diagnostics are being used magnetic NPs linked with antibodies to mark specific molecules or structure needing to be investigate. In tumor diagnostic NPs loaded with different molecules were developed as potential tools for the detection of esophageal adenocarcinoma[41].

Chang et al. proposed a novel nanodimensional artificial red blood cell substitute based on ultrathin polyethylene-glycol-polylactide membrane nanocapsules containing hemoglobin and enzymes typical of blood corpuscles[42]. Not the least, NPs has been used as antibacterial agents[43, 44], antivirals[43, 45, 46], antitumorals[47], analgesic and anti-inflammatory nanodrugs[48] and vaccines [49] for many different therapy requirements.

- Fullerenes

As nanoparticles, fullerenes are a pioneer class of carbon-based 0-D structure for targeted delivery. They possess a unique structure due to the disposition of carbon atoms that are interconnected through a specific geometry in pentagonal and hexagonal rings and that allows the interaction with cellular environment. They have the disadvantage to be insoluble in water and low soluble in many organic solvents, so they have been largely modified during the time, with chemical modifications, encapsulations, colloidal solutions or polymers to decrease their high hydrophobicity.

Nevertheless, they are widely used for cancer therapy, photodynamic therapy, antioxidants, antibacterials, neuroprotective agents and as contrast agents in MRI and X-Ray imaging[50-52 53].

- Carbon nanotubes (CNTs)

Carbon nanotubes are 1-D structures composed by one or more sheets of carbon wound to form a tube presenting a diameter between 0,6 and 10nm. They possess a huge number of interesting characteristics as electrical and mechanical properties beyond chemical stability[54]. Exactly due to their chemical stability and their large inner volume, CNTs can be easily functionalized internally or externally with adhesive molecules or active molecules, or in other different ways. Their medical application encompasses from molecule delivery to tissue engineering, but they have the huge disadvantage to stimulate the host immune response[55-57].

- Nanowires (NWs)

Nanowires are 1-D structures that mimic very well the ECM of some tissues and organs; as described above, nanostructure dimension and shape play a pivotal role in the interaction with the biological system, and 1-D nanostructures find a large purpose especially in tissue engineering research, because they mime the biological environment. It has been shown that titanium oxide nanofilaments stimulate cell proliferation and cell death in a dose-dependent manner[58], that zinc oxide nanowires were cytotoxic for human monocyte macrophages[59] and cell

viability of NIH3T3 fibroblasts and mouse macrophage cell line [60] decreased on zinc oxide nanorods. On the contrary, it has been seen that metal nanowires are essentially cytocompatible. In fact, silver nanowires have a significant antimicrobial activity, without inducing cytotoxic response or autophagy[61, 62], differently from silver nanoparticles, whose toxicity was due to the oxidation of Ag^+ salts on the surface. Moreover, iron nanowires and iron oxide nanowires are being tested as non-cytotoxic *in vitro* and used as magnetic nanomaterials, also indicated for several biomedical applications.

Actually, nanowires are of common use in different applications especially for the detection of circulating tumor cells [63, 64], photodynamic therapy and the development of different kind of biosensors. Moreover, silicon NWs have successfully detected many viruses as Dengue, Influenza A H3N2, H1N1 and HIV and specific sequences of DNA with incredible high sensitivity and precision[65].

NWs will be explained in detail in chapter 4.

References

1. Cao, Z.; Zhu, W.; Wang, W.; Zhang, C.; Xu, M.; Liu, J.; Feng, S. T.; Jiang, Q.; Xie, X., Stable cerasomes for simultaneous drug delivery and magnetic resonance imaging. Int J Nanomedicine 2014, 9, 5103-16. DOI: 10.2147/ijn.s66919.

2. Banizs, A. B.; Huang, T.; Dryden, K.; Berr, S. S.; Stone, J. R.; Nakamoto, R. K.; Shi, W.; He, J., In vitro evaluation of endothelial exosomes as carriers for small interfering ribonucleic acid delivery. Int J Nanomedicine 2014, 9, 4223-30. DOI: 10.2147/ijn.s64267.

3. Eroglu, E.; Tiwari, P. M.; Waffo, A. B.; Miller, M. E.; Vig, K.; Dennis, V. A.; Singh, S. R., A nonviral pHEMA+chitosan nanosphere-mediated high-efficiency gene delivery system. Int J Nanomedicine 2013, 8, 1403-15. DOI: 10.2147/ijn.s43168.

4. Liu, L.; Liu, X.; Xu, Q.; Wu, P.; Zuo, X.; Zhang, J.; Deng, H.; Wu, Z.; Ji, A., Self-assembled nanoparticles based on the c(RGDfk) peptide for the delivery of siRNA targeting the VEGFR2 gene for tumor therapy. Int J Nanomedicine 2014, 9, 3509-26. DOI: 10.2147/ijn.s63717.

5. Rodriguez-Gascon, A.; del Pozo-Rodriguez, A.; Solinis, M. A., Development of nucleic acid vaccines: use of self-amplifying RNA in lipid nanoparticles. Int J Nanomedicine 2014, 9, 1833-43. DOI: 10.2147/ijn.s39810.

6. Kircher, M. F.; Mahmood, U.; King, R. S.; Weissleder, R.; Josephson, L., A multimodal nanoparticle for preoperative magnetic resonance imaging and intraoperative optical brain tumor delineation. Cancer Res 2003, 63 (23), 8122-5.

7. Amrol, D., Single-dose azithromycin microsphere formulation: a novel delivery system for antibiotics. Int J Nanomedicine 2007, 2 (1), 9-12.

8. Mahajan, S. D.; Aalinkeel, R.; Law, W. C.; Reynolds, J. L.; Nair, B. B.; Sykes, D. E.; Yong, K. T.; Roy, I.; Prasad, P. N.; Schwartz, S. A., Anti-HIV-1 nanotherapeutics: promises and challenges for the future. Int J Nanomedicine 2012, 7, 5301-14. DOI: 10.2147/ijn.s25871.

9. Madani, S. Y.; Shabani, F.; Dwek, M. V.; Seifalian, A. M., Conjugation of quantum dots on carbon nanotubes for medical diagnosis and treatment. Int J Nanomedicine 2013, 8, 941-50. DOI: 10.2147/ijn.s36416.

10. Tonelli, F. M.; Santos, A. K.; Gomes, K. N.; Lorencon, E.; Guatimosim, S.; Ladeira, L. O.; Resende, R. R., Carbon nanotube interaction with extracellular matrix proteins producing scaffolds for tissue engineering. Int J Nanomedicine 2012, 7, 4511-29. DOI: 10.2147/ijn.s33612.

11. Peng, Q.; Zhang, Z. R.; Gong, T.; Chen, G. Q.; Sun, X., A rapid-acting, long-acting insulin formulation based on a phospholipid complex loaded PHBHHx nanoparticles. Biomaterials 2012, 33 (5), 1583-8. DOI: 10.1016/j.biomaterials.2011.10.072.

12. Yih, T. C.; Al-Fandi, M., Engineered nanoparticles as precise drug delivery systems. J Cell Biochem 2006, 97 (6), 1184-90. DOI: 10.1002/jcb.20796.

13. Yang, H.; Lopina, S. T.; DiPersio, L. P.; Schmidt, S. P., Stealth dendrimers for drug delivery: correlation between PEGylation, cytocompatibility, and drug payload. J Mater Sci Mater Med 2008, 19 (5), 1991-7. DOI: 10.1007/s10856-007-3278-0.

14. Allen, T. M.; Cullis, P. R., Liposomal drug delivery systems: from concept to clinical applications. Adv Drug Deliv Rev 2013, 65 (1), 36-48. DOI: 10.1016/j.addr.2012.09.037.

15. Riehemann, K.; Schneider, S. W.; Luger, T. A.; Godin, B.; Ferrari, M.; Fuchs, H., Nanomedicine--challenge and perspectives. Angew Chem Int Ed Engl 2009, 48 (5), 872-97. DOI: 10.1002/anie.200802585.

16. Cassano, D.; Pocovi-Martinez, S.; Voliani, V., Ultrasmall-in-Nano Approach: Enabling the Translation of Metal Nanomaterials to Clinics. Bioconjug Chem 2018, 29 (1), 4-16. DOI: 10.1021/acs.bioconjchem.7b00664.

17. Kim, C. S.; Wilder-Smith, P.; Ahn, Y. C.; Liaw, L. H.; Chen, Z.; Kwon, Y. J., Enhanced detection of early-stage oral cancer in vivo by optical coherence tomography using multimodal delivery of gold nanoparticles. J Biomed Opt 2009, 14 (3), 034008. DOI: 10.1117/1.3130323.

18. Thomas, R.; Park, I. K.; Jeong, Y. Y., Magnetic iron oxide nanoparticles for multimodal imaging and therapy of cancer. Int J Mol Sci 2013, 14 (8), 15910-30. DOI: 10.3390/ijms140815910.

19. Longmire, M.; Choyke, P. L.; Kobayashi, H., Dendrimer-based contrast agents for molecular imaging. Curr Top Med Chem 2008, 8 (14), 1180-6.

20. Dubertret, B.; Skourides, P.; Norris, D. J.; Noireaux, V.; Brivanlou, A. H.; Libchaber, A., In vivo imaging of quantum dots encapsulated in phospholipid micelles. Science 2002, 298 (5599), 1759-62. DOI: 10.1126/science.1077194.

21. Zhang, L.; Webster, T. J., Nanotechnology and nanomaterials: Promises for improved tissue regeneration. Nano Today, 2009 Vol. 4, pp 66-80

22. Miller, D. C.; Thapa, A.; Haberstroh, K. M.; Webster, T. J., Endothelial and vascular smooth muscle cell function on poly(lactic-co-glycolic acid) with nano-structured surface features. Biomaterials 2004, 25 (1), 53-61.

23. Miller, D. C.; Haberstroh, K. M.; Webster, T. J., Mechanism(s) of increased vascular cell adhesion on nanostructured poly(lactic-co-glycolic acid) films. J Biomed Mater Res A 2005, 73 (4), 476-84. DOI: 10.1002/jbm.a.30318.

24. Degasne, I.; Basle, M. F.; Demais, V.; Hure, G.; Lesourd, M.; Grolleau, B.; Mercier, L.; Chappard, D., Effects of roughness, fibronectin and vitronectin on attachment, spreading, and proliferation of human osteoblast-like cells (Saos-2) on titanium surfaces. Calcif Tissue Int 1999, 64 (6), 499-507.

25. Webster, T. J.; Ergun, C.; Doremus, R. H.; Siegel, R. W.; Bizios, R., Specific proteins mediate enhanced osteoblast adhesion on nanophase ceramics. J Biomed Mater Res 2000, 51 (3), 475-83.

26. Webster, T. J.; Schadler, L. S.; Siegel, R. W.; Bizios, R., Mechanisms of enhanced osteoblast adhesion on nanophase alumina involve vitronectin. Tissue Eng 2001, 7 (3), 291-301. DOI: 10.1089/10763270152044152.

27. Koh, H. S.; Yong, T.; Chan, C. K.; Ramakrishna, S., Enhancement of neurite outgrowth using nano-structured scaffolds coupled with laminin. Biomaterials 2008, 29 (26), 3574-82. DOI: 10.1016/j.biomaterials.2008.05.014.

28. Prabhakaran, M. P.; Venugopal, J. R.; Chyan, T. T.; Hai, L. B.; Chan, C. K.; Lim, A. Y.; Ramakrishna, S., Electrospun biocomposite nanofibrous scaffolds for neural tissue engineering. Tissue Eng Part A 2008, 14 (11), 1787-97. DOI: 10.1089/ten.tea.2007.0393.

29. Yang, F.; Murugan, R.; Ramakrishna, S.; Wang, X.; Ma, Y. X.; Wang, S., Fabrication of nano-structured porous PLLA scaffold intended for nerve tissue engineering. Biomaterials 2004, 25 (10), 1891-900.

30. Holmes, T. C.; de Lacalle, S.; Su, X.; Liu, G.; Rich, A.; Zhang, S., Extensive neurite outgrowth and active synapse formation on self-assembling peptide scaffolds. Proc Natl Acad Sci U S A 2000, 97 (12), 6728-33. DOI: 10.1073/pnas.97.12.6728.

31. Harrington, D. A.; Cheng, E. Y.; Guler, M. O.; Lee, L. K.; Donovan, J. L.; Claussen, R. C.; Stupp, S. I., Branched peptide-amphiphiles as self-assembling coatings for tissue engineering scaffolds. J Biomed Mater Res A 2006, 78 (1), 157-67. DOI: 10.1002/jbm.a.30718.

32. Baker, S. C.; Atkin, N.; Gunning, P. A.; Granville, N.; Wilson, K.; Wilson, D.; Southgate, J., Characterisation of electrospun polystyrene scaffolds for three-dimensional in vitro biological studies. Biomaterials 2006, 27 (16), 3136-46. DOI: 10.1016/j.biomaterials.2006.01.026.

33. McManus, M.; Boland, E.; Sell, S.; Bowen, W.; Koo, H.; Simpson, D.; Bowlin, G., Electrospun nanofibre fibrinogen for urinary tract tissue reconstruction. Biomed Mater 2007, 2 (4), 257-62. DOI: 10.1088/1748-6041/2/4/008.

34. Veiseh, O.; Tang, B. C.; Whitehead, K. A.; Anderson, D. G.; Langer, R., Managing diabetes with nanomedicine: challenges and opportunities. Nat Rev Drug Discov 2015, 14 (1), 45-57. DOI: 10.1038/nrd4477.

35. Zhang, X. D.; Wu, D.; Shen, X.; Chen, J.; Sun, Y. M.; Liu, P. X.; Liang, X. J., Size-dependent radiosensitization of PEG-coated gold nanoparticles for cancer radiation therapy. Biomaterials 2012, 33 (27), 6408-19. DOI: 10.1016/j.biomaterials.2012.05.047.

36. Wang, Y.; Shang, W.; Niu, M.; Tian, J.; Xu, K., Hypoxia-active nanoparticles used in tumor theranostic. Int J Nanomedicine 2019, 14, 3705-3722. DOI: 10.2147/ijn.s196959.

37. Ravindran Girija, A.; Balasubramanian, S., Theragnostic potentials of core/shell mesoporous silica nanostructures. Nanotheranostics 2019, 3 (1), 1-40. DOI: 10.7150/ntno.27877.

38. Ekimov AI, E. A., Onushchenko AA.; 0.0px, p. p. m. p. p. p.; Roman', f. p. T. N.; 15.0px}, m.-h.; 0.0px, p. p. m. p. p. p.; Roman'}, f. p. T. N., Quantum size effect in semiconductor microcrystals. . Solid State Commun. 88: 947–950., 1993.

39. Harguindey, A.; Domaille, D. W.; Fairbanks, B. D.; Wagner, J.; Bowman, C. N.; Cha, J. N., Synthesis and Assembly of Click-Nucleic-Acid-Containing PEG-PLGA Nanoparticles for DNA Delivery. Adv Mater 2017, 29 (24). DOI: 10.1002/adma.201700743.

40. Dutta, P.; Shrivastava, S.; Dey, J., Amphiphilic polymer nanoparticles: characterization and assessment as new drug carriers. Macromol Biosci 2009, 9 (11), 1116-26. DOI: 10.1002/mabi.200900135.

41. Dassie, E.; Arcidiacono, D.; Wasiak, I.; Damiano, N.; Dall'Olmo, L.; Giacometti, C.; Facchin, S.; Cassaro, M.; Guido, E.; De Lazzari, F.; Marin, O.; Ciach, T.; Fery-Forgues, S.; Alberti, A.; Battaglia, G.; Realdon, S., Detection of fluorescent organic nanoparticles by confocal laser endomicroscopy in a rat model of Barrett's esophageal adenocarcinoma. Int J Nanomedicine 2015, 10, 6811-23. DOI: 10.2147/ijn.s86640.

42. Chang, T. M.; Powanda, D.; Yu, W. P., Analysis of polyethylene-glycol-polylactide nano-dimension artificial red blood cells in maintaining systemic hemoglobin levels and prevention of methemoglobin formation. Artif Cells Blood Substit Immobil Biotechnol 2003, 31 (3), 231-47.

43. Ge, L.; Li, Q.; Wang, M.; Ouyang, J.; Li, X.; Xing, M. M., Nanosilver particles in medical applications: synthesis, performance, and toxicity. Int J Nanomedicine 2014, 9, 2399-407. DOI: 10.2147/ijn.s55015.

44. Murugan, K.; Senthilkumar, B.; Senbagam, D.; Al-Sohaibani, S., Biosynthesis of silver nanoparticles using Acacia leucophloea extract and their antibacterial activity. Int J Nanomedicine 2014, 9, 2431-8. DOI: 10.2147/ijn.s61779.

45. Sun, R. W.; Chen, R.; Chung, N. P.; Ho, C. M.; Lin, C. L.; Che, C. M., Silver nanoparticles fabricated in Hepes buffer exhibit cytoprotective activities toward HIV-1 infected cells. Chem Commun (Camb) 2005, (40), 5059-61. DOI: 10.1039/b510984a.

46. Lu, L.; Sun, R. W.; Chen, R.; Hui, C. K.; Ho, C. M.; Luk, J. M.; Lau, G. K.; Che, C. M., Silver nanoparticles inhibit hepatitis B virus replication. Antivir Ther 2008, 13 (2), 253-62.

47. England, C. G.; Priest, T.; Zhang, G.; Sun, X.; Patel, D. N.; McNally, L. R.; van Berkel, V.; Gobin, A. M.; Frieboes, H. B., Enhanced penetration into 3D cell culture using two and three layered gold nanoparticles. Int J Nanomedicine 2013, 8, 3603-17. DOI: 10.2147/ijn.s51668.

48. Kumar, R.; Chen, M. H.; Parmar, V. S.; Samuelson, L. A.; Kumar, J.; Nicolosi, R.; Yoganathan, S.; Watterson, A. C., Supramolecular assemblies based on copolymers of PEG600 and functionalized aromatic diesters for drug delivery applications. J Am Chem Soc 2004, 126 (34), 10640-4. DOI: 10.1021/ja039651w.

49. Mahony, D.; Cavallaro, A. S.; Mody, K. T.; Xiong, L.; Mahony, T. J.; Qiao, S. Z.; Mitter, N., In vivo delivery of bovine viral diahorrea virus, E2 protein using hollow mesoporous silica nanoparticles. Nanoscale 2014, 6 (12), 6617-26. DOI: 10.1039/c4nr01202j.

50. Hu, Y.; Mignani, S.; Majoral, J. P.; Shen, M.; Shi, X., Construction of iron oxide nanoparticle-based hybrid platforms for tumor imaging and therapy. Chem Soc Rev 2018, 47 (5), 1874-1900. DOI: 10.1039/c7cs00657h.

51. Kraemer, A. B.; Parfitt, G. M.; Acosta, D. D. S.; Bruch, G. E.; Cordeiro, M. F.; Marins, L. F.; Ventura-Lima, J.; Monserrat, J. M.; Barros, D. M., Fullerene (C60) particle size implications in neurotoxicity following infusion into the hippocampi of Wistar rats. Toxicol Appl Pharmacol 2018, 338, 197-203. DOI: 10.1016/j.taap.2017.11.022.

52. Borowik, A.; Prylutskyy, Y.; Kawelski, L.; Kyzyma, O.; Bulavin, L.; Ivankov, O.; Cherepanov, V.; Wyrzykowski, D.; Kazmierkiewicz, R.; Golunski, G.; Woziwodzka, A.; Evstigneev, M.; Ritter, U.; Piosik, J., Does C60 fullerene act as a transporter of small aromatic molecules? Colloids Surf B Biointerfaces 2018, 164, 134-143. DOI: 10.1016/j.colsurfb.2018.01.026.

53. Kepley, C.; Dellinger, A., Study examining fullerene toxicity raises questions as to the purity of the nanomaterials and erroneous experimental conclusions. In Toxicol Sci, United States, 2014; Vol. 141, pp 326-7. DOI: 10.1093/toxsci/kfu182.

54. Bhattacharyya, S.; Guillot, S.; Dabboue, H.; Tranchant, J. F.; Salvetat, J. P., Carbon nanotubes as structural nanofibers for hyaluronic acid hydrogel scaffolds. Biomacromolecules 2008, 9 (2), 505-9. DOI: 10.1021/bm7009976.

55. Ladeira, M. S.; Andrade, V. A.; Gomes, E. R.; Aguiar, C. J.; Moraes, E. R.; Soares, J. S.; Silva, E. E.; Lacerda, R. G.; Ladeira, L. O.; Jorio, A.; Lima, P.; Leite, M. F.; Resende, R. R.; Guatimosim, S., Highly efficient siRNA delivery system into human and murine cells using single-wall carbon nanotubes. Nanotechnology 2010, 21 (38), 385101. DOI: 10.1088/0957-4484/21/38/385101.
56. de Menezes, V. M.; Michelon, E.; Rossato, J.; Zanella, I.; Fagan, S. B., Carbon nanostructures interacting with vitamins A, B3 and C: ab initio simulations. J Biomed Nanotechnol 2012, 8 (2), 345-9.
57. Madani, S. Y.; Tan, A.; Dwek, M.; Seifalian, A. M., Functionalization of single-walled carbon nanotubes and their binding to cancer cells. Int J Nanomedicine 2012, 7, 905-14. DOI: 10.2147/ijn.s25035.
58. Magrez, A.; Horvath, L.; Smajda, R.; Salicio, V.; Pasquier, N.; Forro, L.; Schwaller, B., Cellular toxicity of TiO2-based nanofilaments. ACS Nano 2009, 3 (8), 2274-80. DOI: 10.1021/nn9002067.
59. Muller, K. H.; Kulkarni, J.; Motskin, M.; Goode, A.; Winship, P.; Skepper, J. N.; Ryan, M. P.; Porter, A. E., pH-dependent toxicity of high aspect ratio ZnO nanowires in macrophages due to intracellular dissolution. ACS Nano 2010, 4 (11), 6767-79. DOI: 10.1021/nn101192z.
60. Park, E. J.; Lee, G. H.; Shim, H. W.; Kim, J. H.; Cho, M. H.; Kim, D. W., Comparison of toxicity of different nanorod-type TiO2 polymorphs in vivo and in vitro. J Appl Toxicol 2014, 34 (4), 357-66. DOI: 10.1002/jat.2932.
61. An, D.; Su, J.; Weber, J. K.; Gao, X.; Zhou, R.; Li, J., A Peptide-Coated Gold Nanocluster Exhibits Unique Behavior in Protein Activity Inhibition. Journal of the American Chemical Society 2015, 137 (26), 8412-8418. DOI: 10.1021/jacs.5b00888.
62. Baldassarre, F.; Cacciola, M.; Ciccarella, G., A predictive model of iron oxide nanoparticles flocculation tuning Z-potential in aqueous environment for biological application. Journal of Nanoparticle Research 2015, 17 (9), 377. DOI: 10.1007/s11051-015-3163-6.
63. Hosokawa, M.; Hayata, T.; Fukuda, Y.; Arakaki, A.; Yoshino, T.; Tanaka, T.; Matsunaga, T., Size-selective microcavity array for rapid and efficient detection of circulating tumor cells. Anal Chem 2010, 82 (15), 6629-35. DOI: 10.1021/ac101222x.
64. Stott, S. L.; Hsu, C. H.; Tsukrov, D. I.; Yu, M.; Miyamoto, D. T.; Waltman, B. A.; Rothenberg, S. M.; Shah, A. M.; Smas, M. E.; Korir, G. K.; Floyd, F. P., Jr.; Gilman, A. J.; Lord, J. B.; Winokur, D.; Springer, S.; Irimia, D.; Nagrath, S.; Sequist, L. V.; Lee, R. J.; Isselbacher, K. J.; Maheswaran, S.; Haber, D. A.; Toner, M., Isolation of circulating tumor cells using a microvortex-generating herringbone-chip. Proc Natl Acad Sci U S A 2010, 107 (43), 18392-7. DOI: 10.1073/pnas.1012539107.
65. Zhang, G. J.; Zhang, G.; Chua, J. H.; Chee, R. E.; Wong, E. H.; Agarwal, A.; Buddharaju, K. D.; Singh, N.; Gao, Z.; Balasubramanian, N., DNA sensing by silicon nanowire: charge layer distance dependence. Nano Lett 2008, 8 (4), 1066-70. DOI: 10.1021/nl072991l.

Chapter 3 – Safety issues of nanomedicine

The advent of nanotechnologies and nanomedicine revolutionized the approach in numerous fields such as electronics, engineering, telecommunications, medicine and even dentistry due to the possibility to improve mechanical and physical properties of materials through the unique properties presented by the material at the nanosize. The peculiarity of nanomaterials is that they can arrange themselves in a number of packing configurations and subsequently be easily manipulated due to their high surface to core ratio, meaning that there are more atoms on the surface of the nanoparticle than deep within its core. This appear a very useful characteristic in nanomedicine, because atoms have unbound surface and they can be used to create new strong bonds. Moreover, nanomaterials possess the ability to interact on a molecular level, by that increasing the overall efficacy and affinity in comparison to biological molecules interacting with macro- and micro-sized particles, resulting in a feasible use in various application fields[1].

Anyway, there is no question that the risk profile of a technology is strongly correlated with the social and ethical issues that will encourage or subvert its acceptance in the culture. Since society is the consumer and policy decision maker, the public's attitude towards nanotechnology plays a pivotal role in its success or failure; the most important concepts to deeply analyze are the ethical issue and the toxicological issue.

3.1 The ethical issue

This context of rapid advancement of novel techniques promises to reach substantial benefits and to enhance the level of healthcare through the use of nanosized materials. All the technological developments, at the basis of nanotechnologies, provide in addition a series of not under estimable ethical issues. In fact, the clinical use of nanomaterials needs regulatory guidelines to ensure the appropriate use of new medical devices and drugs originating from nanoscience. The regulatory plan must include toxicological aspects, but also ethical related to the question of the amelioration of quality of life in some cases of severe diseases and the effective costs of treating patients which might be available only for a few. Moreover, nanosized materials have different risk profile given their size, increased biological activity and unknown properties. This profile of risks is largely unknown and obviously creates new ethical and legal challenges about clinical trials, patient use, public and environmental health. Obviously, in the last years, the gap between public's opinion and scientific progress has been partially bridged and people has become more accepting of the new sparking technologies as the perceived benefits

outweigh the risks. The presence of this new technologies integrated in fields that directly affect the society, such as pollution control or health care diagnostic, created some kind of fear for the fact that advanced in technology will require a generation of new trained workers with advanced set of operational and managerial skills to accommodate a more machinery reliant system[2].

There is a constant legislative change about ethical concerns, especially during the development of a new multidisciplinary regulatory framework to assess the control of nanotechnologies use, but the more urgent issue is to govern the emerging technologies responsibly during this period of international norm creation. In fact, the health risk of engineered nanomaterials from public interest groups, the lack of regulation and an environment of legal uncertainty are putting the industry's long-term economic viability at risk[3].

Herein, in absence of well-developed regulatory protocols, it becomes fundamental to carefully consider all the potentially deriving risks. In this regard, the US Food and Drug Administration (FDA), published several nanotechnology-specific guidance documents instructing industries on agency policy[4]. In July 2007 FDA concluded that it is not necessary a particular regulatory for nanosized materials, but it will be used a case-by-case approach for every product.

Nevertheless, three main challenges stand out:

- the adequacy of the regulatory framework itself – in nanomedicine the old definition of chemical and mechanical action is not still valid and for the purpose of evaluating such products. The new definition must be accompanied by legal requirements for review, approval and postmarket surveillance; in fact, as the current regulatory may works for actual products, but the increasing complexity of nanotechnology and its entrance in many fields will likely strain their limits. In this regard, obviously, the implementation of new frameworks is necessary to ensure safety and efficacy[4];
- the analysis of potential novel risks, which raise question about traditional safety and efficacy requirements' appropriateness; nanoscale properties alters the established risk-benefit measures, the assessment of clinical trials and of research protocols;
- the labeling of nanomedicine products for consumer's education and safety, in order to promote also a positive perception and understanding of potential applications.

As it is clear, the traditional process of ethical decision is no more able to keep up with the rapid increase and change of nano-technological developments, leading to a necessary deeper understanding of the technology itself and to a specific analysis of risks/benefits correlated with ethical considerations in order to guide nanotechnology introduction towards an ethically acceptable outcome[3, 5].

3.2 The toxicological issue

Although the promises of nanomedicine are of substantial scientific and economic benefits and that space from aerospace engineering and nano-electronic to environmental remediation and medical healthcare. Currently, over 800 products already in commerce contains nanomaterials, confirming that human exposure is already occurring and its projection of increase in the next years is a reality. Thus, given the considerable lack of certain about nanomaterials safety, it is imperative to understand and thereafter minimize any potential toxicological hazard associated to their use, not only to preserve human and environmental safety, but also to avoid an incalculable damage to nanotechnology industry in the long period. Moreover, as private companies are not forced to perform post-marketing studies on their product, it become essential to predispose a network of investigation concerning long term effects of these materials and to report any adverse effect to the competent regulatory body.

The peculiarity of nanomaterials to possess different characteristics if compared to bulk materials create another issue relative to the size-dependent toxicity of the material. This means that a particles 100nm sized normally nontoxic could dramatically transform into a toxic element if its size changes of 1nm; a nontoxic element can disintegrate or aggregate creating toxic reaction materials. It is exactly this unpredictability of nanomaterial behavior and body response, in terms also of immune system to the nanoproducts, since it is different than the reaction in cell culture, that has to be deeply understood. In the United States of America, the proper agency adopted a four-stage structure to evaluate the dimension of any health concern: problem identification, dose-response assessment, exposure assessment and risk characterization[6]. It is clear that before nanomedicine products can be used in clinical routine they must undergo extensive pre-clinical and clinical testing[7]; many international organizations launched programs aimed to study the risks bounded to the use of nanomaterials, but researchers have only just begun to explore the toxicological, pharmacological and immunological properties of nanomaterials. Unfortunately, the extensive pre-clinical research may only provide reasonable indications about the possible use in humans of nanomaterials, but, there have been recorded many cases of phase I trials where humans exposed to 500 times lower dose of the recorded toxic limit in animal studies presented very serious adverse reactions[7]. This tricky point is probably due to the extreme difficulty in assessing nanomaterials safety, because they are not a unified class and they have no other properties in common in addition to the size. The huge variation of size and shape could have dramatically unpredictable effects on the physical or chemical properties of the material.

In particular, the toxicological, immunological and mechanical risks for human health enfold effects at the moment of the interaction with the medical device; as medical device the EU Medical Devices Directive means “every tools for diagnosis, monitoring, treatment or alleviation of or compensation for an injury or handicap; instruments for

investigation, replacement or modification of anatomy or physiology processes". This definition clarify that nanomaterials have a broad range of applications in biomedical field and the first step to undergo to assess the use of a biomaterial is to verify its biocompatibility. Biocompatibility is defined as the ability of a material to perform an appropriate host response in a specific application and the main guidelines for its evaluation are the International Organization for Standardization (ISO) 10993. Understanding the level of risk associated with the exposure to a new material and the collection of safety data are fundamental to carefully track its safety, on short and long term, and to record the presence of adverse effects, with the final aim to ensure the safety and wellbeing of people.

Nanomaterials used for biomedical applications may affect human health in different ways, also depending on the exposure route (e.g. some nanomaterials are toxic if inhaled and not toxic in ingested).

There are three common ways of nanomaterial uptake by the human body: inhalation, contact with the skin and ingestion. The exposure through the respiratory system leads to the deposition of nanomaterials in the respiratory tract and lungs, resulting in respiratory related diseases such as asthma, bronchitis, etc. Moreover, the uptake and translocation of the material could reach the brain through blood system. If nanomaterials come in contact with the skin, absorption can occur; nanoparticle may penetrate into sweat glands and hair follicles resulting in a detrimental accumulation (e.g. the use of nanoparticles in cosmetology is strictly regulated). There have been a few reports on nanoparticle penetration into the skin, Baroli et al. reported that metallic nanoparticles smaller than 10 nm could penetrate the hair follicle and stratum corneum as well as sometimes reach the viable epidermis[8]. The ingestion of nanomaterials may lead to the uptake at gastrointestinal level. It can occur with daily food, drinks, and medicines, but may cause cytotoxic effects. Cytotoxicity is defined as the presence of nanomaterials that can prevent cell division, hinder cell proliferation, damage DNA and biological systems, and eventually lead to cell death by apoptosis.

Once a nanomaterial entered the human body, it can give side effects or toxicity in different ways. The main known side risks related to the use of nanomaterials are:

- DNA damage
- ROS formation
- Translocation of the nanomaterial from the exposure site to other parts of the body
- Crossing of cell membrane, blood-brain barrier, capillaries and penetration in the circulatory system
- Penetration and accumulation in peripheral organs (liver, spleen, lymph nodes, bone marrow, etc.).

Obviously, the effect of the nanomaterial depends on the organ which it comes into contact, but almost every district of the body tends to behave the same way and acting an acute inflammation that can exacerbate in chronic inflammation. The presence of an inflamed tissue leads to the production of radical oxygen species (ROS), which can damage protein, DNA, mitochondria and membranes. The mechanisms through nanomaterials can induce DNA damage are multiple because they can enter the human body in different ways, as cited before, and alternative pathways could induce DNA damage, immunoreaction, inflammation or cancer. Moreover, once penetrated the organism, nanomaterials can be internalized from the cells and spread through the nucleic membrane, binding to DNA molecules or DNA-related proteins creating physical damage to the genetic material and invalidating cellular mitosis or enhancing inflammation and consequently oxidative stress levels with genotoxic effects. It is still unknown the potential of causing diseases on a long term of nanoparticles that had entered the organism and are not excreted but accumulated in cell tissues. For example, nanoparticles for drug delivery accumulates in the liver causing chronic inflammation of the organ or leading to the dissemination in other parts of the body with the possibility to cause further pathologies. Moreover, it has been seen that inhalation of ultrafine particles is critical for pulmonary inflammation, as well as inhalation of carbon nanotubes[9, 10].

Moreover, nanomaterials penetrated in a specific district of the organism can cross the blood system barriers and translocate to another organ or tissue of the body. This is very dangerous especially in case of reaching the brain or in case of accumulation in the target organ, where they can induce blood clotting alteration, autoimmune response, alteration of metabolism, necrosis of the tissue, or they can be uptaken from resident cells and subsequently induce protein denaturation, apoptosis, alteration of cell cycle, carcinogenesis. Finally, it is important to control the clearance of the nanomaterial, in order to avoid persisting organ accumulation.

The fundamental aspects of size and shape

Size and shape of the nanomaterial are fundamental to control the risk of side effects and the damage to organisms and they may also affect the disposition and translocation of particles in the organism. In fact, particle size can clearly have a dramatic effect on the way in which an organism responds upon exposure to foreign materials. There are several aspects to consider in this issue:

1. Size can control the exposure of the body; some studies underlined how it is possible to hypostatize the material distribution in a particular organ depending on the nanostructures size[11, 12].
2. Size is a factor in the ability of the body to clear foreign particles (clearance mechanisms)[13]. For example, the ciliatory system in the lung is designed to clear particulate matter from the upper airways,

phagocytosis by macrophages and giant cells is a common mechanism by which the body's innate immune system attempts to clear particles of the order of a few microns or less[14].

3. Size can be a factor in the ultimate fate (in terms of location) of particles that are not cleared (translocation, fibrosis)[15].
4. Particle size can potentially influence direct mechanisms and extent of toxicity within cells and tissues (cytotoxicity, necrosis and mutagenicity).

Instead, nanostructures shape has been implicated in several forms of toxic effects, mostly relating to the inhalation toxicity of certain inorganic fibers such as asbestos[16]. The toxicity of quartz has been definitively connected to its crystal structure. Although there are a few examples of high aspect ratio fibers showing increased toxicity, it is not generally proven that all such shapes are dangerous, particularly at the nano-scale[17]. Recent research into the potential toxicity of carbon nanotubes has suggested that there may be some asbestos-like toxicity associated with carbon nanotubes longer than 20 microns[18-20].

Obviously, there must be considered also other characteristics designing a nanomaterial for biomedical applications, such as surface properties, surface area, surface charge and reactivity and for their use it is necessary to precisely understand the correct concentration of use. Table 3.1 resumes some of the important characteristics.

Table 3.1: Brief description of the risks associated with specific characteristics of nanomaterials.

Nanomaterial properties	Risk description
Agglomeration or aggregation	Agglomeration or aggregation (fusion of particles) are significant risk criteria as they lead to poor corrosion resistance, high solubility and phase change of nanomaterials, leading to deterioration and lack in structure maintenance.
Reactivity of charge	Chemical species characterizing nanomaterials and their charge-related critical functional groups will be a significant factor for specific functionality and bioavailability of nanomaterials.
Impurity	Nanomaterials interact with impurities due to their high reactivity. Due to this reason, encapsulation becomes a prime necessity for solution-based synthesis of nanomaterials. In the encapsulation process, the reactive nano-entities are encapsulated by nonreactive species to provide stability to the material.
Size	Reactivity and agglomeration of nanomaterials is mostly dependent on their particle size. It is well known that the process of agglomeration will happen at slower rates in smaller particles. Penetration in human tissues and inhalation are also linked to nanomaterials dimension.
Shape	Shape is fundamental to understand the risk of contact with the material. Nanomaterials with different shapes interact differently with human cells and tissues and can be internalized in different ways, leading to very various side effects.
Contaminant dissociation	The contamination of residual impurities from the synthesis is considered as a major risk factor for nanomaterials.

Evaluation of toxicity *in vitro*

The *in vitro* research is the most common and easy way to screen the toxicity of a nanomaterial. *In vitro* toxicity testing is used to evaluate the potential hazards of a variety of materials, including pesticides, pharmaceutical, food additive and medical devices, but it requires a limiting prerequisite for a correct outcome that is the availability of an appropriate validated test system. Studies using epithelial and macrophage cell lines in the respiratory and gastrointestinal tracts, as well as in the skin and vasculature, are among the most common *in vitro* models used in evaluating the toxicity of nanoparticles (as it occurred for pulmonary response to inhaled asbestos)[21]. Fiber characteristics such as concentration, type and size have been shown to be important factors in the development of the inflammatory response to inhaled asbestos, and have helped to develop more stringent requirements for regulation and importation of amphiboles[21].

Proper control of all variables involved in the study is essential to understand deeply the cell–nanoparticle interactions mechanism. Also, mimicking the *in vitro* environment as much as possible is crucial to obtaining representative results that may later be applied *in vivo*. Finally, the appropriate tests must be performed to measure accurately the cellular response under question. When these three factors are kept under consideration, *in vitro* analysis of nanotoxicity offers investigators a powerful tool for mechanistic and high throughput analysis. Normally *in vitro* studies of toxicity of nanomaterials must follow the guidelines ISO 10993-5, with as intended endpoint to show the degree of damage that a specific nanomaterial caused. Many endpoints are possible, as the loss of membrane integrity, the release of cytosolic enzymes, the alteration of metabolic processes, the reduction of DNA synthesis or the block of cell cycle.

There are many variables in an experiment, just to cite some of them:

- variations in size, shape, surface area, surface chemistry and charge of the nanoparticles before and during the study
- variables linked to cell suspension and cell line
- reaction of nanomaterials to the *in vitro* environment (proteins in serum, amino acids, salts)
- difficulties in standardization of nanomaterial concentration (typically these reports are in terms of µg/ml, but large variations expand the range of concentration from ng/ml to mg/ml)
- different time of incubation with nanomaterials.

Limitations

Although the *in vitro* toxicity assays provide easy methods of assessing cell viability, they provide little input in determining the mechanism of cellular toxicity and death. Many of the colorimetric assays using tetrazolium salts

measure cell viability as a function of metabolic function, but questions regarding why these cells stopped mitochondrial activity remains unanswered. Any number of deleterious consequences from nanoparticle exposure may contribute to these effects, such as membrane lysis, cell cycle arrest and apoptosis. Another limitation of colorimetric assays is the potential interactions of the nanoparticles with the color-generating dyes such as formazan crystals. Other variables such as surfactants used to stabilize the particles have also been shown to interfere with the dyes being measured[22]. Results from these studies indicate that the validity of these methods needs to be assessed in the presence of nanoparticles before results can be interpreted as absolute.

Much of the actual literature investigated systems which seem to display a relatively little risk, but all the studies were conducted on the short period. Nevertheless, since the risks of these new technology are still unknown, it is necessary to develop a systematic risk assessment in parallel with technological development, to keep hazardous potential as small as possible[23]. Moreover, researchers and public institution should educate the society about how nanotechnologies can be used in medicine and about the risks and benefits related, because people not properly educated and informed on the matter are likely to view it as dangerous.

References

1. Li, L.; Pan, H.; Tao, J.; Xu, X.; Mao, C.; Gu, X.; Tang, R., Repair of enamel by using hydroxyapatite nanoparticles as the building blocks. Journal of Materials Chemistry 2008, 18 (34), 4079-4084. DOI: 10.1039/B806090H.

2. Gupta, N.; Fischer, A. R.; Frewer, L. J., Ethics, Risk and Benefits Associated with Different Applications of Nanotechnology: a Comparison of Expert and Consumer Perceptions of Drivers of Societal Acceptance. Nanoethics 2015, 9 (2), 93-108. DOI: 10.1007/s11569-015-0222-5.

3. Malsch, I.; Subramanian, V.; Semenzin, E.; Hristozov, D.; Marcomini, A.; Mullins, M.; Hester, K.; McAlea, E.; Murphy, F.; Tofail, S. A., Empowering citizens in international governance of nanotechnologies. J Nanopart Res 2015, 17 (5), 215. DOI: 10.1007/s11051-015-3019-0.

4. Paradise, J., Regulating Nanomedicine at the Food and Drug Administration. AMA J Ethics 2019, 21 (4), E347-355. DOI: 10.1001/amajethics.2019.347.

5. Sollie, P., Ethics, technology development and uncertainty: an outline for any future ethics of technology. Journal of Information, Communication and Ethics in Society 2007, 5 (4), 293-306. DOI: 10.1108/14779960710846155.

6. Stander, L.; Theodore, L., Environmental Implications of Nanotechnology—An Update. International Journal of Environmental Research and Public Health 2011, 8 (2). DOI: 10.3390/ijerph8020470.

7. Resnik, D. B.; Tinkle, S. S., Ethics in nanomedicine. Nanomedicine (Lond) 2007, 2 (3), 345-50. DOI: 10.2217/17435889.2.3.345.

8. Baroli, B.; Ennas, M. G.; Loffredo, F.; Isola, M.; Pinna, R.; Lopez-Quintela, M. A., Penetration of metallic nanoparticles in human full-thickness skin. J Invest Dermatol 2007, 127 (7), 1701-12. DOI: 10.1038/sj.jid.5700733.

9. Mangum, J. B.; Turpin, E. A.; Antao-Menezes, A.; Cesta, M. F.; Bermudez, E.; Bonner, J. C., Single-walled carbon nanotube (SWCNT)-induced interstitial fibrosis in the lungs of rats is associated with increased levels of PDGF mRNA and the formation of unique intercellular carbon structures that bridge alveolar macrophages in situ. Part Fibre Toxicol 2006, 3, 15.

10. Shvedova, A. A.; Kisin, E. R.; Mercer, R.; Murray, A. R.; Johnson, V. J.; Potapovich, A. I.; Tyurina, Y. Y.; Gorelik, O.; Arepalli, S.; Schwegler-Berry, D.; Hubbs, A. F.; Antonini, J.; Evans, D. E.; Ku, B. K.; Ramsey, D.; Maynard, A.; Kagan, V. E.; Castranova, V.; Baron, P., Unusual inflammatory and fibrogenic pulmonary responses to single-walled carbon nanotubes in mice. Am J Physiol Lung Cell Mol Physiol 2005, 289 (5), L698-708. DOI: 10.1152/ajplung.00084.2005.

11. R. Bailey, M.; Ansoborlo, E.; A. Guilmette, R.; Paquet, F., Practical application of the ICRP human respiratory tract model. Radiation Protection Dosimetry 2003, 105 (1-4), 71-76. DOI: 10.1093/oxfordjournals.rpd.a006324.

12. Heyder, J., Deposition of inhaled particles in the human respiratory tract and consequences for regional targeting in respiratory drug delivery. Proc Am Thorac Soc 2004, 1 (4), 315-20. DOI: 10.1513/pats.200409-046TA.

13. Renwick, L. C.; Donaldson, K.; Clouter, A., Impairment of alveolar macrophage phagocytosis by ultrafine particles. Toxicol Appl Pharmacol 2001, 172 (2), 119-27. DOI: 10.1006/taap.2001.9128.

14. Lucarelli, M.; Gatti, A. M.; Savarino, G.; Quattroni, P.; Martinelli, L.; Monari, E.; Boraschi, D., Innate defence functions of macrophages can be biased by nano-sized ceramic and metallic particles. Eur Cytokine Netw 2004, 15 (4), 339-46.

15. Oberdörster, G.; Ferin, J.; Lehnert, B. E., Correlation between particle size, in vivo particle persistence, and lung injury. Environmental Health Perspectives 1994, 102 (suppl 5), 173-179. DOI: 10.1289/ehp.102-1567252.

16. Berry, C. C.; Dalby, M. J.; McCloy, D.; Affrossman, S., The fibroblast response to tubes exhibiting internal nanotopography. Biomaterials 2005, 26 (24), 4985-4992. DOI: 10.1016/j.biomaterials.2005.01.046.

17. Hart, G. A.; Hesterberg, T. W., In vitro toxicity of respirable-size particles of diatomaceous earth and crystalline silica compared with asbestos and titanium dioxide. J Occup Environ Med 1998, 40 (1), 29-42. DOI: 10.1097/00043764-199801000-00008.
18. Poland, C. A.; Duffin, R.; Kinloch, I.; Maynard, A.; Wallace, W. A.; Seaton, A.; Stone, V.; Brown, S.; Macnee, W.; Donaldson, K., Carbon nanotubes introduced into the abdominal cavity of mice show asbestos-like pathogenicity in a pilot study. Nat Nanotechnol 2008, 3 (7), 423-8. DOI: 10.1038/nnano.2008.111.
19. Kostarelos, K., The long and short of carbon nanotube toxicity. Nature Biotechnology 2008, 26 (7), 774-776. DOI: 10.1038/nbt0708-774.
20. Takagi, A.; Hirose, A.; Nishimura, T.; Fukumori, N.; Ogata, A.; Ohashi, N.; Kitajima, S.; Kanno, J., Induction of mesothelioma in p53+/- mouse by intraperitoneal application of multi-wall carbon nanotube. J Toxicol Sci 2008, 33 (1), 105-16. DOI: 10.2131/jts.33.105.
21. Mossman, B. T.; Bignon, J.; Corn, M.; Seaton, A.; Gee, J. B., Asbestos: scientific developments and implications for public policy. Science 1990, 247 (4940), 294-301. DOI: 10.1126/science.2153315.
22. Belyanskaya, L.; Manser, P.; Spohn, P.; Bruinink, A.; Wick, P., The reliability and limits of the MTT reduction assay for carbon nanotubes–cell interaction. Carbon 2007, 45, 2643-2648. DOI: 10.1016/j.carbon.2007.08.010.
23. Powell, M. C.; Griffin, M. P.; Tai, S., Bottom-up risk regulation? How nanotechnology risk knowledge gaps challenge federal and state environmental agencies. Environ Manage 2008, 42 (3), 426-43. DOI: 10.1007/s00267-008-9129-z.

Chapter 4 – Nanowires: an overview

4.1 Overview on nanowires

The interesting properties and performances showed by nanomaterials if compared to the equivalent bulk led to the rapid development of new materials and growth methods. Nanostructured materials, nanowires (NWs) in particular, are very stimulating for the fabrication and the design of nanosized devices. This new field of study crosses many fields, from nanoelectronics and nanophotonic to medical devices, in order to obtain better performances.

As described in the previous chapter, nanowires are structures with two dimensions in the nanometer range and the length in the micron range; usually the ratio length/width is greater than 1000.

NWs growth arose in the late 60's, when Wagner employed the Vapor-Liquid-Solid (VLS) method to create microwires with a 0,1μm diameter; the obtained whiskers were the first evidence of the real possibility to scale the dimensions of semiconductors at the submicronscale[1]. Continuous advancement in research allowed in 1998 to Morales and coworkers to grew the first single-crystalline silicon and germanium nanowires with the VLS method, making it the most precise NWs synthesis technique[2].

The peculiarities of NWs are radically different from those of the massive form, for example the already mentioned high surface to volume ratio, due to the quantum confinement effect that render nanowires optimal candidates for the more varied applications (e.g. nano-sensors, nano-probes) for biomedical applications[3, 4].

4.2 VLS growth and CVD technique

Nanowires, as the other nanostructures, can be produced with two totally different approaches: the "top-down" and the "bottom-up" techniques.

- Top-down approach

The top-down approach is based on micro-fabrication standard methods, consisting in the application of deposition and subsequently etching of a planar substrate in order to reduce the object dimension until the nanosize is reached. Working in subtractive fashion, NWs can be synthetized by etching out crystal planes from

the substrate[5]. The most attractive advantage of top-down technique is its capability of forming randomly ordered shapes of nanostructure and the possibility to adopt the technologies already in use in the semi-conductor's manufactory. Moreover, top-down fabrication methods allow to maintain during the process all the chemical-physical characteristics of the starting material. The disadvantages are represented by the elevated costs and long times of production, the dimensional limitations due to the dimension of the nanostructure or of the massive sample to treat.

Examples of predominant top-down techniques are photolithography, focussed ion beam, nanoimprinting lithography, optical and electronic lithography.

- Bottom-up technique

The milestone in man's ability to build things is the ability to build things using individual atoms as the building blocks, to build things from the bottom up, by placing atoms where we want them. Bottom-up has been defined also as a sort of natural auto-organization method, because, during the process the auto-organization of the basic components (atoms and molecules) of a nanostructure is induced.

This technique assembles the final structure by adding sub-components to the substrate; nanostructures are synthetized by stacking atoms onto each other, producing new crystal planes. Subsequently, as occurred for atoms, crystal planet stack onto each other results in the synthesis of nanostructures. Generally, the idea is to control the assembly of atoms and molecules taking advantage of the molecular recognition to create the final structure principally with chemical processes. The advantages of the bottom-up technique are that allows the production of an unlimited number of nanomaterials not existing in nature, with different properties if compared to the crystal material with the same chemical composition existing in nature and consents to obtain chemically homogeneous structures almost free from structural defects.

The most studied techniques for the bottom-up approach are generally defined as epitaxy, namely the deposition of thin layer of crystal matter on a massive crystal substrate, defining both the growth and the structural properties. They include the Vapor-Liquid-Solid (VLS) process, the chemical vapor deposition (CVD), the laser ablation and molecular beam epitaxy (MBE) and the atomic layer deposition (ALD).

Figure 4.1 resumes the different approach to nanomaterial synthesis.

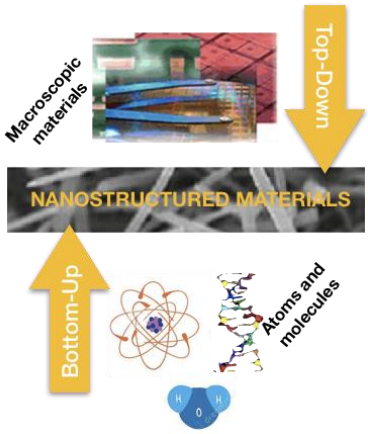

Figure 4.1: Scheme of the Top-down and Bottom-up processes.

After Morales et al. experiment the process was applied to more controllable methods, such as chemical vapour deposition with Vapor-Liquid-Solid, that become the dominant option for their growth due to its simple realization, flexible and excellent control of many aspects of the synthesis process.

4.2.1 Vapor-Liquid-Solid process

The VLS process is one of the most widely bottom-up growth techniques. The name derives from the nature of the three phases present in the growth interface.

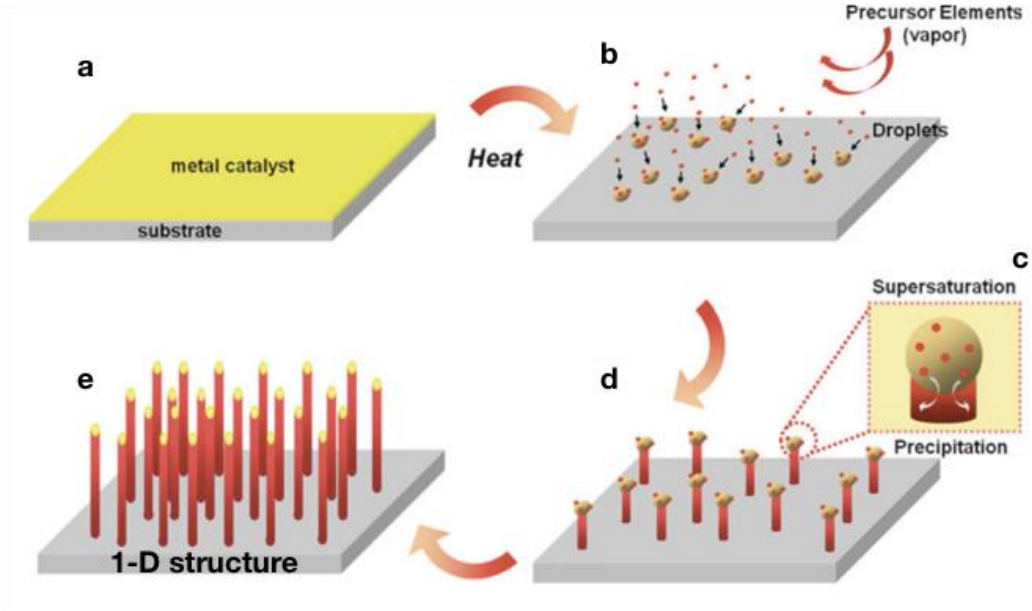

Figure 4.2: Growth of 1-D structures by VLS mechanism. a) deposition of a thin layer of catalyst on the growth substrate. b) Dewetting phase, the precursor elements allow the formation of the eutectic alloy droplets. c) Droplets supersaturation and material precipitation. d) Precipitation and nanowire growth. e) Final 1-D structure.

The typical VLS growth process involves the use of a metal catalyst (usually iron, gold or nickel) which is deposed on the substrate surface (usually a semi-conductor as silicon), creating a thin metal layer (Figure 4.2 a). During the growth, the system (catalyst and substrate) is heated over the eutectic temperature and leads to the formation of a liquid eutectic alloy between catalyst and the material of the substrate. Subsequently, the phenomenon called "dewetting" takes place and the liquid-alloy aggregates form droplets on the substrate surface, due to its surface tension (Figure 4.2b).

In this context, is fundamental the presence of semiconductor source material acting as precursor elements in the vapor phase, because it consents to the eutectic alloy to continue to incorporate material through the vapor/liquid interface, resulting in a short time in the supersaturation of the semi-conductor in the eutectic alloy. At the moment of supersaturation, inside each droplet the concentration of the material become higher than the equilibrium point and further addition of semiconductor source material will eventually result in a nucleation, otherwise a precipitation of the material creating a liquid-solid growth interface (Figure 4.2c-d). Nanowires growth is thus achieved through the continuous transfer of semi-conductor material from the vapor source into the eutectic resulting in the addition of solid at the liquid-solid interface, ending in a final solid crystal stage[1].

During this process, the metal catalyst remains on the tip of nanowires, while this elongates from below (Figure 4.2 e). At the end of the process the nanowire diameter in proportional to the size of the initial catalyst drop and its length is determined by many factors (time of growth, precursor element rate flow, impurity in the droplets etc.).

Summarizing, in VLS process three phases (vapour, liquid, and solid) and two interfaces (vapor/solid and liquid/solid) are involved. As schematized in Figure 4.3 (a-b-c), the VLS mechanism consists of three steps:

1- Metal-substrate liquid alloy droplets formation
2- Gaseous precursors decomposition at the vapor-liquid interface and diffusion through the alloy droplets
3- Nucleation at the growth interface: the NWs growth occurs between the solid phase and the liquid phase, along a single direction.

Figure 4.3 d shows GaN nanowires grown with VLS method.

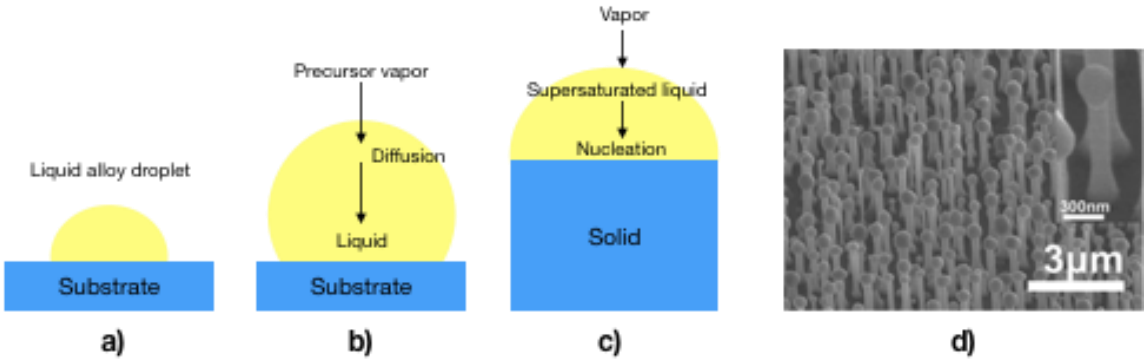

Figure 4.3: a-b-c) Microscopical illustration of kinetic steps in VLS mechanism. d) Vertical growth of GaN nanowires on GaN film deposited sapphire substrate by establishing homoepitaxial relationship between nanowires and substrate. The growth direction of nanowires is same as the orientation of substrate.

In a VLS process the role of metal is double. First, the metal catalyst allows, during the dewetting phase, the formation of the droplets of eutectic metal-substrate alloy, represented in Figure 4.4.

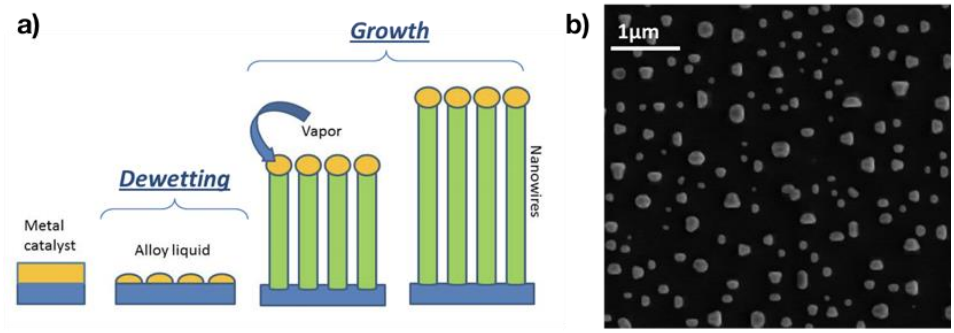

Figure 4.4: a) Schematic representation of VLS process. b) Typical SEM image of dewetting phase.

Moreover, as shown in Figure 4.5, the eutectic temperature is much lower than the melting temperature of its single compounds, reason why nanowires with VLS growth can be carried out at low temperature.

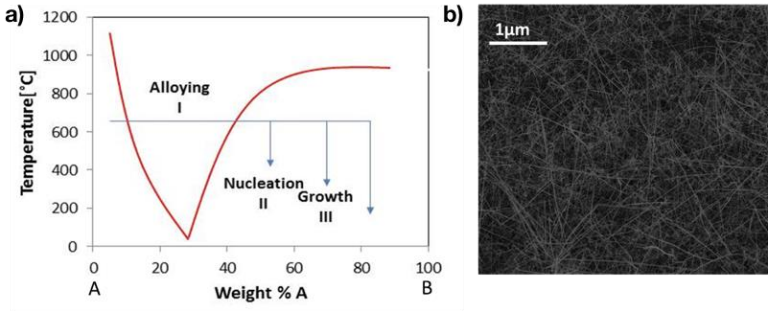

Figure 4.5: a) Binary phase diagram for metal substrate, the red line indicates a typical growth temperature. b) Typical SEM image of NWs.

Secondly, the metal assists both diffusion and incorporation of the species from gaseous precursors, promoting the nucleation and allowing to obtain nanowires with a fixed elemental composition and uniform growth over the whole substrate. Nowadays, VLS is the process of election to create different type of NWs, especially elemental semiconductors (Si, Ge, B)[6], III-V semiconductors (GaN, GaAs, GaP, InP, InAs)[7-9], II-VI semiconductors (ZnS, ZnSe, CdS, CdSe)[10, 11] and metal oxides (ZnO, MgO, CdO, TiO_2, SnO_2, In_2O_3, Ga_2O_3)[12, 13].

4.2.2 Chemical vapor deposition technique

Another process to obtain semiconductors nanowires is the chemical vapor deposition (CVD); the name obviously suggests the phase of the precursor supplied for the reaction (for example, in the case of silicon, it can be silane (SiH_4) or silicon tetrachloride ($SiCl_4$) as silicon source)[14].

The CVD technique is a synthesis process that allows the precursor deposition on a solid substrate. As it occurs in VLS, the precursor is supplied in a gaseous form through a carrier inert gas (hydrogen, nitrogen or argon). The precursor flow into the reactor and once it reacts with the substrate surface it decomposes in its constituent, allowing the binding of silicon with the substrate and the consequently nanowire growth.

The NWs growth velocity is variable due to temperature and silicon precursor used, but generally, through CVD technique, it is variable from 10^{-2} to 10^{3} nm/min; moreover, it consents the epitaxial growth of silicon NWs. CVD has been widely studied and a variety of techniques are available.

4.3 Silicon carbide-based nanomaterials

Silicon carbide (SiC), seems to be the election material for biomedical, environmental and engineering applications, due to its robustness, hardness and resistance to high temperature. SiC is composed of silicon and carbon and it is mostly synthetized industrially through various processes. SiC has shown thermal conductivity, high temperature resistance and electrical properties far superior to those of conventional semiconductors. Single-crystal silicon carbide presents a high Young's modulus (370GPa), excellent hardness (9 on the Mhos scale), low friction coefficient (0,17) and high resistance to acid and basic chemical attack, wear and corrosion that suggests a material resistance in harsh environments such as body fluids[15, 16]. These features, together with low thermal expansion coefficient, low weight and transparency to visible light, elevate SiC as an optimal biomaterial to be used in a wide variety of cutting-edge applications, varying from smart medical implants to environmental biosensors. Moreover, in biomedical applications, it could be the platform of choice to investigate cell response

to semiconductors. Obviously, in this field is fundamental the capability of the material to directly interfacing cells and its biocompatibility, in order to be integrated in living tissue. In this regards, SiC has been seen as safe in contact with blood and useful as barrier for protein adhesion in cardiovascular field including uses[17].

Chemically, SiC is a material formed by the covalent bond of Si and C atoms, typically in biatomic layers, whose form creates tetrahedrally oriented molecules of Si-C characterized by a very short bond length, but a high strength, thus originating the extreme stability of the material. SiC can be formed in amorphous, polycrystalline and monocrystalline solid. The presence of this high bond strength entails that its synthesis normally requires temperatures over 1000°C. One of the important characteristics of SiC is that the bilayers of Si and C can be stacked one upon the other in different crystal orientations: cubic, hexagonal, and rhombohedral. With more than 200 known polytypes reported in the literature, the three technologically relevant forms are one purely cubic form (β-SiC) and two hexagonal forms that actually have some cubic symmetry (α-SiC). The cubic form has the designation 3C-SiC, where the "3" delineates that 3 bilayers of Si-C are needed to form the basic structure and the "C" indicates that the crystal form is cubic. The hexagonal forms are 4H-SiC and 6H-SiC, where the "4" and "6" delineate that 4 and 6 bilayers are needed, while the "H" indicates that the crystal form is hexagonal.

While interesting in their own right, these various forms of SiC actually have different applications.

Silicon-based nanowires actually have a wide range of applications in biomedical field, where they are the key of nanowire-based biosensors able to afford: cancer diagnostics[18], microRNAs detection[19, 20], troponin T detection in cardiovascular diseases and cardiac biomarkers in serum[21] , proteins analysis from blood[22] and infectious diseases revelation[23].

Our interest is for the cubic phase because it can be grown on a silicon substrate, which has a cubic structure although with different lattice parameter. In this thesis SiC will only refers to the cubic phase; in the next chapters different kind of nanowires based on silicon carbide and their structural functionalization will be analyzed.

4.4 Titanium-based nanomaterials

Titanium is one of the materials of election for replacing hard tissues that incur heavy loads, such as the bone and teeth due to its unique combination of strength and biocompatibility. In particular, titanium alloys are being widely developed for medical application because of the possibility to modify titanium natural properties leading to a material with peculiar lightness, strength, corrosion resistance, and biocompatibility. From the late 60's titanium covers the vast majority of dental implants owing to its excellent bone bonding capacity, biocompatibility, and clinical success of osteointegration[24].

The mechanical properties of titanium are significantly altered by the presence of trace amounts of impurities such as oxygen, carbon, and nitrogen; generally, titanium used for surgical implants is classified into four grades depending on the quantity of impurities, and mechanical properties. Its extensive applications for biomedical devices and dental or orthopedic implants are conferred to its low corrosion rate, due to its high reactivity in contact with oxygen, resulting in the formation of an oxide protective layer on the surface with high adherence. Normally, after the implant in the human body, oxygen atoms react with titanium atoms creating a 3-6nm of thickness TiO_2 layer. The thickness of the layer depends on many environmental conditions, as its composition; generally, it is formed by TiO_2, TiO_3 or TiO, but the first is the more stable and the most common on endosseous implant surfaces. Titanium dioxide (TiO_2) is known for its excellent stability and physical-chemical properties; its crystal structure exhibit four different symmetries typical of the four titanium polymorphisms: rutile, anatase, brookite and TiO_2-B.

Titanium surface characteristics are not only linked to the dioxide layer, but also to the microtopography, the charge distribution and chemistry of the material.

Titanium implant surfaces presents different morphologies, due to the manufacturing processes. It has been seen that the mechanical stability of the implant and its anchorage is determined by the geometry of the topography and by the interaction between implant surface and tissue; the micro rugosity of titanium is directly related with cellular response to the biomaterial, with the molecular events implicated and with new osteogenesis[24]. Increasingly studies shifted from the microtopography of the material to the nanotopography, due to its ability to stimulate osteoblasts maturation and subsequently bone formation.

Titanium is largely used for orthopedic and dental implants because it is biologically stable and inert and due to the direct contact built between the implant surface and the bone tissue. In fact, implant surface characteristics modulate differentiation and cell behavior; titanium should enhance the cellular differentiation in order to allow the new osteogenesis. The development of an osteoinductive surface is fundamental to reach tissue regeneration and it is possible through the production of scaffolds with porous structure able to ameliorate the biological anchorage for the bone. A key factor in the rapid osteointegration of an implant is the rapid formation of hydroxyapatite at the surface and the subsequently deposition of new bone. It has been seen that bone regeneration can be strongly influenced in presence of a nanostructured surface if compared to the flat TiO_2 surface[25, 26].

Titanium-based nanostructures (nanowires, nanotubes, etc.) are already in use in dental clinic daily experience since they have been used to improve the mechanical properties of certain polymeric materials as resin

composites[27, 28], flowable resin composites[29], orthodontic resin cement[30] and glass ionomer cements[31], creating an effective functional material due to the unique properties nanosized TiO_2 can provide.

The creation of a substrate of titanium with a NWs surfaces may present many advantages in terms of bone integration and regeneration due to its unique physical-chemical properties and its high reactivity; in chapter 9 of this thesis dioxide titanium nanowires and their effect on biological environment will be analyzed.

4.5 Nanowires in nanomedicine: the biocompatibility

Nanotechnology opened a new way for investigation and development of nanomaterials and devices with unique properties for many fields, include nanomedicine, but these new properties may cause toxicological events that have not been yet properly studied and whose possible long-term impact must be analyzed.

The idea to tailor material properties to clinical needs allowed the design of devices and system useful in health care applications. First, every innovative biomaterial which encountered animal or human cells and tissues needs the fundamental characteristic to be cytocompatible and, to maximize the treatment efficacy, it should be internalized into the targeted cell. To investigate the main risks bounded to this new branch of medicine, many tools have been developed and adapted to allow the standardization of tests for nanomaterials interaction with body structure as biological barriers.

The safety evaluation of nanostructures, and in particular NWs, cytotoxicity is a crucial step for their transition from potential to effective materials for the development of biomedical tools and requires considerably more attention to fill in the current knowledge gap[32].

Among 1-D nanostructures cytotoxicity results are very contradictory and highlight the variability due to dimensions, surface properties, bio-durability, dose and exposure time. In fact, it has been seen that some classes of materials, as crystalline oxide nanowires (ZnO[33], Tio_2[34]) are cytostatic or induce cell death, while other as metal nanowires (gold[35], iron[36], silver[37], nickel[38]) are essentially cytocompatible, the most of the time in a dose-dependent manner.

Unless there are several studies demonstrating that nanomaterials size does not influence the toxicological outcome, in general, inhalation studies showed that penetration of nanoparticles deep in the respiratory tract can cause great inflammatory response, often associated with toxicity due to cellular internalization[39-41]. Nanomaterial internalization by cells can occur in different ways, the most prominent of which is diffusion across the plasma membrane, that can take place directly across the membrane or through membrane channels (10-30nm). The

alternative to diffusion across the plasma membrane is endocytosis, an energy depending mechanism that can occur in many different ways and that is normally the way in of the major part of nanoscale macromolecules and molecular assemblies through the enclosing in membrane vesicles. When a material binds to the receptors on plasma membrane, it facilitates receptor-mediated endocytosis, instead, it can activate clathrin-mediated endocytosis or caveolae-mediated endocytosis, resulting in the production of pits of 80-120nm on the membrane, regulating the dimensions of the material they are able to incorporate[42]. These endocytosed nanomaterials are confined in little vesicles called endolysosomes that prevent nanomaterials to reach the cytosol. The endocytic fate of nanomaterials has been already described in literature, for example it has been seen that 3-4nm gold nanoparticles 24 hours after internalizations were found in lysosomal bodies in perinuclear region[43]. The same has been seen for iron oxide nanoparticles[44, 45], fullerenes[46] and silicon-based nanowires[47]. Qualitative observation showed that in most cases nanomaterials are contained within vesicular structure and cannot breach cell membrane barrier, but the kinetics, amount and mechanism of up-take depend on a number of factors such as purity of the material, nanomaterial-cells incubation conditions, cell treatment, type if cell and type of nanomaterial. Moreover, the internalization process creates pores in the cell membrane that possibly lead to the disruption of the delicate osmotic balance between intra and extracellular environment concerning ions, protein and macromolecule, and subsequently toxicity.

Nevertheless, for many biomedical applications is fundamental to allow the effect of the material to penetrate the cell membrane and to enter in the nucleus; the localization of the englobed materials plays a pivotal role in some applications as photodynamic therapy or intracellular imaging.

Nanomaterials shape can highly change the rate of internalization; for example, spherical nanoparticle has a better chance to be internalized than nanowires, the uptake of nanorods is strongly influenced by their dimensions. Moreover, as a particle decreases in size, the exposed area enhances and the surface free for chemical reactions and catalytic activity is higher, leading to a major reaction potential due to the surface atoms which tend to have unsatisfied high energy bonds[32]. In the case that these nanomaterials can penetrate cell membrane, they have a much greater chance to interact with biomolecules (causing direct damage and enhancing oxidative stress) if compared to the same microsized materials.

Another important aspect is the purity of the nanomaterial; residual contaminating materials, especially metals, may be responsible of genotoxic responses, maybe more than the nanomaterial itself.

The agglomeration of nanomaterials is not under estimable, because they have the tendency to agglomerate if hydrophobic, in particular under physiological conditions. Agglomeration will dramatically increase the material dimension and the surface area of the original structure. Various methods are being used to enhance

hydrophilicity of nanomaterials through the use of surfactants or chemical modification (functionalization) of their surfaces and as a result, the genotoxic responses are also altered[32].

All these parameters are of vital importance in studying cellular up-take of nanomaterials; hydrophilicity/hydrophobicity, dimension and charge of the particle surface are essential because they alter the dispersion of the material in the experimental medium, influencing proteins adsorption on the surface and changing the internalization.

In this regard, International Organization for Standardization (ISO), a worldwide federation of national standards, emanates a guideline for the biological *in vitro* evaluation of medical devices. In particular, ISO 10993 part 5 is related to *in vitro* preliminary analysis for the cytotoxicity of materials for biomedical applications. These methods specify the incubation of cultured cells in contact with a device and/or extracts of a device either directly or through diffusion; these guidelines are designed to determine the biological response of mammalian and/or fibroblast cells *in vitro* using appropriate biological parameters. As stated in ISO 10993-5 guidelines "an important quality issue of materials for medical devices having direct or indirect contact with the body tissue is the biocompatibility". Any biomaterial promising for *in vivo* implanting has to be analyzed for biocompatibility evaluation with specific *in vitro* tests, starting from cytotoxicity tests, as recommended by American Society for Quality Control.

Given the lack of literature about silicon-based and titanium-based nanowires, in this thesis we will show *in vitro* preliminary results about these kinds of NWs.

References

1. Wagner, R. S.; Ellis, W. C., VAPOR-LIQUID-SOLID MECHANISM OF SINGLE CRYSTAL GROWTH. Applied Physics Letters 1964, 4 (5), 89-90. DOI: 10.1063/1.1753975.

2. Morales, A. M.; Lieber, C. M., A laser ablation method for the synthesis of crystalline semiconductor nanowires. Science 1998, 279 (5348), 208-11. DOI: 10.1126/science.279.5348.208.

3. Viguier, B.; Zor, K.; Kasotakis, E.; Mitraki, A.; Clausen, C. H.; Svendsen, W. E.; Castillo-Leon, J., Development of an electrochemical metal-ion biosensor using self-assembled peptide nanofibrils. ACS Appl Mater Interfaces 2011, 3 (5), 1594-600. DOI: 10.1021/am200149h.

4. Tian, B.; Lieber, C. M., Design, synthesis, and characterization of novel nanowire structures for photovoltaics and intracellular probes. Pure Appl Chem 2011, 83 (12), 2153-2169. DOI: 10.1351/pac-con-11-08-25.

5. Tong, H. D.; Chen, S.; van der Wiel, W. G.; Carlen, E. T.; van den Berg, A., Novel top-down wafer-scale fabrication of single crystal silicon nanowires. Nano Lett 2009, 9 (3), 1015-22. DOI: 10.1021/nl803181x.

6. Westwater, J.; Gosain, D. P.; Tomiya, S.; Usui, S.; Ruda, H., Growth of silicon nanowires via gold/silane vapor–liquid–solid reaction. Journal of Vacuum Science & Technology B: Microelectronics and Nanometer Structures Processing, Measurement, and Phenomena 1997, 15 (3), 554-557. DOI: 10.1116/1.589291.

7. S, B.; T, K.; Y, W.; S, F.; K, T., Metalorganic vapor-phase epitaxial growth and characterization of vertical InP nanowires Appl. Phys. Lett. 83 3371 2003.

8. Bao, X. Y.; Soci, C.; Susac, D.; Bratvold, J.; Aplin, D. P.; Wei, W.; Chen, C. Y.; Dayeh, S. A.; Kavanagh, K. L.; Wang, D., Heteroepitaxial growth of vertical GaAs nanowires on Si(111) substrates by metal-organic chemical vapor deposition. Nano Lett 2008, 8 (11), 3755-60. DOI: 10.1021/nl802062y.

9. Lin H-M; Chen Y-L; Yang J; Liu Y-C; Yin K-M; Kai J-J; Chen F-R; Chen L-C, C. Y.-F. C. C.-C., Synthesis and Characterization of Core–Shell GaP@GaN and GaN@GaP Nanowires. Nano Letters, 2003; Vol. 3, pp 537–41.

10. Barrelet, C. J.; Wu, Y.; Bell, D. C.; Lieber, C. M., Synthesis of CdS and ZnS nanowires using single-source molecular precursors. J Am Chem Soc 2003, 125 (38), 11498-9. DOI: 10.1021/ja036990g.

11. T, Z. X.; Z, L.; P, L. Y.; Q, L.; K, H. S., Growth and luminescence of zinc-blende-structured ZnSe nanowires by metalorganic chemical vapor deposition Appl. Phys. Lett. 83 5533 2003.

12. Park, H.-K.; Yang, B.; Kim, S.-W.; Kim, G.-H.; Youn, D.-H.; Kim, S.-H.; Maeng, S.-L., Formation of silicon oxide nanowires directly from Au/Si and Pd–Au/Si substrates. Phys. E Low-dimensional Syst. Nanostructures 37 158–62 2007.

13. G, C. P.-C. F. Z. D. W.-Y. W.-A. J. J., ZnO Nanowires Synthesized by Vapor Trapping CVD Method. Chem. Mater. 16 5133–7, 2004.

14. Kodambaka, S.; Tersoff, J.; Reuter, M. C.; Ross, F. M., Diameter-Independent Kinetics in the Vapor-Liquid-Solid Growth of Si Nanowires. Physical Review Letters 2006, 96 (9), 096105. DOI: 10.1103/PhysRevLett.96.096105.

15. Monnink S H, v. B. A. J., Peels H O, Tigchelaar I, de Kam P J, Crijns H J van Oeveren W, Silicon-carbide coated coronary stents have low platelet and leukocyte adhesion during platelet activation. . J. Investig. Med. 47 304–10, 1999.

16. Li X, W. X., Bondokov R, Morris J, An Y H and Sudarshan T S, Micro/nanoscale mechanical and tribological characterization of SiC for orthopedic applications. . J. Biomed. Mater. Res. B. Appl. Biomater. 72 353–61, 2005.

17. Bolz, A.; Schaldach, M., Artificial heart valves: improved blood compatibility by PECVD a-SiC:H coating. Artif Organs 1990, 14 (4), 260-9.

18. Zheng, G.; Patolsky, F.; Cui, Y.; Wang, W. U.; Lieber, C. M., Multiplexed electrical detection of cancer markers with nanowire sensor arrays. Nat Biotechnol 2005, 23 (10), 1294-301. DOI: 10.1038/nbt1138.

19. Cattani-Scholz, A.; Pedone, D.; Dubey, M.; Neppl, S.; Nickel, B.; Feulner, P.; Schwartz, J.; Abstreiter, G.; Tornow, M., Organophosphonate-based PNA-functionalization of silicon nanowires for label-free DNA detection. ACS Nano 2008, 2 (8), 1653-60. DOI: 10.1021/nn800136e.

20. Calin, G. A.; Croce, C. M., MicroRNA-cancer connection: the beginning of a new tale. Cancer Res 2006, 66 (15), 7390-4. DOI: 10.1158/0008-5472.can-06-0800.

21. Chua, J. H.; Chee, R. E.; Agarwal, A.; Wong, S. M.; Zhang, G. J., Label-free electrical detection of cardiac biomarker with complementary metal-oxide semiconductor-compatible silicon nanowire sensor arrays. Anal Chem 2009, 81 (15), 6266-71. DOI: 10.1021/ac901157x.

22. Shajaripour Jaberi, S. Y.; Ghaffarinejad, A.; Omidinia, E., An electrochemical paper based nano-genosensor modified with reduced graphene oxide-gold nanostructure for determination of glycated hemoglobin in blood. Anal Chim Acta 2019, 1078, 42-52. DOI: 10.1016/j.aca.2019.06.018.

23. Huang, M. J.; Xie, H.; Wan, Q.; Zhang, L.; Ning, Y.; Zhang, G. J., Serotype-specific identification of Dengue virus by silicon nanowire array biosensor. J Nanosci Nanotechnol 2013, 13 (6), 3810-7.

24. Buser, D.; Broggini, N.; Wieland, M.; Schenk, R. K.; Denzer, A. J.; Cochran, D. L.; Hoffmann, B.; Lussi, A.; Steinemann, S. G., Enhanced Bone Apposition to a Chemically Modified SLA Titanium Surface. Journal of Dental Research 2004, 83 (7), 529-533. DOI: 10.1177/154405910408300704.

25. Tsuchiya, H.; Macak, J. M.; Muller, L.; Kunze, J.; Muller, F.; Greil, P.; Virtanen, S.; Schmuki, P., Hydroxyapatite growth on anodic TiO2 nanotubes. J Biomed Mater Res A 2006, 77 (3), 534-41. DOI: 10.1002/jbm.a.30677.

26. Oh, S. H.; Finones, R. R.; Daraio, C.; Chen, L. H.; Jin, S., Growth of nano-scale hydroxyapatite using chemically treated titanium oxide nanotubes. Biomaterials 2005, 26 (24), 4938-43. DOI: 10.1016/j.biomaterials.2005.01.048.

27. Xia, Y.; Zhang, F.; Xie, H.; Gu, N., Nanoparticle-reinforced resin-based dental composites. J Dent 2008, 36 (6), 450-5. DOI: 10.1016/j.jdent.2008.03.001.

28. Sun, J.; Forster, A. M.; Johnson, P. M.; Eidelman, N.; Quinn, G.; Schumacher, G.; Zhang, X.; Wu, W. L., Improving performance of dental resins by adding titanium dioxide nanoparticles. Dent Mater 2011, 27 (10), 972-82. DOI: 10.1016/j.dental.2011.06.003.

29. Dafar, M. O.; Grol, M. W.; Canham, P. B.; Dixon, S. J.; Rizkalla, A. S., Reinforcement of flowable dental composites with titanium dioxide nanotubes. Dent Mater 2016, 32 (6), 817-26. DOI: 10.1016/j.dental.2016.03.022.

30. Poosti, M.; Ramazanzadeh, B.; Zebarjad, M.; Javadzadeh, P.; Naderinasab, M.; Shakeri, M. T., Shear bond strength and antibacterial effects of orthodontic composite containing TiO2 nanoparticles. Eur J Orthod 2013, 35 (5), 676-9. DOI: 10.1093/ejo/cjs073.

31. Elsaka, S. E.; Hamouda, I. M.; Swain, M. V., Titanium dioxide nanoparticles addition to a conventional glass-ionomer restorative: influence on physical and antibacterial properties. J Dent 2011, 39 (9), 589-98. DOI: 10.1016/j.jdent.2011.05.006.

32. Singh, N.; Manshian, B.; Jenkins, G. J.; Griffiths, S. M.; Williams, P. M.; Maffeis, T. G.; Wright, C. J.; Doak, S. H., NanoGenotoxicology: the DNA damaging potential of engineered nanomaterials. Biomaterials 2009, 30 (23-24), 3891-914. DOI: 10.1016/j.biomaterials.2009.04.009.

33. Wang, Z. L.; Song, J., Piezoelectric nanogenerators based on zinc oxide nanowire arrays. Science 2006, 312 (5771), 242-6. DOI: 10.1126/science.1124005.

34. Magrez, A.; Horvath, L.; Smajda, R.; Salicio, V.; Pasquier, N.; Forro, L.; Schwaller, B., Cellular toxicity of TiO2-based nanofilaments. ACS Nano 2009, 3 (8), 2274-80. DOI: 10.1021/nn9002067.

35. Shevach, M.; Fleischer, S.; Shapira, A.; Dvir, T., Gold nanoparticle-decellularized matrix hybrids for cardiac tissue engineering. Nano Lett 2014, 14 (10), 5792-6. DOI: 10.1021/nl502673m.

36. Song, M. M.; Song, W. J.; Bi, H.; Wang, J.; Wu, W. L.; Sun, J.; Yu, M., Cytotoxicity and cellular uptake of iron nanowires. Biomaterials 2010, 31 (7), 1509-17. DOI: 10.1016/j.biomaterials.2009.11.034.

37. Richter, A. P.; Brown, J. S.; Bharti, B.; Wang, A.; Gangwal, S.; Houck, K.; Cohen Hubal, E. A.; Paunov, V. N.; Stoyanov, S. D.; Velev, O. D., An environmentally benign antimicrobial nanoparticle based on a silver-infused lignin core. Nat Nanotechnol 2015, 10 (9), 817-23. DOI: 10.1038/nnano.2015.141.

38. Perez, J. E.; Contreras, M. F.; Vilanova, E.; Felix, L. P.; Margineanu, M. B.; Luongo, G.; Porter, A. E.; Dunlop, I. E.; Ravasi, T.; Kosel, J., Cytotoxicity and intracellular dissolution of nickel nanowires. Nanotoxicology 2016, 10 (7), 871-80. DOI: 10.3109/17435390.2015.1132343.

39. Geiser, M.; Rothen-Rutishauser, B.; Kapp, N.; Schurch, S.; Kreyling, W.; Schulz, H.; Semmler, M.; Im Hof, V.; Heyder, J.; Gehr, P., Ultrafine particles cross cellular membranes by nonphagocytic mechanisms in lungs and in cultured cells. Environ Health Perspect 2005, 113 (11), 1555-60. DOI: 10.1289/ehp.8006.

40. Baggs, R. B.; Ferin, J.; Oberdorster, G., Regression of pulmonary lesions produced by inhaled titanium dioxide in rats. Vet Pathol 1997, 34 (6), 592-7. DOI: 10.1177/030098589703400607.

41. Wang, B.; Feng, W. Y.; Wang, T. C.; Jia, G.; Wang, M.; Shi, J. W.; Zhang, F.; Zhao, Y. L.; Chai, Z. F., Acute toxicity of nano- and micro-scale zinc powder in healthy adult mice. Toxicol Lett 2006, 161 (2), 115-23. DOI: 10.1016/j.toxlet.2005.08.007.

42. Patel, L. N.; Zaro, J. L.; Shen, W. C., Cell penetrating peptides: intracellular pathways and pharmaceutical perspectives. Pharm Res 2007, 24 (11), 1977-92. DOI: 10.1007/s11095-007-9303-7.

43. Wayteck, L.; Dewitte, H.; De Backer, L.; Breckpot, K.; Demeester, J.; De Smedt, S. C.; Raemdonck, K., Hitchhiking nanoparticles: Reversible coupling of lipid-based nanoparticles to cytotoxic T lymphocytes. Biomaterials 2016, 77, 243-54. DOI: 10.1016/j.biomaterials.2015.11.016.

44. Li, T.; Murphy, S.; Kiselev, B.; Bakshi, K. S.; Zhang, J.; Eltahir, A.; Zhang, Y.; Chen, Y.; Zhu, J.; Davis, R. M.; Madsen, L. A.; Morris, J. R.; Karolyi, D. R.; LaConte, S. M.; Sheng, Z.; Dorn, H. C., Correction to "A New Interleukin-13 Amino-Coated Gadolinium Metallofullerene Nanoparticle for Targeted MRI Detection of Glioblastoma Tumor Cells". J Am Chem Soc 2016, 138 (5), 1723. DOI: 10.1021/jacs.6b00117.

45. Fernandes, R. S.; Mota, L. G.; Kalbasi, A.; Moghbel, M.; Werner, T. J.; Alavi, A.; Rubello, D.; Cardoso, V. N.; de Barros, A. L., 99mTc-phytate as a diagnostic probe for assessing inflammatory reaction in malignant tumors. Nucl Med Commun 2015, 36 (10), 1042-8. DOI: 10.1097/mnm.0000000000000358.

46. Zhao, X.; Chang, S.; Long, J.; Li, J.; Li, X.; Cao, Y., The toxicity of multi-walled carbon nanotubes (MWCNTs) to human endothelial cells: The influence of diameters of MWCNTs. Food Chem Toxicol 2019, 126, 169-177. DOI: 10.1016/j.fct.2019.02.026.

47. Cacchioli, A.; Ravanetti, F.; Alinovi, R.; Pinelli, S.; Rossi, F.; Negri, M.; Bedogni, E.; Campanini, M.; Galetti, M.; Goldoni, M.; Lagonegro, P.; Alfieri, R.; Bigi, F.; Salviati, G., Cytocompatibility and cellular internalization mechanisms of SiC/SiO2 nanowires. Nano Lett 2014, 14 (8), 4368-75. DOI: 10.1021/nl501255m.

Chapter 5 – Nanodentistry

Oral health care can be hauled as never before with the application of various nanomaterials (e.g. nanoparticles, quantum dots, nanorods, nanowires, etc.). Starting from the evidence that all the natural materials and systems establish their foundation at the nanoscale and that all the biological building blocks of life are nano-entities, it become obvious that nanotechnologies can be the turning point of medicine. Dentistry is a field particularly suitable for the use of nanodevices due to the easily reaching of the site of interest in patients' mouth, the short time of applications and the relative low costs. With the advent of nanotechnology and new materials obviously come new properties and new opportunities in many fields of everyday life; the two main properties at the basis of the use of nanomaterials are the increase in relative surface area and the quantum effect. The first is referred to the increase of the percentage of total atoms on the surface of the material (with increased reactivity of the material), while the second refers to the ability of size to influence the properties of matter, intended as optical, electrical and magnetic behaviour of materials.

The use of nanomaterials in dentistry and the growing interest for the future led to the emerging of a new field called nanodentistry. The advent of nanodestistry will allow to maintain a nearly perfect oral health through the use of different nanomaterials (e.g. nanorobots, nanorods, etc.) and the extension of their use in applications as local anesthesia, dentition renaturalization, permanent cure of hypersensitivity, orthodontics, enamel reconstruction and caries cure[1].

The following paragraphs will show some of the current applications of nanotechnology in dentistry.

5.1 Preventive nanodentistry

The main aim of dentistry is to prevent rather than treat diseases as caries or periodontal disease, caused by the presence of a bacterial biofilm formation. Dental caries is caused by the presence of bacteria in aggregates attached one to each other on tooth surface to form oral plaque and it is one of the most destructive diseases affecting oral structures. Assuming that the first fight against caries is to maintain an adequate oral hygiene, several nanoparticles have been incorporated into dental composites, to inhibit bacterial growth through the disruption of bacterial cell membrane, inhibition of sugar metabolism, generation of ROS, prevention of DNA replication or displacement of magnesium ions (normally required for the enzymatic activity of oral biofilm)[2-8].

Moreover, bacterial colony produces acids which cause the loss of calcium and phosphate, but this demineralizing action could be reversed promoting the remineralization of tooth, providing calcium and phosphorous ions from

an external source, in order to favor ions precipitations into the damaged dental structure and to furnish an anti-cariogenetic effect.

One of the newest applications is certainly to induce anesthesia with nanomaterials. The gingiva of the patients is instilled with a colloidal suspension containing millions of active, analgesic, micron-sized dental robots whose aim is to reach the pulp due to the different chemical gradient and temperature, through the gingiva sulcus, lamina propria and dentinal tubules, reaching to the control over nerve-impulse traffic in any tooth that requires treatment. The giant achievement of this application is the lack of use of needles, thereby providing patients, especially kids, with anxiety-free comfort[1, 9].

5.2 Diagnostic and therapeutic nanodentistry

Diagnostic of dental and oral conditions is still nowadays routinely undertaken in clinic using a set of guidelines which have not changed in the last decades. In the era of improving diagnostics, also nanomaterials for oral bio-sensing have been developed. The concept of biosensor is related to the use of a device which incorporates a fluid or an element and generates a measurable signal, proportional to the concentration of the desired analyte. Nano-diagnostic devices can be very useful in the diagnosis of the early stage of some diseases identifiable at molecular or cellular level, as it occurs with tumor cells or viruses infection[1, 10]. For example, in the case of oral cancer diagnosis, saliva is used as an inexpensive and noninvasively obtained diagnostic medium that contains proteomic and genomic markers for molecular disease identification. Nanobiosensor are also very practice in use, since they can afford to be placed and deformed in response to very low forces, being enough sensitive to feel the breaking of chemical bonds[11]. Moreover, nanomaterials can help in cancer management and treatment plan design, since standard clinical images obtained through computer tomography or magnetic resonance are exceptional in the definition of tumor location and size but are less reliable to distinguish between benign and cancerous metastasis (<5mm)[12, 13].

Even in oral diseases treatment nanotechnology presence is important, due to the use of nanomaterials as quantum dots or nanoshells covered with outer metallic layers to selectively destroy cancel cells, leaving untouched normal cells; other applications are the use of nanomaterials in photodynamic therapy and gene therapy. In cancer radiation therapy, nanomaterials have been used as radiosensitizer, causing cell death after gamma radiation; in cancer chemotherapy nanoparticles and nanodelivery vehicles are commonly used to improve both, the stability of the drug and the controlled drug delivery[14, 15]. In addition to cancer treatment,

nanoderlivery transbuccal system was developed to rapidly and efficiently deliver opioid analgesia at a consistent and controlled diffusion to more effectively manage the breakthrough pain cancer associated[16].

The prevention of biofilm-dependent oral diseases is another goal of nanotechnology use in dentistry, in fact, understanding the main factors of bacterial adhesion, colonization and pathogenesis, a lot of oral diseases may be defeat[5]. Through the use of atomic force microscope and nanomechanical biosensors, the two ways of bacterial adhesion to tooth surface or dental implants have been revealed, helping to understand the early phase of oral biofilm formation and pathogenesis of diseases.

Certainly, one of the most fascinating uses of nanotechnology on oral diagnostic is the development of microchips. Microchips are substrates able to perform many diagnostic tests simultaneously; in particular microelectronical systems able to perform saliva diagnostic and to identify or measure proteins, DNA, mRNA, electrolytes, small molecules or miRNA which are normally correlated with a profile of a particular disease (e.g. cardiovascular diseases, cancer, etc.)[17, 18]. Moreover, also diagnostic cytology-on-a-chip technique plays a pivotal role in the advancement of oral cancer early detection[19, 20].

Therapeutic nanodentistry has also a number of applications in the treatment of dentin hypersensitivity, root canal disinfection or tissue engineering. Dentin is normally protected by a layer of enamel in the crown or by cementum in the root; the exposure of dentinal tubules leads to alterations of the fluid pressure hydrodynamics of the fluids inside the dentinal tubules. This alteration is believed to be responsible for hypersensitivity, which can be treated with the use of nanoparticles that can be adsorbed on the inner dentinal tubules walls and can selectively and precisely occlude the tubules, reducing dentin sensitivity. Furthermore, nanorobots may provide a permanent cure for dentinal sensitivity occluding the tubules with biological material[1].

Nanoparticles as zinc oxide or chitosan have been incorporated into root canal scalers in attempt to disinfect root canals, resulting in an enhanced antibacterial action and a significant reduction of Enterococcus faecalis presence[21]. Metal oxides have also been used as root canal irrigants with longer antibacterial activity if compared to the classical NaOCl solution[22].

Nowadays, potential applications of TE in dentistry include the treatment of orofacial fractures, cartilage regeneration, pulp repair, periodontal ligament regeneration, bone augmentation and implant osseointegration; nanotechnologies play a pivotal role in TE development. For example, nanocrystalline hydroxyapatite could be used to ameliorate the properties of commonly used bone grafts, in order to stimulate the cell proliferation required for periodontal tissue regeneration.

Bio-nanointerfaces of clinical relevance

Normally, to restore the loss partially (as enamel or dentin) or completely of a toot, dental composite and implants are used and their retention is mainly obtained with micromechanical retention. This can underline the importance of resin composite-tooth interface and bone-implant interface for the success of the restoration. Nowadays nanotechnologies are of common use in the modification and stabilization of these interfaces, to increase the longevity of the treatment. The bond of dental composites and tooth generally occurs with different adhesive resin systems depending on separate etchant, primer and adhesive resin. The use of etchant, demineralize dentin, via hydroxyapatite crystal removal, but the polymerized adhesive resin aims to protect the exposed collagen from enzymatic degradation. The long-term success of resin composite depends on the integrity and durability of resin-dentin interface, that can be jeopardized by the incomplete penetration or polymerization of the monomers, the degradation of collagen matrix or the hydrolysis of the monomer. Once the interface integrity is compromised, a lot of nanoleakge may occur, with consequent pain, sensitivity and failure of the restoration. In this regard, nanotechnology product may be used to prevent nanoleakge and to enhance the longevity of resin-dentin bond (e.g. reinforcement of cross-linking of collagen and biomimetic remineralization, inhibition of MMPs action, modification of the resin monomer adhesion, etc.)[23, 24]. Some examples of nanomaterials used for ameliorating the interface resistance are: zirconia nanoparticles (20-50nm), hydroxyapatite nanoparticles (20-70nm), colloidal silica (5-40nm), barium aluminosilicate nanofillers (400nm) and reactive nanogels[25-28].

More or less the same importance of the resin-dentin interface is the one of the implant-tissue interface. Implant osseointegration is the main challenge to allow peri-implant healing process. Primary mechanical and secondly biological anchorage are the keys for the osseointegration, which involves also osteoconduction and de novo bone formation to provide contact osteogenesis. Moreover, the intimate contact between the neck of the implant and the gingival tissue if fundamental to avoid bacterial infiltration and attachment. Implant micro- and nano-topography obviously induce the direct contact between cells and implant; nanotechnology has been introduced to mediate bone formation and implant osseointegration[29]. Many methods (e.g. lithography, anodization, ion implantation, plasma treatments, etc.) have been used to control dental implant topography at the level of nanosurface features (e.g. nanotubules), since cell behaviour changes in function of the dimension and spaces between the nanostructured patterns. For example, a change in the diameter of nanotubes of about 50-60nm can cause the transition of cells from proliferative to differentiate; spacing of 58nm have been demonstrated to enhance the formation of focal adhesions, while higher density of nanostructures and distances of about 60nm instead of 120nm induce a higher bone-implant contact[30-33].

In Table 3.1 a list of the most used nanomaterials and their applications in dental field is presented.

Table 5.1: Nanomaterials commonly used in dentistry.

NANOMATERIALS	DENTAL APPLICATIONS
Silver nanoparticles	High antimicrobial activity due to their interaction with the lipid components of bacterial cell wall, especially in the regard of *Streptococcus mutans*, the main factor related to caries formation[34-37].
Nanosized calcium fluoride	Administered through a spray-drying system are very useful in the attempt to provide a labile fluoride reservoir to improve dental remineralization[38].
Carbonate hydroxyapatite crystals	Hydroxyapatite found common use in the filling of demineralized enamel and in providing a reservoir of calcium ions, or in the treatment of dentinal hypersensitivity [39-41].
Nanosized amorphous calcium phosphate particles	Encourage cell proliferation and tissue calcification, with a high degree of mineral complexes deposition to the lesioned surface[42, 43].
Casein phosphopeptide amorphous calcium phosphate nanocomplexes	Enhancers of enamel remineralization in a dose- and time-dependent manner[44, 45].
Nanoparticulate bioactive glass	Higher degree of antimicrobial activity due to the silica release and acts as nucleation site for calcium and phosphates, leading to a general reduction of mineral loss[46, 47].
Calcium carbonate nanoparticles	Calcium carbonate nanoparticles have been incorporated in an experimental dentifrice which allows the slow and continuous release of high concentrations of calcium ions into the surrounding oral fluids, acting as a delivery vehicle, resulting in an effective remineralization of early stage enamel lesions[39].
Gold nanoparticles	Gold nanoparticles have been developed as vehicles for the delivery of antimicrobial agents and to act as antifungal material[48].
Nano-toothbrush	Silver and gold colloidal nanoparticles have been incorporated inside toothbrush bristles to mechanically improve plaque removal and to enhance antibacterial effect with the final goal to reduce periodontal disease complications. Specifically, in an experimental periodontal model,

	the local application of nanostructured doxycycline gel prevented bone loss[49].
Carbon nanotubes	Teeth filling or coating of the tooth surface, due to its large surface area can easily adhere to the tooth, dentin or cementum surface and bringing active molecules[50, 51].
Graphene	Its high fracture resistance allows to perform teeth or implant coatings forming a uniform crystal lattice[52, 53].
Zirconia nanoparticles	Reduces bacterial adhesion to the tooth surface with a high fracture resistance[54, 55].
Silica nanoparticles	Development of homogeneous suspension of silica nanoparticles in nanofillers that enhance the mechanical properties and the remineralization of dentin[56].
Titanium dioxide nanoparticles	Improvement of antibacterial activity and mechanical properties in resins and restorative materials[57, 58].
Gold nanoparticles	Usually improve mechanical properties of dentin adhesive, they enhance bone formation and maintenance without showing cellular toxicity. Also used as contrast agents for imaging[59, 60].
Iron oxide nanoparticles	Prevent bacterial biofilm formation but their toxicity is size-dependent[61].
Copper oxide nanoparticles	The coating of dental implants with copper nanoparticles showed a lower degree of bacterial infiltration, due to the high antibacterial activity of copper[62, 63].
Chitosan nanoparticles	Improved cell response in presence of chitosan nanofibers, low cytotoxicity and controlled release of chlorhexidine[64, 65].
Zinc oxide nanoparticles	Zinc nanoparticles prevent the formation of bacterial colonies and of biofilm[66].
PLGA nanoparticles	Prevention of bacterial activity in root canal infections and possibility to incorporate drugs against specific kind of bacteria[67].

References

1. Freitas, R. A., Jr., Nanodentistry. J Am Dent Assoc 2000, 131 (11), 1559-65. DOI: 10.14219/jada.archive.2000.0084.

2. Gu, H.; Fan, D.; Gao, J.; Zou, W.; Peng, Z.; Zhao, Z.; Ling, J.; LeGeros, R. Z., Effect of ZnCl2 on plaque growth and biofilm vitality. Arch Oral Biol 2012, 57 (4), 369-75. DOI: 10.1016/j.archoralbio.2011.10.001.

3. Xie, Y.; He, Y.; Irwin, P. L.; Jin, T.; Shi, X., Antibacterial activity and mechanism of action of zinc oxide nanoparticles against Campylobacter jejuni. Appl Environ Microbiol 2011, 77 (7), 2325-31. DOI: 10.1128/aem.02149-10.

4. Kasraei, S.; Sami, L.; Hendi, S.; Alikhani, M. Y.; Rezaei-Soufi, L.; Khamverdi, Z., Antibacterial properties of composite resins incorporating silver and zinc oxide nanoparticles on Streptococcus mutans and Lactobacillus. Restor Dent Endod 2014, 39 (2), 109-14. DOI: 10.5395/rde.2014.39.2.109.

5. Chen, C.; Weir, M. D.; Cheng, L.; Lin, N. J.; Lin-Gibson, S.; Chow, L. C.; Zhou, X.; Xu, H. H., Antibacterial activity and ion release of bonding agent containing amorphous calcium phosphate nanoparticles. Dent Mater 2014, 30 (8), 891-901. DOI: 10.1016/j.dental.2014.05.025.

6. Foldbjerg, R.; Olesen, P.; Hougaard, M.; Dang, D. A.; Hoffmann, H. J.; Autrup, H., PVP-coated silver nanoparticles and silver ions induce reactive oxygen species, apoptosis and necrosis in THP-1 monocytes. Toxicol Lett 2009, 190 (2), 156-62. DOI: 10.1016/j.toxlet.2009.07.009.

7. Song, B.; Leff, L. G., Influence of magnesium ions on biofilm formation by Pseudomonas fluorescens. Microbiol Res 2006, 161 (4), 355-61. DOI: 10.1016/j.micres.2006.01.004.

8. Birla, S. S.; Tiwari, V. V.; Gade, A. K.; Ingle, A. P.; Yadav, A. P.; Rai, M. K., Fabrication of silver nanoparticles by Phoma glomerata and its combined effect against Escherichia coli, Pseudomonas aeruginosa and Staphylococcus aureus. Lett Appl Microbiol 2009, 48 (2), 173-9. DOI: 10.1111/j.1472-765X.2008.02510.x.

9. Saravana, K. R.; Vijayalakshmi, R., Nanotechnology in dentistry. Indian J Dent Res 2006, 17 (2), 62-5.

10. Ilic, B.; Yang, Y.; Craighead, H. G., Virus detection using nanoelectromechanical devices. Applied Physics Letters 2004, 85 (13), 2604-2606. DOI: 10.1063/1.1794378.

11. Burg, T. P.; Godin, M.; Knudsen, S. M.; Shen, W.; Carlson, G.; Foster, J. S.; Babcock, K.; Manalis, S. R., Weighing of biomolecules, single cells and single nanoparticles in fluid. Nature 2007, 446 (7139), 1066-1069. DOI: 10.1038/nature05741.

12. Popovtzer, R.; Agrawal, A.; Kotov, N. A.; Popovtzer, A.; Balter, J.; Carey, T. E.; Kopelman, R., Targeted gold nanoparticles enable molecular CT imaging of cancer. Nano Lett 2008, 8 (12), 4593-6.

13. Reuveni, T.; Motiei, M.; Romman, Z.; Popovtzer, A.; Popovtzer, R., Targeted gold nanoparticles enable molecular CT imaging of cancer: an in vivo study. Int J Nanomedicine 2011, 6, 2859-64. DOI: 10.2147/ijn.s25446.

14. Zhang, X. D.; Wu, D.; Shen, X.; Chen, J.; Sun, Y. M.; Liu, P. X.; Liang, X. J., Size-dependent radiosensitization of PEG-coated gold nanoparticles for cancer radiation therapy. Biomaterials 2012, 33 (27), 6408-19. DOI: 10.1016/j.biomaterials.2012.05.047.

15. Sulfikkarali, N.; Krishnakumar, N.; Manoharan, S.; Nirmal, R. M., Chemopreventive efficacy of naringenin-loaded nanoparticles in 7,12-dimethylbenz(a)anthracene induced experimental oral carcinogenesis. Pathol Oncol Res 2013, 19 (2), 287-96. DOI: 10.1007/s12253-012-9581-1.

16. Payne, R.; Coluzzi, P.; Hart, L.; Simmonds, M.; Lyss, A.; Rauck, R.; Berris, R.; Busch, M. A.; Nordbrook, E.; Loseth, D. B.; Portenoy, R. K., Long-term safety of oral transmucosal fentanyl citrate for breakthrough cancer pain. J Pain Symptom Manage 2001, 22 (1), 575-83. DOI: 10.1016/s0885-3924(01)00306-2.

17. Herr, A. E.; Hatch, A. V.; Throckmorton, D. J.; Tran, H. M.; Brennan, J. S.; Giannobile, W. V.; Singh, A. K., Microfluidic immunoassays as rapid saliva-based clinical diagnostics. Proc Natl Acad Sci U S A 2007, 104 (13), 5268-73. DOI: 10.1073/pnas.0607254104.

18. Liu, C. J.; Kao, S. Y.; Tu, H. F.; Tsai, M. M.; Chang, K. W.; Lin, S. C., Increase of microRNA miR-31 level in plasma could be a potential marker of oral cancer. Oral Dis 2010, 16 (4), 360-4. DOI: 10.1111/j.1601-0825.2009.01646.x.

19. Weigum, S. E.; Floriano, P. N.; Christodoulides, N.; McDevitt, J. T., Cell-based sensor for analysis of EGFR biomarker expression in oral cancer. Lab Chip 2007, 7 (8), 995-1003. DOI: 10.1039/b703918b.

20. Weigum, S. E.; Floriano, P. N.; Redding, S. W.; Yeh, C. K.; Westbrook, S. D.; McGuff, H. S.; Lin, A.; Miller, F. R.; Villarreal, F.; Rowan, S. D.; Vigneswaran, N.; Williams, M. D.; McDevitt, J. T., Nano-bio-chip sensor platform for examination of oral exfoliative cytology. Cancer Prev Res (Phila) 2010, 3 (4), 518-28. DOI: 10.1158/1940-6207.capr-09-0139.

21. Kishen, A.; Shi, Z.; Shrestha, A.; Neoh, K. G., An investigation on the antibacterial and antibiofilm efficacy of cationic nanoparticulates for root canal disinfection. J Endod 2008, 34 (12), 1515-20. DOI: 10.1016/j.joen.2008.08.035.

22. Monzavi, A.; Eshraghi, S.; Hashemian, R.; Momen-Heravi, F., In vitro and ex vivo antimicrobial efficacy of nano-MgO in the elimination of endodontic pathogens. Clin Oral Investig 2015, 19 (2), 349-56. DOI: 10.1007/s00784-014-1253-y.

23. Malacarne-Zanon, J.; de Andrade, E. S. S. M.; Wang, L.; de Goes, M. F.; Martins, A. L.; Narvaes-Romani, E. O.; Anido-Anido, A.; Carrilho, M. R., Permeability of Dental Adhesives - A SEM Assessment. Eur J Dent 2010, 4 (4), 429-39.

24. Hashimoto, M.; De Munck, J.; Ito, S.; Sano, H.; Kaga, M.; Oguchi, H.; Van Meerbeek, B.; Pashley, D. H., In vitro effect of nanoleakage expression on resin-dentin bond strengths analyzed by microtensile bond test, SEM/EDX and TEM. Biomaterials 2004, 25 (25), 5565-74. DOI: 10.1016/j.biomaterials.2004.01.009.

25. Lohbauer, U.; Wagner, A.; Belli, R.; Stoetzel, C.; Hilpert, A.; Kurland, H. D.; Grabow, J.; Muller, F. A., Zirconia nanoparticles prepared by laser vaporization as fillers for dental adhesives. Acta Biomater 2010, 6 (12), 4539-46. DOI: 10.1016/j.actbio.2010.07.002.

26. Wagner, A.; Belli, R.; Stotzel, C.; Hilpert, A.; Muller, F. A.; Lohbauer, U., Biomimetically- and hydrothermally-grown HAp nanoparticles as reinforcing fillers for dental adhesives. J Adhes Dent 2013, 15 (5), 413-22. DOI: 10.3290/j.jad.a29534.

27. Di Hipolito, V.; Reis, A. F.; Mitra, S. B.; de Goes, M. F., Interaction morphology and bond strength of nanofilled simplified-step adhesives to acid etched dentin. Eur J Dent 2012, 6 (4), 349-60.

28. Moraes, R. R.; Garcia, J. W.; Wilson, N. D.; Lewis, S. H.; Barros, M. D.; Yang, B.; Pfeifer, C. S.; Stansbury, J. W., Improved dental adhesive formulations based on reactive nanogel additives. J Dent Res 2012, 91 (2), 179-84. DOI: 10.1177/0022034511426573.

29. Mendonca, G.; Mendonca, D. B.; Aragao, F. J.; Cooper, L. F., Advancing dental implant surface technology--from micron- to nanotopography. Biomaterials 2008, 29 (28), 3822-35. DOI: 10.1016/j.biomaterials.2008.05.012.

30. Brammer, K. S.; Oh, S.; Cobb, C. J.; Bjursten, L. M.; van der Heyde, H.; Jin, S., Improved bone-forming functionality on diameter-controlled TiO(2) nanotube surface. Acta Biomater 2009, 5 (8), 3215-23. DOI: 10.1016/j.actbio.2009.05.008.

31. Oh, S.; Brammer, K. S.; Li, Y. S.; Teng, D.; Engler, A. J.; Chien, S.; Jin, S., Stem cell fate dictated solely by altered nanotube dimension. Proc Natl Acad Sci U S A 2009, 106 (7), 2130-5. DOI: 10.1073/pnas.0813200106.

32. Cavalcanti-Adam, E. A.; Volberg, T.; Micoulet, A.; Kessler, H.; Geiger, B.; Spatz, J. P., Cell spreading and focal adhesion dynamics are regulated by spacing of integrin ligands. Biophys J 2007, 92 (8), 2964-74. DOI: 10.1529/biophysj.106.089730.

33. Ballo, A.; Agheli, H.; Lausmaa, J.; Thomsen, P.; Petronis, S., Nanostructured model implants for in vivo studies: influence of well-defined nanotopography on de novo bone formation on titanium implants. Int J Nanomedicine 2011, 6, 3415-28. DOI: 10.2147/ijn.s25867.

34. Martinez-Gutierrez, F.; Thi, E. P.; Silverman, J. M.; de Oliveira, C. C.; Svensson, S. L.; Vanden Hoek, A.; Sanchez, E. M.; Reiner, N. E.; Gaynor, E. C.; Pryzdial, E. L.; Conway, E. M.; Orrantia, E.; Ruiz, F.; Av-Gay, Y.; Bach, H., Antibacterial activity, inflammatory response, coagulation and cytotoxicity effects of silver nanoparticles. Nanomedicine 2012, 8 (3), 328-36. DOI: 10.1016/j.nano.2011.06.014.

35. Lu, Z.; Rong, K.; Li, J.; Yang, H.; Chen, R., Size-dependent antibacterial activities of silver nanoparticles against oral anaerobic pathogenic bacteria. J Mater Sci Mater Med 2013, 24 (6), 1465-71. DOI: 10.1007/s10856-013-4894-5.

36. Rosenblatt, A.; Stamford, T. C.; Niederman, R., Silver diamine fluoride: a caries "silver-fluoride bullet". J Dent Res 2009, 88 (2), 116-25. DOI: 10.1177/0022034508329406.

37. Santos, V. E., Jr.; Vasconcelos Filho, A.; Targino, A. G.; Flores, M. A.; Galembeck, A.; Caldas, A. F., Jr.; Rosenblatt, A., A new "silver-bullet" to treat caries in children--nano silver fluoride: a randomised clinical trial. J Dent 2014, 42 (8), 945-51. DOI: 10.1016/j.jdent.2014.05.017.

38. Sun, L.; Chow, L. C., Preparation and properties of nano-sized calcium fluoride for dental applications. Dental materials : official publication of the Academy of Dental Materials 2008, 24 (1), 111-116. DOI: 10.1016/j.dental.2007.03.003.

39. Nakashima, S.; Yoshie, M.; Sano, H.; Bahar, A., Effect of a test dentifrice containing nano-sized calcium carbonate on remineralization of enamel lesions in vitro. J Oral Sci 2009, 51 (1), 69-77.

40. Lelli, M.; Putignano, A.; Marchetti, M.; Foltran, I.; Mangani, F.; Procaccini, M.; Roveri, N.; Orsini, G., Remineralization and repair of enamel surface by biomimetic Zn-carbonate hydroxyapatite containing toothpaste: a comparative in vivo study. Frontiers in physiology 2014, 5, 333-333. DOI: 10.3389/fphys.2014.00333.

41. Besinis, A.; van Noort, R.; Martin, N., Infiltration of demineralized dentin with silica and hydroxyapatite nanoparticles. Dent Mater 2012, 28 (9), 1012-23. DOI: 10.1016/j.dental.2012.05.007.

42. Elkassas, D.; Arafa, A., Remineralizing efficacy of different calcium-phosphate and fluoride based delivery vehicles on artificial caries like enamel lesions. J Dent 2014, 42 (4), 466-74. DOI: 10.1016/j.jdent.2013.12.017.

43. Zhang, X.; Li, Y.; Sun, X.; Kishen, A.; Deng, X.; Yang, X.; Wang, H.; Cong, C.; Wang, Y.; Wu, M., Biomimetic remineralization of demineralized enamel with nano-complexes of phosphorylated chitosan and amorphous calcium phosphate. J Mater Sci Mater Med 2014, 25 (12), 2619-28. DOI: 10.1007/s10856-014-5285-2.

44. Reynolds, E. C., Anticariogenic complexes of amorphous calcium phosphate stabilized by casein phosphopeptides: a review. Spec Care Dentist 1998, 18 (1), 8-16.

45. Reynolds, E. C.; Cai, F.; Shen, P.; Walker, G. D., Retention in plaque and remineralization of enamel lesions by various forms of calcium in a mouthrinse or sugar-free chewing gum. J Dent Res 2003, 82 (3), 206-11. DOI: 10.1177/154405910308200311.

46. Tai, B. J.; Bian, Z.; Jiang, H.; Greenspan, D. C.; Zhong, J.; Clark, A. E.; Du, M. Q., Anti-gingivitis effect of a dentifrice containing bioactive glass (NovaMin) particulate. J Clin Periodontol 2006, 33 (2), 86-91. DOI: 10.1111/j.1600-051X.2005.00876.x.

47. Gjorgievska, E.; Nicholson, J. W., Prevention of enamel demineralization after tooth bleaching by bioactive glass incorporated into toothpaste. Aust Dent J 2011, 56 (2), 193-200. DOI: 10.1111/j.1834-7819.2011.01323.x.

48. Zhang, Y.; Shareena Dasari, T. P.; Deng, H.; Yu, H., Antimicrobial Activity of Gold Nanoparticles and Ionic Gold. Journal of Environmental Science and Health, Part C 2015, 33 (3), 286-327. DOI: 10.1080/10590501.2015.1055161.

49. Botelho, M. A.; Martins, J. G.; Ruela, R. S.; Queiroz, D. B.; Ruela, W. S., Nanotechnology in ligature-induced periodontitis: protective effect of a doxycycline gel with nanoparticules. J Appl Oral Sci 2010, 18 (4), 335-42. DOI: 10.1590/s1678-77572010000400003.

50. Akasaka, T.; Nakata, K.; Uo, M.; Watari, F., Modification of the dentin surface by using carbon nanotubes. Biomed Mater Eng 2009, 19 (2-3), 179-85. DOI: 10.3233/bme-2009-0578.

51. Kou, W.; Akasaka, T.; Watari, F.; Sjogren, G., An in vitro evaluation of the biological effects of carbon nanotube-coated dental zirconia. ISRN Dent 2013, 2013, 296727. DOI: 10.1155/2013/296727.

52. Yin, P. T.; Shah, S.; Chhowalla, M.; Lee, K. B., Design, synthesis, and characterization of graphene-nanoparticle hybrid materials for bioapplications. Chem Rev 2015, 115 (7), 2483-531. DOI: 10.1021/cr500537t.

53. He, J.; Zhu, X.; Qi, Z.; Wang, C.; Mao, X.; Zhu, C.; He, Z.; Li, M.; Tang, Z., Killing dental pathogens using antibacterial graphene oxide. ACS Appl Mater Interfaces 2015, 7 (9), 5605-11. DOI: 10.1021/acsami.5b01069.

54. Asadpour, E.; Sadeghnia, H. R.; Ghorbani, A.; Boroushaki, M. T., Effect of zirconium dioxide nanoparticles on glutathione peroxidase enzyme in PC12 and n2a cell lines. Iran J Pharm Res 2014, 13 (4), 1141-8.

55. Brunner, T. J.; Wick, P.; Manser, P.; Spohn, P.; Grass, R. N.; Limbach, L. K.; Bruinink, A.; Stark, W. J., In vitro cytotoxicity of oxide nanoparticles: comparison to asbestos, silica, and the effect of particle solubility. Environ Sci Technol 2006, 40 (14), 4374-81. DOI: 10.1021/es052069i.

56. Besinis, A.; van Noort, R.; Martin, N., Remineralization potential of fully demineralized dentin infiltrated with silica and hydroxyapatite nanoparticles. Dental Materials 2014, 30 (3), 249-262. DOI: https://doi.org/10.1016/j.dental.2013.11.014.

57. Elsaka, S. E.; Hamouda, I. M.; Swain, M. V., Titanium dioxide nanoparticles addition to a conventional glass-ionomer restorative: influence on physical and antibacterial properties. J Dent 2011, 39 (9), 589-98. DOI: 10.1016/j.jdent.2011.05.006.

58. Sun, J.; Forster, A. M.; Johnson, P. M.; Eidelman, N.; Quinn, G.; Schumacher, G.; Zhang, X.; Wu, W. L., Improving performance of dental resins by adding titanium dioxide nanoparticles. Dent Mater 2011, 27 (10), 972-82. DOI: 10.1016/j.dental.2011.06.003.

59. Heo, D. N.; Ko, W.-K.; Lee, H. R.; Lee, S. J.; Lee, D.; Um, S. H.; Lee, J. H.; Woo, Y.-H.; Zhang, L. G.; Lee, D.-W.; Kwon, I. K., Titanium dental implants surface-immobilized with gold nanoparticles as osteoinductive agents for rapid osseointegration. Journal of Colloid and Interface Science 2016, 469, 129-137. DOI: https://doi.org/10.1016/j.jcis.2016.02.022.

60. Regiel-Futyra, A.; Kus-Liśkiewicz, M.; Sebastian, V.; Irusta, S.; Arruebo, M.; Stochel, G.; Kyzioł, A., Development of Noncytotoxic Chitosan–Gold Nanocomposites as Efficient Antibacterial Materials. ACS Applied Materials & Interfaces 2015, 7 (2), 1087-1099. DOI: 10.1021/am508094e.

61. Thukkaram, M.; Sitaram, S.; Kannaiyan, S. k.; Subbiahdoss, G., Antibacterial Efficacy of Iron-Oxide Nanoparticles against Biofilms on Different Biomaterial Surfaces. International Journal of Biomaterials 2014, 2014, 6. DOI: 10.1155/2014/716080.

62. Gutiérrez, M. F.; Malaquias, P.; Matos, T. P.; Szesz, A.; Souza, S.; Bermudez, J.; Reis, A.; Loguercio, A. D.; Farago, P. V., Mechanical and microbiological properties and drug release modeling of an etch-and-rinse adhesive containing copper nanoparticles. Dental Materials 2017, 33 (3), 309-320. DOI: https://doi.org/10.1016/j.dental.2016.12.011.

63. Ren, G.; Hu, D.; Cheng, E. W. C.; Vargas-Reus, M. A.; Reip, P.; Allaker, R. P., Characterisation of copper oxide nanoparticles for antimicrobial applications. International Journal of Antimicrobial Agents 2009, 33 (6), 587-590. DOI: https://doi.org/10.1016/j.ijantimicag.2008.12.004.

64. Chronopoulou, L.; Nocca, G.; Castagnola, M.; Paludetti, G.; Ortaggi, G.; Sciubba, F.; Bevilacqua, M.; Lupi, A.; Gambarini, G.; Palocci, C., Chitosan based nanoparticles functionalized with peptidomimetic derivatives for oral drug delivery. New Biotechnology 2016, 33 (1), 23-31. DOI: https://doi.org/10.1016/j.nbt.2015.07.005.

65. Jing, X.; Mi, H.-Y.; Peng, J.; Peng, X.-F.; Turng, L.-S., Electrospun aligned poly(propylene carbonate) microfibers with chitosan nanofibers as tissue engineering scaffolds. Carbohydrate Polymers 2015, 117, 941-949. DOI: https://doi.org/10.1016/j.carbpol.2014.10.025.

66. Khan, S.; Zaheer, S.; Gupta, N., Oral psoriasis: A diagnostic dilemma. European Journal of General Dentistry 2013, 2 (1), 67-71. DOI: 10.4103/2278-9626.106822.

67. Pagonis, T. C.; Chen, J.; Fontana, C. R.; Devalapally, H.; Ruggiero, K.; Song, X.; Foschi, F.; Dunham, J.; Skobe, Z.; Yamazaki, H.; Kent, R.; Tanner, A. C. R.; Amiji, M. M.; Soukos, N. S., Nanoparticle-based Endodontic Antimicrobial Photodynamic Therapy. Journal of Endodontics 2010, 36 (2), 322-328. DOI: https://doi.org/10.1016/j.joen.2009.10.011.

Chapter 6 – Silicon oxycarbide and titanium dioxide-based nanowires: growth methods

6.1 Introduction

As mentioned before, nanomaterials have paved the way to the investigation and development of new materials with many different potential applications, due to their unique properties (i.e. mechanical, physical, optical properties). The recently occurred change in the concept of designing biomimetic materials, arose the importance of the nanotopographical organization (rather than micrometrical one) of extracellular signals necessary for cellular response. In particular, it has been demonstrated that cells respond to distinct spatial nanopatterns, in fact, cell adhesion, spreading, proliferation, migration have been shown to be influenced by specific nanopatterning ranging from 15nm to 140nm[1-3]. This peculiar response to nanoscale geometry has been reported for many cell lines, such as, osteoblasts, endothelial cells, mesenchymal stem cells, smooth muscle cells and nerve cells[4-10].

Obviously, to be used in nanomedicine, nanomaterials need to be assessed as safe for human and animal health; in this regards, the most important results in terms of cytocompatibility were recently obtained on silicon-based nano-systems by Tian et al., and on titanium-based nanowires by the group of Park et al., both showing stability and dose-dependent cytotoxic effect of nanostructures[11, 12].

The nanowires treated in thesis are semiconducting NWs, silicon and titanium-based, obtained through a CVD method: silicon oxycarbide (SiO_xC_y) NWs and titanium dioxide (TiO_2) NWs

- Silicon oxycarbide nanowires (SiO_xC_y)

Silicon oxycarbide NWs have been shown to possess a high elastic modulus, bending strength, chemical resistance in harsh environment, high temperature stability, hardness and biocompatibility. Moreover, its biodegradability and ability to avoid immune system responses make them a suitable nano-biomaterial for biomedical implants in various body districts[13-16]. Furthermore, nanometrical size allows the development of a surface topography similar to the ECM, fundamental for cell adhesion and proliferation in regenerative medicine.

Silicon oxycarbide can easily be functionalized with macromolecules or nanoparticles which make it an ideal platform for several experimental approaches.

- Titanium dioxide nanowires (TiO_2 NWs)

One of the most common implant materials is titanium, after a number of surface treatments aimed to create a rough surface for a better bone integration. In this regard, the development of a nanostructured titanium surface represents a step forward in the mimic of the ECM structure (e.g. disposition of collagen bundles). The suitability of TiO_2 as inorganic material is prevalently due to its biocompatibility, already proved in currently clinically used orthopedic prostheses and dental implants[17, 18]. Moreover, titanium dioxide has been proved to be a semiconductor material that can provide a favorable substrate for cell growth and differentiation[5].

6.2 Nanowires growth method

All the NWs used for the project were produced at IMEM-CNR Institute of Parma in a growth apparatus, designed by Dr. Giovanni Attolini, through a CVD technique.

Many of the produced SiC-based NWs are covered by a thin layer of oxide (core/shell) and some by C-rich phases in the shell, i.e. they consist of a continuous crystalline core encapsulated in a sheath of a different crystalline or amorphous material, even if, it had minor influence on physical properties and was often removed during the manufacturing process[19].

All the substrates were previously cleaned in an ultrasonic bath with organic solvent and cleaned in hydrofluoric acid (HF) aqueous solution (HF : H_2O = 1 : 50) for 2 min. Once cleaned the surface from every silicon oxide residue, substrates were rinsed in deionized water, dried in a nitrogen atmosphere and covered with the catalyst solution, which was dried at 40°C in air.

The CVD technique principles foresee the injection of a gaseous precursors in presence of a gas carrier and subsequently its deposition on a solid substrate. The carrier gas flow with the precursors in the growth chamber, where the precursors decompose on the substrate surface, and removes gaseous byproduct from the system.

The growth apparatus built at IMEM-CNR consists of: the system for the gas supply (carrier gas and precursor gas), controlled by mass flow controllers (MFC), the purge system for the carrier gas, the growth chamber, the furnace, and the aspiration tool for the removal of reaction byproducts and for the prevention of accidental gas loss.

Figure 6.1 shows the CVD apparatus.

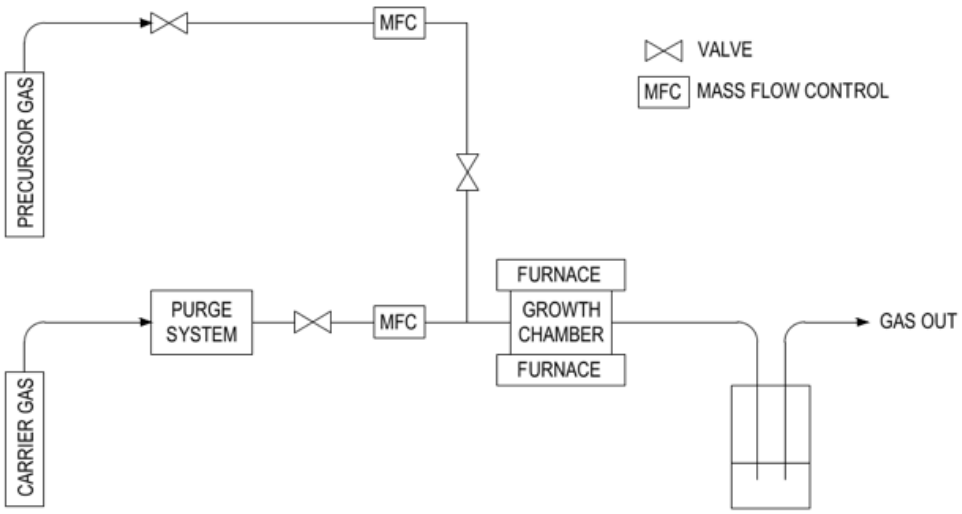

Figure 6.1: CVD apparatus diagram.

The growth chamber is surrounded by a tubular furnace, in order to reach the homogeneous high temperature needed for NWs growth (both, the substrate and the reactor wall reach the same temperature during the growth) and is defined as an "hot wall" type; moreover, the reactor uses an "open tube" growth method, hence the growth is characterized by the continuous flow of carrier gas at atmospheric pressure. The carrier gas selected for the growth was nitrogen (N_2), also fluxed to remove oxygen from the chamber, and the precursor gas was carbon monoxide (CO).

6.2.1 Silicon oxycarbide nanowires

Silicon oxycarbide (SiO_xC_y) nanowires growth occurred on silicon (001) and (111) substrates through the established CVD process (as described before for core-shell NWs) lowering the temperature to 1050°C for 45 minutes and rapidly quenched to ambient temperature after the growth. Ferric nitrate ($Fe(NO_3)_3$) was used as catalyst and carbon monoxide was flowed during the process acted as dopant precursor, so that carbon-doped under-stoichiometric silicon dioxide nanowires were obtained[19].

X-Ray Photoemission Spectroscopy (XPS) measurements indicated that the content at the surface of NWs was carbon 13,4%, silicon 35,8% and oxygen 50,8%.

Nanowire were subsequently characterized at IMEM-CNR by scanning electron microscopy (SEM), high resolution transmission electron microscopy (HR-TEM) and high angle annular dark field imaging in scanning mode (HAADF-STEM)[20].

Figure 6.2 shows the dense bundle of NWs long interwoven fibers cover the whole sample surface and that morphology was comparable for all the NWs; moreover, the STEM-HAADF characterization presented an amorphous structure of silicon oxycarbide and the carbon map confirmed the presence of carbon inside the SiO_xC_y structure[19].

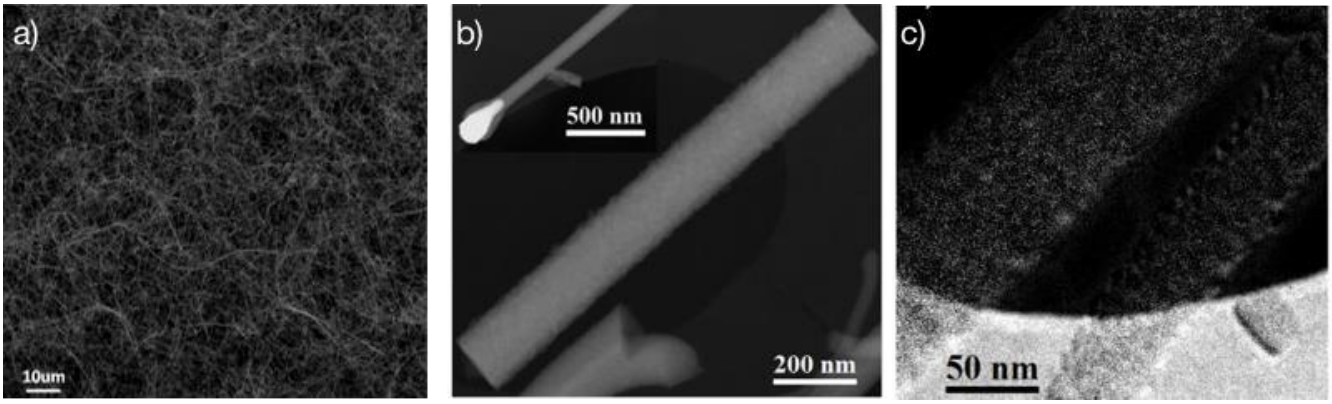

Figure 6.2: a) SEM image of a SiO_xC_y NWs bundle. b) STEM-HAADF image of representative SiO_xC_y NW, and nanowire tip clearly visible in the enlargement. c) Carbon map obtained through TEM with energy filtered (the white area is the carbon support film of the TEM grid)[19].

The medium length of SiO_xC_y NWs is several tens of μm and the substrates are homogeneously covered by NWs after the growth (Figure 6.2 a). The diameter of SiO_xC_y NWs appears slightly larger than the other kinds of NWs and it was about 80nm[19].

6.2.2 Titanium dioxide nanowires

Titanium dioxide nanowires were grown by a CVD process, as previously described, on commercially pure (c.p.) polycrystalline titanium disks (Institut Straumann AG, Waldenburg, CH), with nickel nitrate as catalyst. After the initial cleaning in HF, samples were dipped in a solution of $Ni(NO_3)_2$ and dried in air; subsequently, substrates were positioned in the CVD growth chamber and heated at the growth temperature of 1120 °C with a constant CO flux for 20 min.

This particular process does not require a specific titanium precursor to be fluxed, because titanium was already provided by the substrate. Carbon oxide acted as the oxidation agent and allowed the conversion of Ti into TiO_2; the presence of nickel nitrate as catalyst favored the anisotropic growth of the NWs.

Titanium oxide nanowires morphology was analyzed through SEM, NWs crystalline structure was studied by X-Ray Diffraction (XRD) in a Siemens D-500 diffractometer with a Cu Kα radiation and finally, a TEM analysis of a single

NW was performed in a JEOL 2200FS microscope operating at 200kV in conventional scanning (STEM) mode, after transfer of NWs on a carbon-coated copper grid.

The characterization and biological evaluation of TiO_2 NWs will be detailed in chapter 9.

Any innovative biomaterial, nano or not, which aim to be in contact with animal or human cells, must be cytocompatible, in order to perform its final objective (e.g. drug delivery, tissue regeneration, etc). In the following chapters the biological response of different cell lines to NWs will be evaluated, also after chemical modification of the substrates.

References

1. Park, J.; Bauer, S.; Schlegel, K. A.; Neukam, F. W.; von der Mark, K.; Schmuki, P., TiO2 nanotube surfaces: 15 nm--an optimal length scale of surface topography for cell adhesion and differentiation. Small 2009, 5 (6), 666-71. DOI: 10.1002/smll.200801476.

2. Cavalcanti-Adam, E. A.; Volberg, T.; Micoulet, A.; Kessler, H.; Geiger, B.; Spatz, J. P., Cell spreading and focal adhesion dynamics are regulated by spacing of integrin ligands. Biophys J 2007, 92 (8), 2964-74. DOI: 10.1529/biophysj.106.089730.

3. Massia, S. P.; Hubbell, J. A., An RGD spacing of 440 nm is sufficient for integrin alpha V beta 3-mediated fibroblast spreading and 140 nm for focal contact and stress fiber formation. J Cell Biol 1991, 114 (5), 1089-100. DOI: 10.1083/jcb.114.5.1089.

4. Dalby, M. J.; McCloy, D.; Robertson, M.; Agheli, H.; Sutherland, D.; Affrossman, S.; Oreffo, R. O., Osteoprogenitor response to semi-ordered and random nanotopographies. Biomaterials 2006, 27 (15), 2980-7. DOI: 10.1016/j.biomaterials.2006.01.010.

5. Popat, K. C.; Leoni, L.; Grimes, C. A.; Desai, T. A., Influence of engineered titania nanotubular surfaces on bone cells. Biomaterials 2007, 28 (21), 3188-97. DOI: 10.1016/j.biomaterials.2007.03.020.

6. Brammer, K. S.; Oh, S.; Gallagher, J. O.; Jin, S., Enhanced cellular mobility guided by TiO2 nanotube surfaces. Nano Lett 2008, 8 (3), 786-93. DOI: 10.1021/nl072572o.

7. Park, J.; Bauer, S.; Schmuki, P.; von der Mark, K., Narrow window in nanoscale dependent activation of endothelial cell growth and differentiation on TiO2 nanotube surfaces. Nano Lett 2009, 9 (9), 3157-64. DOI: 10.1021/nl9013502.

8. Peng, L.; Eltgroth, M. L.; LaTempa, T. J.; Grimes, C. A.; Desai, T. A., The effect of TiO2 nanotubes on endothelial function and smooth muscle proliferation. Biomaterials 2009, 30 (7), 1268-72. DOI: 10.1016/j.biomaterials.2008.11.012.

9. Raja, P. M.; Connolley, J.; Ganesan, G. P.; Ci, L.; Ajayan, P. M.; Nalamasu, O.; Thompson, D. M., Impact of carbon nanotube exposure, dosage and aggregation on smooth muscle cells. Toxicol Lett 2007, 169 (1), 51-63. DOI: 10.1016/j.toxlet.2006.12.003.

10. Belyanskaya, L.; Weigel, S.; Hirsch, C.; Tobler, U.; Krug, H. F.; Wick, P., Effects of carbon nanotubes on primary neurons and glial cells. Neurotoxicology 2009, 30 (4), 702-11. DOI: 10.1016/j.neuro.2009.05.005.

11. Park, E. J.; Lee, G. H.; Shim, H. W.; Kim, J. H.; Cho, M. H.; Kim, D. W., Comparison of toxicity of different nanorod-type TiO2 polymorphs in vivo and in vitro. J Appl Toxicol 2014, 34 (4), 357-66. DOI: 10.1002/jat.2932.

12. Tian, B.; Liu, J.; Dvir, T.; Jin, L.; Tsui, J. H.; Qing, Q.; Suo, Z.; Langer, R.; Kohane, D. S.; Lieber, C. M., Macroporous nanowire nanoelectronic scaffolds for synthetic tissues. Nat Mater 2012, 11 (11), 986-94. DOI: 10.1038/nmat3404.

13. Lagonegro, P.; Rossi, F.; Galli, C.; Smerieri, A.; Alinovi, R.; Pinelli, S.; Rimoldi, T.; Attolini, G.; Macaluso, G.; Macaluso, C.; Saddow, S. E.; Salviati, G., A cytotoxicity study of silicon oxycarbide nanowires as cell scaffold for biomedical applications. Mater Sci Eng C Mater Biol Appl 2017, 73, 465-471. DOI: 10.1016/j.msec.2016.12.096.

14. Onclin, S.; Ravoo, B. J.; Reinhoudt, D. N., Engineering Silicon Oxide Surfaces Using Self-Assembled Monolayers. Angewandte Chemie International Edition 2005, 44 (39), 6282-6304. DOI: 10.1002/anie.200500633.

15. Tamayo, A.; Rubio, J.; Rubio, F.; Oteo, J. L.; Riedel, R., Texture and micro-nanostructure of porous silicon oxycarbide glasses prepared from hybrid materials aged in different solvents. Journal of the European Ceramic Society 2011, 31 (9), 1791-1801. DOI: https://doi.org/10.1016/j.jeurceramsoc.2011.02.039.

16. Du P, W. X., Lin I K, Zhang X, Effects of composition and thermal annealing on the mechanical properties of silicon oxycarbide films. Sensors Actuators, A Phys. 176 90–8, 2012.

17. Dafar, M. O.; Grol, M. W.; Canham, P. B.; Dixon, S. J.; Rizkalla, A. S., Reinforcement of flowable dental composites with titanium dioxide nanotubes. Dent Mater 2016, 32 (6), 817-26. DOI: 10.1016/j.dental.2016.03.022.

18. Freitas, R. A., Jr., Nanodentistry. J Am Dent Assoc 2000, 131 (11), 1559-65. DOI: 10.14219/jada.archive.2000.0084.
19. Fabbri, F.; Rossi, F.; Negri, M.; Tatti, R.; Aversa, L.; Dhanabalan, S. C.; Verucchi, R.; Attolini, G.; Salviati, G., Carbon-doped SiO(x) nanowires with a large yield of white emission. Nanotechnology 2014, 25 (18), 185704. DOI: 10.1088/0957-4484/25/18/185704.
20. Rossi F, F. F., Attolini G, Bosi M, Watts B E, Salviati G, TEM and SEM-CL Studies of SiC Nanowires Mater. Sci. Forum 645-648 387–390 2010

Chapter 7 – Study of silicon oxycarbide nanowires cytotoxicity

From: A cytotoxicity study of silicon oxycarbide nanowires as cell scaffold for biomedical applications.[1]
Published in Journal of Material Science and Engineering C, 73 (2017) 465-471.
DOI: 10.1016/j.msec.2016.12.096

Abstract

Tissue engineering requires the development of new 3-dimensional biomaterials to promote cell colonization, proliferation and differentiation; as the ECM is a complex structure which possess both micro and nano-scaled patterns of chemistry and topography, the synthesis of nanowires, due to their particular morphology and three-dimensional arrangement, strongly resemble its architecture, as they appear as promising candidates for artificial matrix development in different biomedical fields. In particular, silicon oxycarbide presents high elastic modulus, bending strength and hardness in aggressive environments and high temperature if compared to conventional silicate glasses. In this chapter a preliminary study about silicon oxycarbide nanowires cytotoxicity is presented in order to verify the possibility to use them for biomedical applications. As stated in the ISO 10993-5 guidelines "an important quality issue of materials for medical devices having direct or indirect contact with the body tissue is the biocompatibility". Any biomaterial promising for *in-vivo* implanting must be analyzed for biocompatibility evaluation with specific *in-vitro* tests, starting from cytotoxicity tests. In particular, ISO 10993-5 describes test methods to assess the *in vitro* cytotoxicity of medical devices, specifying the incubation of cultured cells in contact with a device and/or extracts of a device either directly or through diffusion. These methods are designed to determine the biological response of cells *in vitro* using appropriate biological parameters; L929 mouse fibroblasts are the standard cell line for cytotoxicity tests, as recommended by American Society for Quality Control.

In our work, SiO_xC_y NWs were synthetized through CVD technique on silicon substrates and they have been tested *in vitro* with a fibroblastic cell line. More specifically, indirect and direct cytotoxicity assays were performed in accordance with ISO 10993-5, by quantitating cell viability at MTT and chemiluminescent assay; a gene expression analysis was performed to understand the alteration in mRNA expression profile and cell cultures were observed with Scanning Electron Microscope (SEM) to analyze the cell-surface interface and morphology. Finally, samples were tested for hemocompatibility, as stated in ISO 10993-4, which defines blood-device interaction as any interaction between blood, or blood components and a device resulting in effects on the blood or on any organ or tissue, or on the device. For our research, Platelet-rich Plasma was assayed at SEM and by ELISA assay. Platelets activation and clotting formation are important steps of acute inflammatory response and they are useful to

increase the tissue regeneration, in fact, platelets activation and subsequent release of growth factors as PDGF, regulates cell growth and division.

SiO_xC_y NWs proved to be biocompatible and to not impair cell proliferation at both, direct and indirect contact assays. L929 cells were able to attach on NWs and proliferate, but the most important result is the interesting ability of cells to reorganize the 3D NWs bundle by displacing the nanostructure and creating tunnels within the NWs network. Silicon oxycarbide nanowires have been shown to did not impair platelet activation and behaved similarly, if nanowires were compared to flat silicon oxycarbide.

Our data showed that SiO_xC_y NWs did not release cytotoxic species and acted as a viable and suitable scaffold for fibroblastic cells, thus representing a promising platform for implantable devices; moreover due to their peculiar chemical, physical and mechanical properties are promising biomaterials for multiple clinical applications, including the stimulation of clot formation.

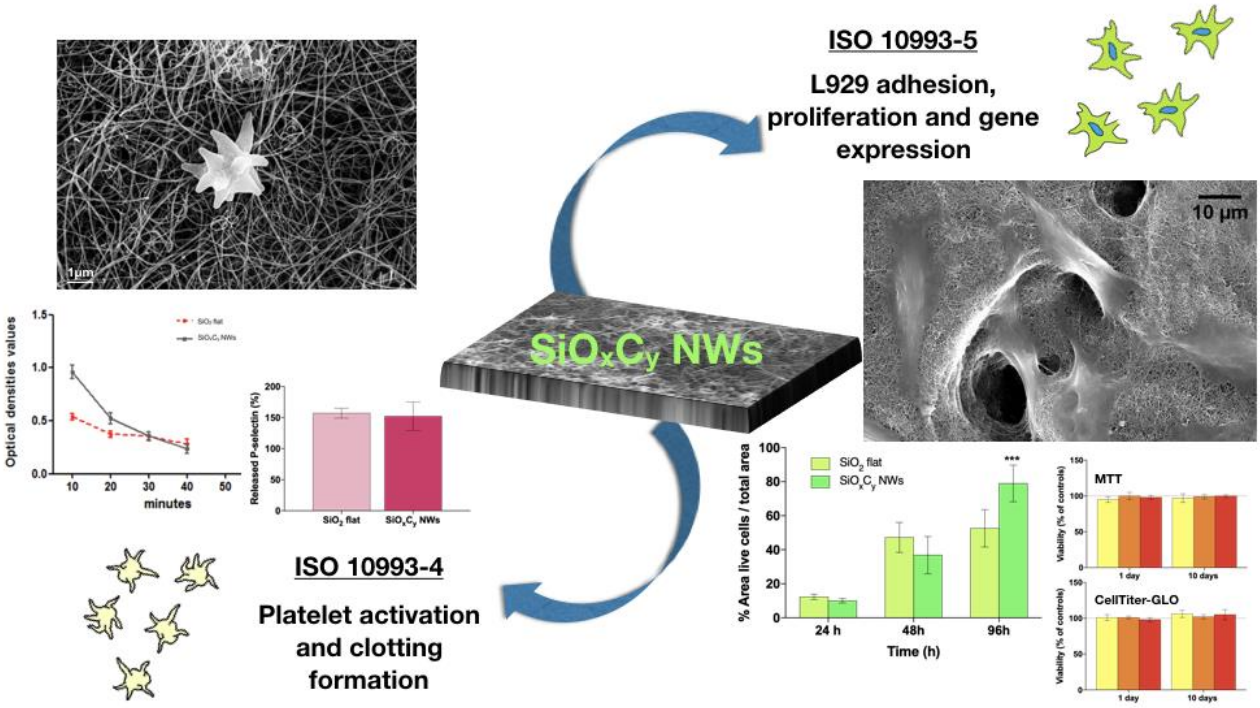

Figure 7.1: Graphical abstract of the chapter.

7.1 Introduction

Regenerative medicine is based on the idea of using biomaterials capable to provide a scaffold for ingrowing cells to replace the missing extracellular matrix (ECM) and consequently allow the regeneration of missing or damaged tissues. The ECM is a complex structure, which create a microenvironment that controls cell fate and activity; in this regard, it becomes of fundamental importance the interaction of cells within scaffolds and physico-chemical characteristics of the biomaterial, in order to synthetize ECM adequate components. In fact, the maturation and maintenance of a suitable extracellular matrix plays a pivotal role in the potential success of any 3D scaffold. Moreover, ECM allows cells to be reached by a vast array of biochemical and mechanical signals leading to their response in terms of proliferation, migration or differentiation in mature cells; for these reasons, biomaterials should possess adequate physical and chemical properties to promote wound healing and regeneration, support cell function, and provide cells with direct stimuli to promote cell growth and differentiation and activate metabolic cascades that are conducive to tissue repair. The actual knowledge leads to the use of tissue extracts or derivates as *in vitro* or *in vivo* scaffolding materials, because they closely mimic the architecture of pristine tissues, but with the big limitation of their availability. Innovative biomaterials, as it occurred for nanomaterials, have been extensively studied in the last decades due to their peculiar abilities and their superficial nanotopographies. In fact, it is known that the surface of interaction between cells and biologically active materials needs to be deeply investigates, topographical modifications might be a powerful tool to understand and facilitate the development of regenerative therapies and to potentially clinical use these nanostructured biomaterials; moreover, native ECM exhibits macroscale to nanoscale patterns of topography, therefore it is not unsurprising that cells respond to a variety of micro and nano scales of features. Silicon oxycarbide nanowires (SiO_xC_y NWs) are nanostructured material obtained by CVD technique with carbon monoxide gas as dopant precursor; they have been shown to have higher elastic modulus, bending strength and hardness, higher chemical durability than conventional silicate glasses in aggressive environments and greater stability at high temperatures[2-4]. As literature data explain, there occur a variety of notable changes with the shift from micro- to nanometer reinforcement as the presence of higher surface area or the significant improvement in mechanical performance (e.g. stiffness and tensile strength), if compared to the same bulk material. Furthermore, silicon oxycarbide has been demonstrated to increase platelet aggregation and activation, thereby promoting rapid clot formation and the onset of the acute inflammatory process, which is necessary for the creation of an adequate provisional matrix and subsequent wound healing[5]. An additional characteristic of SiO_xC_y is its capability to be easily engineered through functionalization and decoration with macro-molecules and nanoparticles which makes it an interesting platform for several experimental approaches[6-8]. The nanometric structure, moreover, can provide specific topographical and mechanical cues in order to ameliorate cell adhesion, cell proliferation and cell differentiation; the synthesis

of silicon oxycarbide nanowires allows the arrangement of 3D bundles that strictly mimic the organization of many ECM components and that could be therefore promising candidate for artificial matrices in different clinical situations[9].

Given that above, the aim of the study was to deeply investigate cellular response of fibroblastic cell line to a 3-dimensional environment of carbon doped silicon oxycarbide nanowires, to create a viable scaffold candidate for the regeneration of connective tissue. Furthermore, platelet activation and clot formation on these substrates were analyzed, in order to verify if the materials were able to start the coagulation cascade fundamental event for the initiation of tissue regeneration[10].

7.2 Materials and methods

Sample growth and characterization

SiO_xC_y NWs were grown, as described in the previous chapter, through a CVD technique on a silicon substrate preventively covered with metal catalyst, with carbon monoxide as dopant precursor and a temperature of 1050°C for 45 min[10]. Samples were characterized and sterilized with absolute ethanol and UVC rays for 15min before the use for cell culture experiments. Samples were characterized through X-Ray Photoemission Spectroscopy (XPS) and obtained results indicated that the content at the surface of NWs was carbon 13,4%, silicon 35,8% and oxygen 50,8%. Nanowires were subsequently characterized by scanning electron microscopy (SEM), high resolution transmission electron microscopy (HR-TEM) and high angle annular dark field imaging in scanning mode (HAADF-STEM)[11]. As previously shown in Figure 6.2 the medium length of SiO_xC_y NWs is several tens of µm and the substrates are homogeneously covered by NWs after the growth (a medium of 5-10NWs per μm^2 were exposed on the samples); the diameter of SiO_xC_y NWs appears slightly larger than the other kinds of NWs and it was about 80nm[10].

Cell assays

Cell cultures – Cell assays were performed with a mouse fibroblast cell line (L929, NCTC, clone 929 of strain L, derived from C3H/An male mouse) obtained from the American Type Culture Collection (ATCC, Manassas, VA, USA, distributed from LGC Standards srl, Sesto S. Giovanni, Milano, Italy). Cells were cultured in Dulbecco's Modified Eagle Medium (D-MEM, Thermo Fisher Scientific) supplemented with 10% FBS, 1% Penicillin and Streptomycin (PenStrep, Thermo Fisher Scientific) and 1% L-Glutamine (Thermo Fisher Scientific).

Indirect contact cytotoxicity assays – To observe the cellular effect of the potential release of cytotoxic agents from the sample in the culturing medium, an indirect contact cytotoxicity test in accordance with ISO 10993-5 guidelines, was performed to exclude the release of any cytotoxic agents from the nanowires substrate. According to ISO 10993-5, a material is accepted as biocompatible if the viability is greater than 70%. To this purpose, 30.000 cells/ml were seeded in 96 multi-well plates in complete D-MEM and the plates were maintained at 37 °C and 5% CO_2 in humidified atmosphere for 24 h. Simultaneously, NWs samples were soaked for 1 and 10 days in D-MEM in a 37 °C and controlled humidity environment; as a control, the same volume medium was incubated in the same condition. At days 1 and 10, conditioned medium was collected from the NWs sample and added to the pristine medium at percentages of 50%, 70% and 100% of the total D-MEM volume, following the ISO 10993-5 guidelines

for porous materials, and subsequently added to L929 cells who were cultured for further 24 hours. At the term of the incubation time, an MTT colorimetric assay (Roche Applied Science, Penzberg, Germany), based on the 3-(4,5-dimethylthiazol-2-yl)-2,5-diphenyltetrazolium bromide dye, was performed to assess cell viability, as recommended by ISO guidelines and the result was confirmed through method of determining the number of viable cells based on quantitation of the ATP present, a chemiluminescent proliferation assay (CellTiter-Glo, Promega, Madison, WI, USA).

Direct contact cytotoxicity assays – To observe the effect of a direct contact between L929 cells and SiO_xC_y NWs, a direct contact cytotoxicity test was performed in agreement with ISO 10993-5. Briefly, cell viability and proliferation were assayed at different time points. Seventy-thousand cells/ml were seeded on 1 cm × 1 cm NWs samples and on control flat SiO_2 and cultured in complete medium for 24, 48 and 96 hours. To evaluate the presence of viable or dead cells on the samples, a fluorescent staining with Calcein AM and Propidium Iodide was developed. Briefly, samples were rinsed in PBS (Sigma Aldrich) and incubated for 10min at room temperature (RT) with 4µM Calcein AM (fluorescent dye specific for living cells) and 1µM Propidium Iodide (fluorescent dye specific for dead cells). Samples were then washed in PBS and observed with a fluorescent microscope (Zeiss Axio Imager A2, Zeiss, Oberkochen, Germania) with excitation/emission wavelengths of 495/515 nm for Calcein AM and 560/720 nm for Propidium Iodide. For cell viability quantitation, the area covered by cells was measured with the Zen Pro 2012 software (Zeiss) and normalized to the control.
Moreover, to confirm direct contact cytotoxicity analysis result, 20.000 cells/ml were seeded on NWs samples and cultured for 24, 48 and 96h to perform a viability chemiluminescent assay CellTiter-Glo (Promega).

Gene expression analysis – To observe if there were differences in terms of gene expression between nanowires and bare silicon samples, after 96h of culture total RNA was extracted using TriZol (Thermo Fisher Scientific), according to manufacturer's indications. The purity of extracted RNA was measured through a NanoPhotometer™ P class (Implen GmbH, München, Germania) and subsequently RNA was retrotranscribed to cDNA with a High Capacity cDNA Reverse Transcription Kit (Thermo Fisher Scientific). TaqMan quantitative RT-PCR was performed on samples through a Real Time PCR machine (StepOne Plus, Life Technologies) and using the following primer probe sets from Applied Biosystems (Foster City, CA, USA): Alkaline Phosphatase (Mm00475834_m1); Cyclin D1 (Mm00432359_m1); Collagen 1a1 (Mm00483387_m1). GAPDH (Mm99999915_g1) was used as housekeeping gene.

Scanning electron microscopy – To observe cell morphology and the interaction with the underlying nanowires substrate, SEM morphological analysis was performed after 24, 48 and 96h of culture. Briefly, cells were fixed with 2.5% glutaraldehyde (Sigma-Aldrich) solution in 0,1M Na-Cacodylate buffer for 30 min at RT, thus washed in Na-

Cacodylate buffer for 5 min at RT and subsequently dehydrated in an ascendant series of ethanol (Sigma-Aldrich) at RT, for 10min each alcohol (EtOH 35%, 50%, 70%, 75%, 90%, 95%, 99%). Specimens were then coated with a nanometric gold layer through a SCD 040 coating device (Balzer Union, Wallruf, Germany). Microphotographs of cells distribution and morphology over NWs were taken in a dual beam Zeiss Auriga Compact system equipped with a GEMINI Field-Emission SEM column operated at 5keV.

Blood and platelet interactions – To analyze the interaction of the material with blood and the response in terms of activation of platelets ISO 10993-4 guidelines standards were followed; kinetic blood coagulation test and P-selectin assay were performed. Blood samples were collected from young, healthy, female farm pigs weighting approximately 45kg, free from hepatitis or other blood diseases (blood was provided by the University of South Florida's Center for Advanced Medical Learning and Simulation labs, under Institutional Animal Care and Use Committee, Protocol ID: IS00000216). To obtain platelet rich plasma (PRP), collected whole blood was centrifuged at 1200xg for 10min. To perform the experiment nanowires samples were soaked for 15min in PRP and subsequently they were fixed, dehydrated and covered with a thin layer of gold as previously described for SEM observation. Platelet shape was finally observed through a dual beam Zeiss Auriga Compact system equipped with a GEMINI Field-Emission SEM column operated at 5keV.

For the kinetic blood coagulation test, in order to evaluate the release of hemoglobin by residual erythrocytes that remained free during the clot formation; the assay was performed by recalcification of the anticoagulated whole blood. Samples were heated at 37°C for 5min, then 3ml of anticoagulated blood were putted onto the nanowires surface and incubated for further 5min. At the end of the 5min, calcium chloride solution (0,2mol/l) was added to start the coagulation cascade (time 0). Blood samples were shaked for 1min and incubated al 37°C for 10, 20, 30 and 40min. At experimental time points samples were shaken for other 10min and 500µl of distilled water were added to allow the lysis of free erythrocytes. The absorbance of the supernatants was measured at 540nm; since the relieved signal is due to the free erythrocytes, the absorbance is inversely proportional to the clot dimension. The average of the curve is the result of the average of three replicate experiments.

To perform a P-selectin release assay, nanowires samples were previously warmed at 37°C, then 400µl of PRP were positioned on the substrates and incubated for further 60min. After 60min PRP was collected, plasma was separated by centrifugation and soluble P-selectin was quantified through an immunosorbent assay (sP-Selectin ELISA Kit, Cusabio, Wuhan, P.R.China).

Statistical analysis – Data were analyzed using Prism7 (GraphPad, La Jolla, CA, USA). All the values are reported as the mean ± standard deviation of three repeated experiments. Differences among the groups were evaluated with either t-Test, one-way ANOVA or two-way ANOVA statistical tests and with the Tukey or Bonferroni post-test for multiple comparisons. Differences were considered significant when $p<0.05$.

7.3 Results

Sample characterization

Carbon-doped silica nanowires were grown with the described CVD method and after the process samples were observed through electron scanning microscopy to verify the homogeneous distribution of NWs on the substrates. SEM microphotograph (Figure 7.2) of SiO_xC_y NWs show a bundle of haphazardly disposed NWs which covered the entire substrate and resemble the disposition of collagen fibrils in connective tissues; NWs showed also the expected dimensions of diameter and length as shown in TEM microphotographs (Figure 7.3).

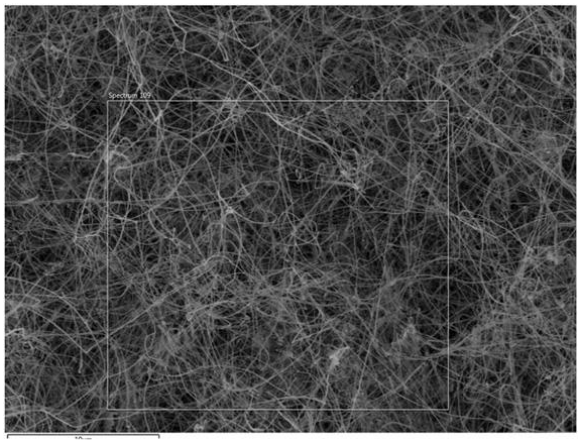

Figure 7.2: SEM microphotograph of SiO_xC_y NWs bundle on silicon substrate. The ROI labelled as Spectrum 109 was analyzed through EDX and the presence of a 3% of carbonium was confirmed.

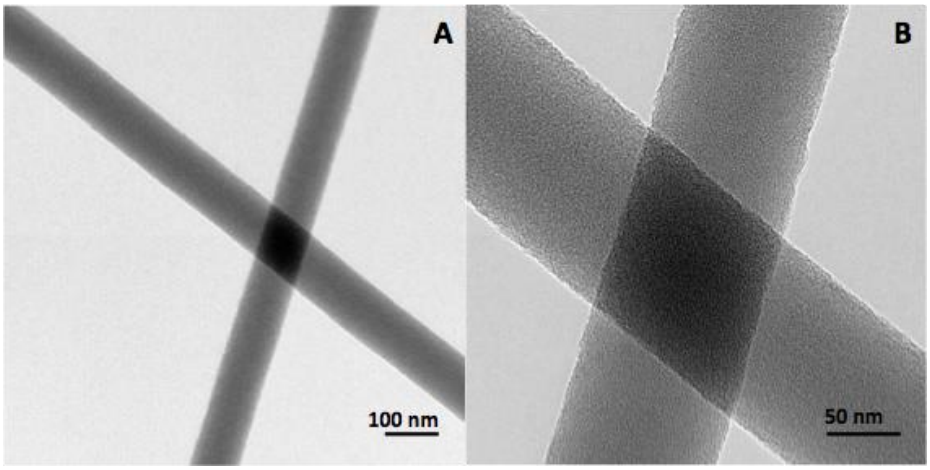

Figure 7.3: TEM microphotographs of two SiO_xC_y nanowires.

EXD analysis result confirmed the presence of a 3% carbonium part in the grown nanowires, as shown by the peaks in Figure 7.4.

Figure 7.4: EDX analysis SiO_xC_y nanowires.

Biological assays

Cell response to nanostructured material was analyzed through *in vitro* indirect and direct cytotoxicity assays. For indirect cytotoxicity assays ISO 10993-5 guidelines for porous materials instructions were followed to investigate the release of chemical agents from nanowires samples. Firstly, samples were soaked in complete medium for 1 or 10 days and the conditioned medium (medium after the incubation with nanowires) was collected and used to perform cell cultures. Cell viability after 24h of culture in conditioned medium was assessed with chemiluminescence assay and MTT assay, as previously described. Obtained data showed (Figure 7.5) that cell viability was unaffected by the conditioned medium at any concentration for both, chemiluminescence and MTT assays, that were very in agreement with each other and attested a viability greater than 95% not affected by any toxic contamination.

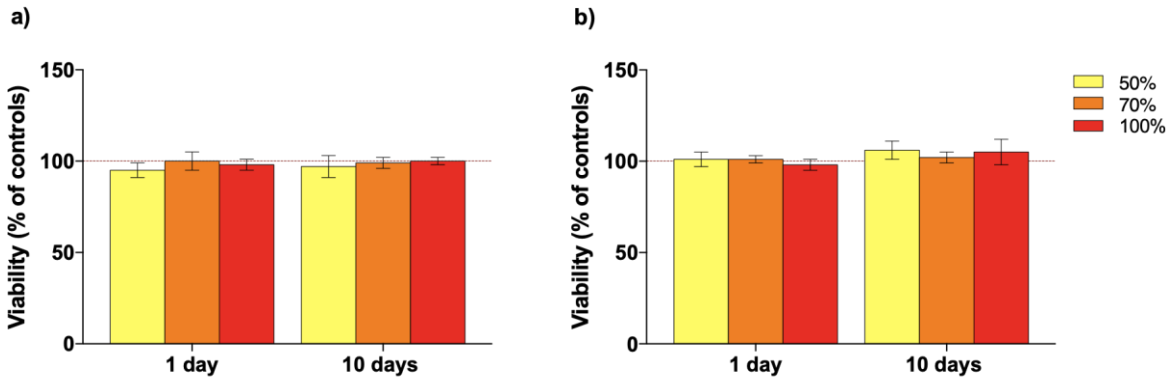

Figure 7.5: Histograms showing the viability of L929 cells according to the ISO 10993-5 protocol for indirect cytotoxicity assays. a) Chemiluminescent assay; b) MTT assay.

As well as indirect cytotoxicity tests, also direct contact test had a positive outcome; cells were seeded directly on nanowires substrates and on control flat SiO_2 and cultured for 24, 48 and 96h. At the experimental time points cells viability was assessed with a live and dead fluorescent staining (Calcein AM/Propidium Iodide), in particular, live cells were labeled in green and dead cells in red. As it is clear from Figure , cells were alive and healthy on both, flat SiO_2 and nanowires substrates, while dead cells were hardly detectable on the materials for every selected time point.

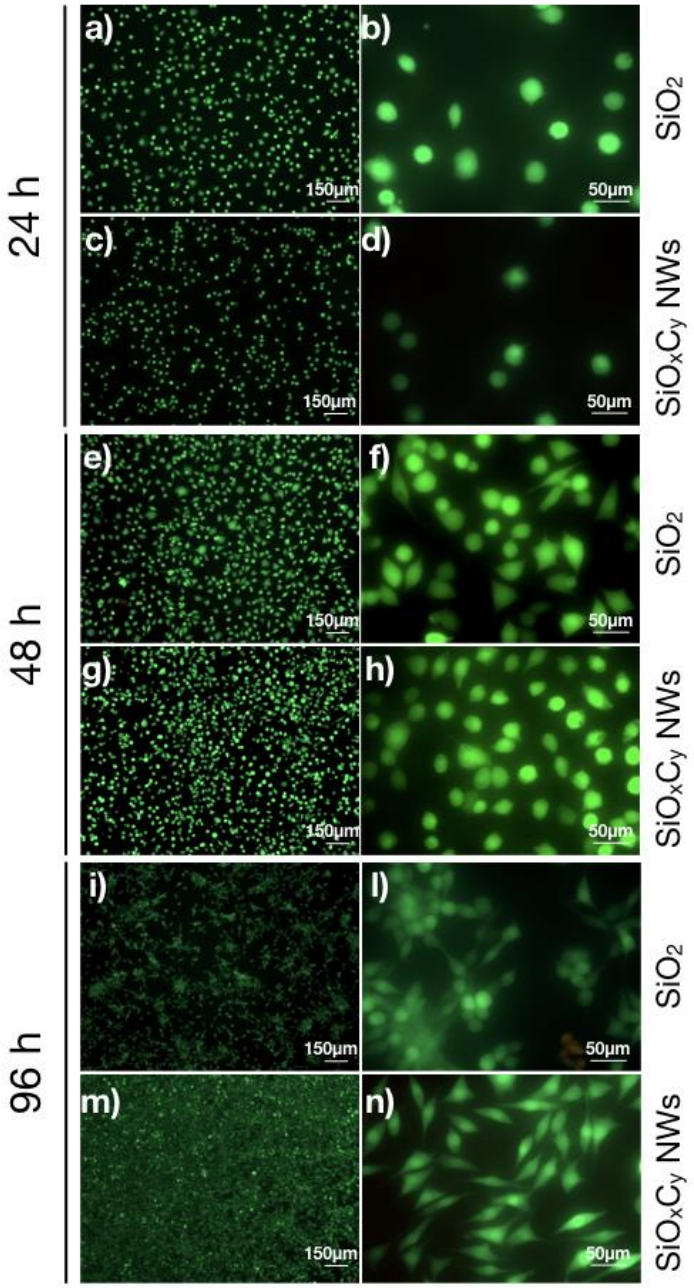

Figure 7.6: Fluorescence images of cells after 24, 48 and 96h from the seeding with a Calcein AM/Propidium iodide staining. The upper panel shows cells on flat SiO_2 substrate (a-b) and SiO_xC_y NWs (c-d) at 24h ; the middle panel shows cells on flat SiO_2 substrate (e-f) and SiO_xC_y NWs (g-h) at 48h and the lower panel shows cells on flat SiO_2 substrate (i-l) and SiO_xC_y NWs (m-n) at 96h.

As observable in the fluorescence images, cells grown on nanowires appeared well spread, elongated and homogeneously distributed (Figure c-d-g-h-m-n), while on flat control surface (Figure a-b-e-f-l-m) cells displayed a rounded shape and after 96 hours they seemed disposed very heterogeneously and well distributed clusters. Nevertheless, the percentage of area covered by live cells on both samples was measured and compared; as shown in Figure 7.6, the percentage of live cells was initially higher on the control, but at 96h cells on NWs caught on rapidly and covered much more substrate.

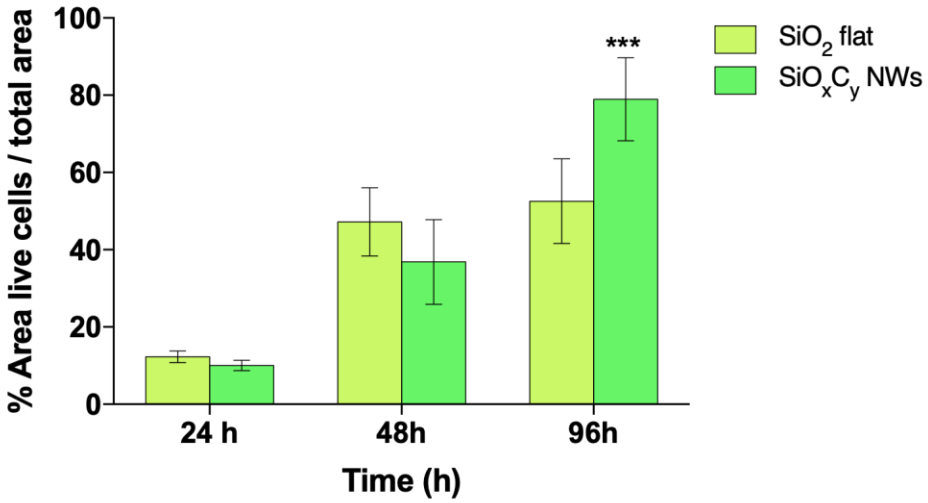

*Figure 7.6: Histogram showing the viability of cells on control flat SiO_2 substrate and silicon oxycarbide nanowires obtained through quantification of the area covered by live cells in the sample from Figure . Cells on nanowires were more numerous if compared to the flat surface after 96h of culture. ***p=0,0001.*

Moreover, to confirm the data, cell viability was quantitated through chemiluminescence (Figure 7.7) and the result was the same obtained with the fluorescence assay.

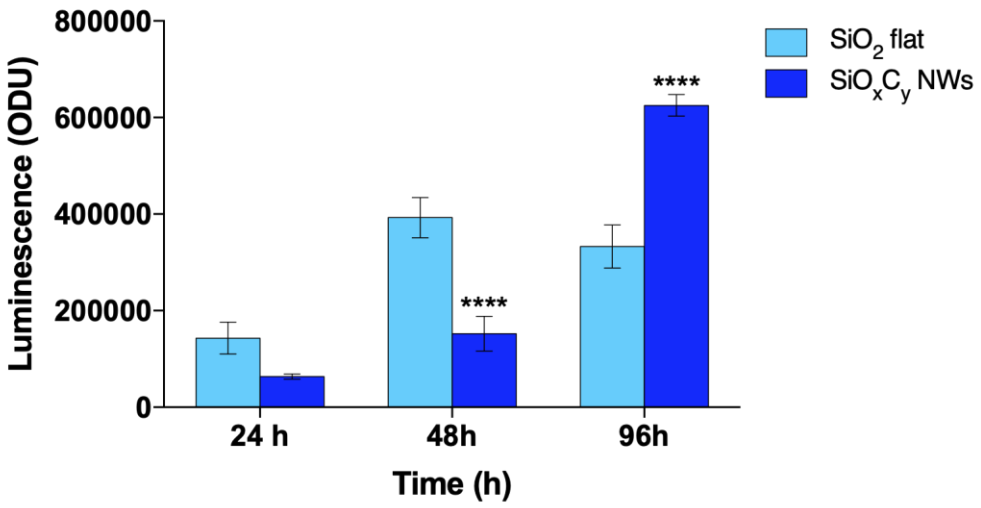

*Figure 7.7: Chemiluminescence assay developed on L929 cells after 24, 48 and 96h of culture on control flat SiO_2 substrate and silicon oxycarbide nanowires; consistently with Figure cells were less on silicon oxide control samples. ****p<0,0001.*

Consistently with the obtained data, cellular gene expression was analyzed through RT-PCR after 96h of culture and the results showed a much higher expression on the nanowires sample of the mRNA encoding for the synthesis of Cyclin D1 (Figure 7.8 a), key gene in the control of the progression of cell cycle. Nevertheless, no differences where observed in the expression of Alkaline Phosphatase and of Collagen type I (Figure 7.8 b-c).

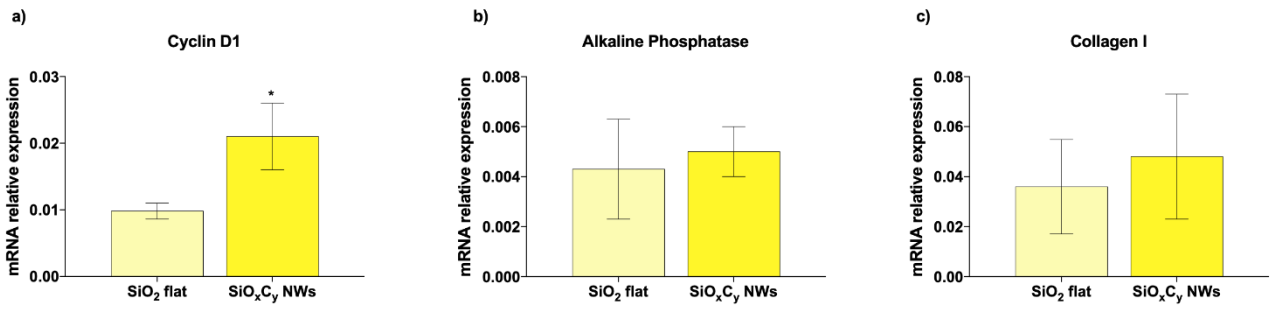

*Figure 7.8: mRNA expression quantitation obtained through RT-PCR for Cyclin D1, Alkaline Phosphatase and Collagen type 1 in L929 cell line cultured for 96h on SiO_2 and SiO_xC_y NWs. *p=0,196.*

To observe cell morphology and spreading, nanowires samples were evaluated by SEM in a time-course observation at 24, 48 and 96h after the seeding. After 24h (Figure 7.9 a-d) cells appeared healthy, with the typical polygonal shape, intact cytoplasm and numerous small cellular extroflections whose main duty seem to be the anchorage to the underlying surface. By 48h (Figure 7.9 b-e) cells were more numerous maybe due to the several mitotic figure easily observable on the samples. Finally, at 96h (Figure 7.9 c-f), a striking modification of the

nanowires bundle occurred, nanowires appeared often displaced and cavities were created in the material. It is worth of note that L929 colonized the material, shaping it in their advantage; in fact, the new established cavities are contoured by well adhered cells who often bridged on the hole surface. Moreover, images at higher magnification (Figure 7.10) underline a complex interaction between cells and surface, characterized by the spreading of cytoplasm across the nanowires and the disposition of cellular extroflections following the path of NWs, thus creating a long appendices that got interlocked with the NWs meshwork.

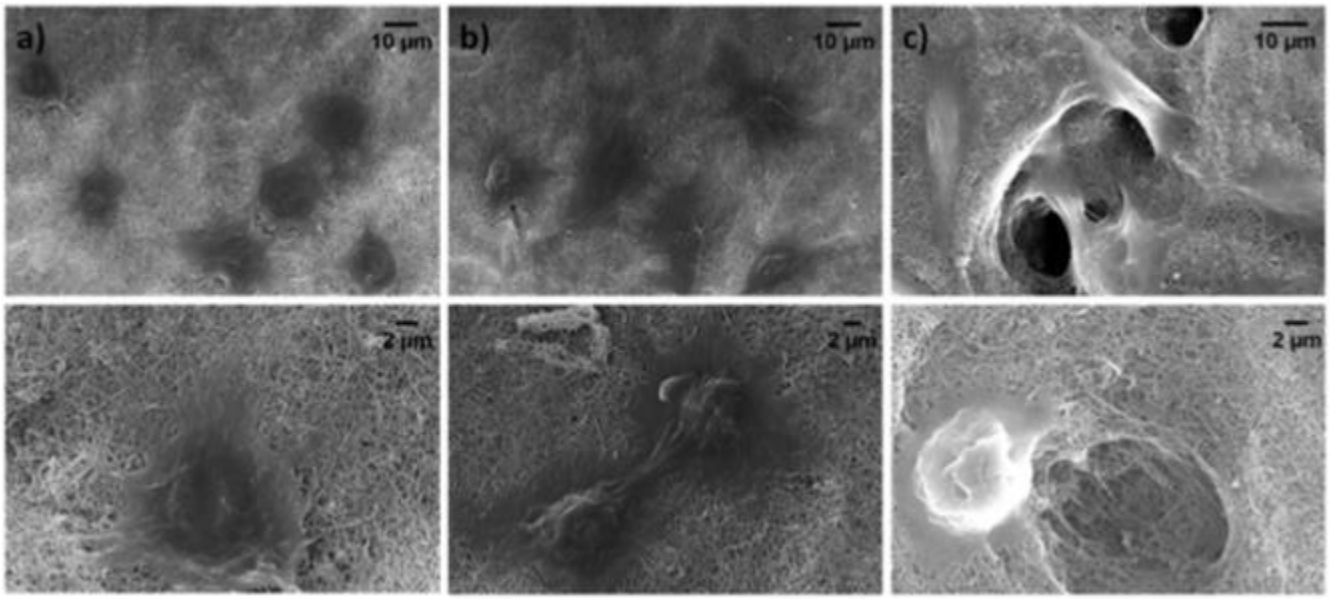

Figure 7.9: SEM images of L929 cultured for 24h (a-d), 48h (b-e) and 96h (c-f) on SiO_xC_y NWs substrates.

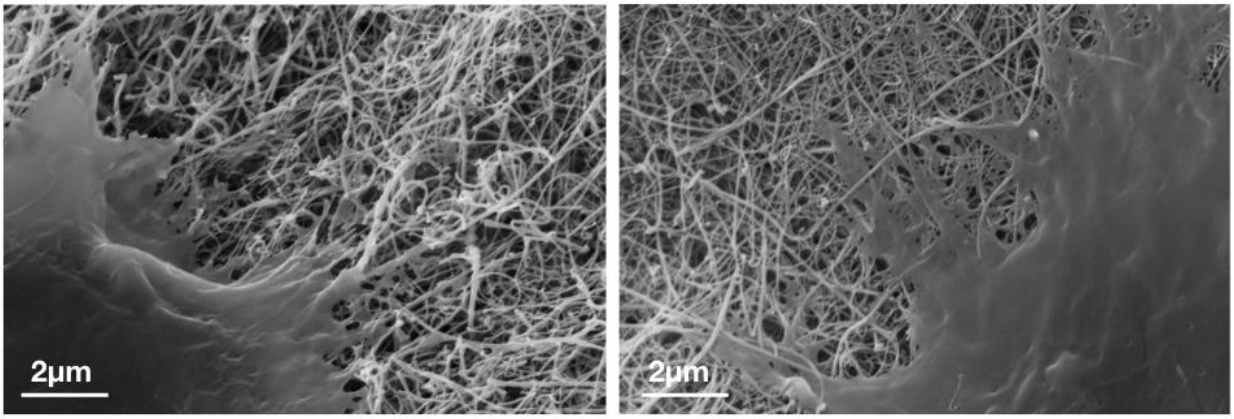

Figure 7.10: SEM enlargements of L929 cells on NWs after 24 hours of culture.

Blood interaction with nanowires sample were then investigated initially with SEM to verify whether nanowires morphology stimulated platelet activation. Figure 7.11 shows the samples of nanowires (a-c) and flat silicon oxide as control (b-d) with activated platelet. The early activation stage of platelet is characterized by the star-like shape

of the cell, while the octopus shape is more related to their complete activation; both the shapes were detectable on all the samples, as statement that nanostructured and bulk materials were quite similar in terms of platelet activation.

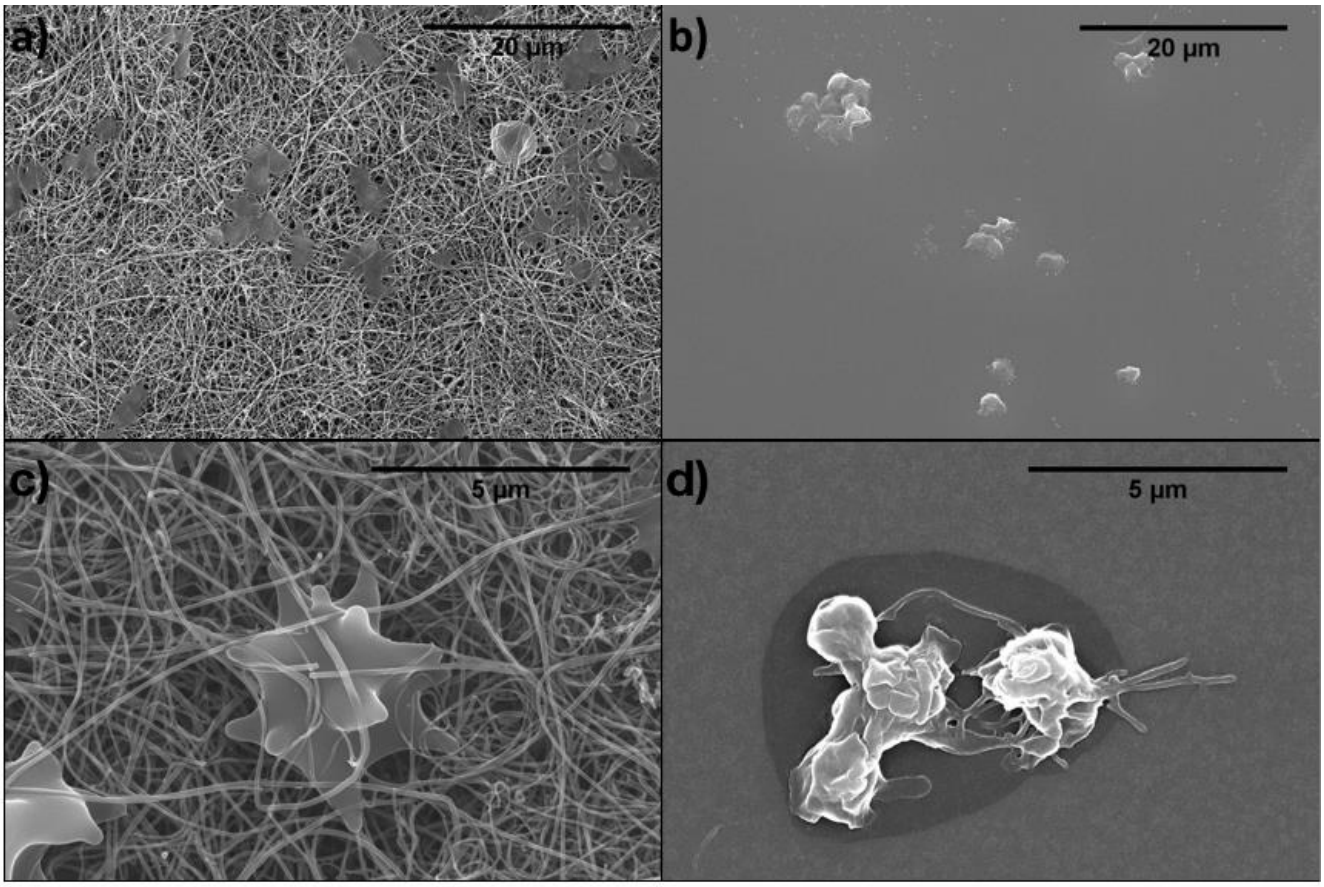

Figure 7.11: SEM microphotographs of platelets on silicon oxycarbide nanowires (a-c) and on flat silicon surface (b-d); the images highlighted the activation (in particular, the star-like shape) of platelets on both surfaces.

The release of P-selectin by platelets was evaluated with ELISA assay; as shown in Figure 7.12 the result confirms what already observed with morphologic investigation. No statistically significant differences of P-selectin release were observed between silicon oxycarbide nanowires and flat silicon oxide surface.

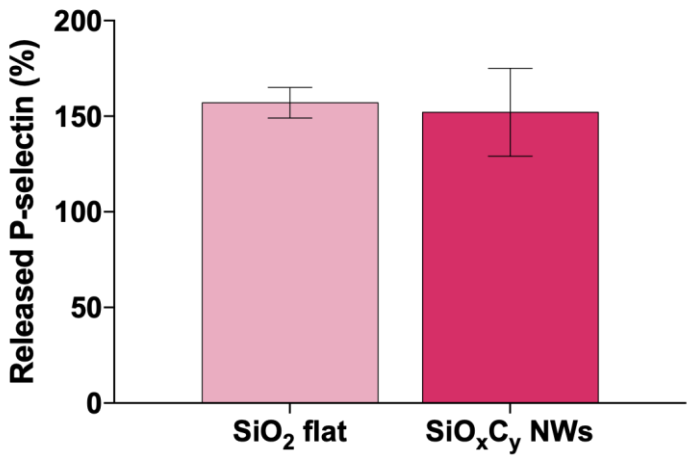

Figure 7.12: Histogram showing the result of ELISA assay for determination of P-selectin release on PRP and nanowires compared to flat silicon. The results confirm what observed in SEM images and shows comparable levels of platelets activation on both surfaces.

To complete the study, a kinetic blood clotting *in vitro* test was performed as previously described, to evaluate the response (for example the degree of activation of intrinsic coagulation factors) of blood when it comes in contact with the samples; the absorbance measured in function of time provide a measure of direct activation, since it represents the release of hemoglobin from erythrocytes. Normally, a biomaterial which has to be implanted needs to favor the blood coagulation cascade, as procoagulant properties are essential to develop a suitable biomaterial for tissue engineering. To this purpose, seen that a proportion of the erythrocytes present in the incubation were included in the clot of coagulation, the remaining ones has been lysate to determine the amount of hemoglobin released during kinetic clotting reactions in recalcified whole blood. Figure 7.13 shows the curves of kinetic of blood clotting of both materials in contact with blood; as it is clear from the image, flat silicon oxide surface had a slower and smooth downward inclined curve, while the slope curve of nanowires sample was more accentuated. This difference between the samples confirmed once again the SEM observations and underlines that on SiO_xC_y NWs sample clot formation is promoted, up until 40min, where the curves converged.

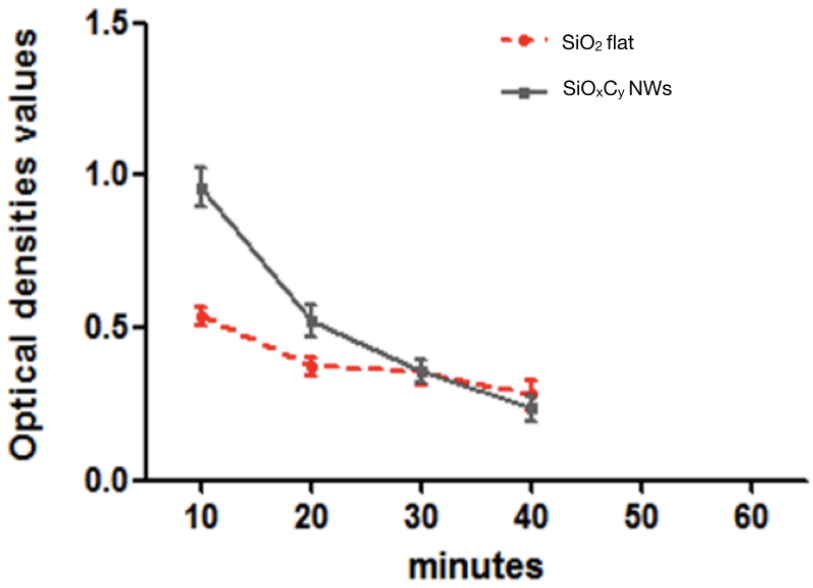

Figure 7.13: Graph showing the kinetic of clotting reactions of flat silicon oxide and silicon oxycarbide nanowires up to 40min. The result suggests different procoagulant propensities, probably due to the different morphology of the samples. A proportion of the erythrocytes present during the incubation was entrapped during the coagulation. Erythrocytes remaining in the solution phase were lysed and the absorbance of the released hemoglobin at 540 nm was determined. Absorbance-time was determined for hemoglobin release during kinetic clotting reactions in recalcified whole blood.

7.4 Discussion

The fundamental idea of regenerative medicine is to promote the creation of new regenerated tissue to replace the damaged one through the use of engineered scaffolds. Scaffolds are biocompatible structures hat provide cells with a support for growth and activity, mimicking the natural extracellular matrix and ideally acting as its surrogate. ECM is composed of many different structures as collagen, elastin, and numerous non-collagenic proteins and it is responsible of the mechanical characteristics of the growth tissue, for the supplying with nutrients resident cells and for governing cell activity[12]. The contact of a biomaterial with cells is important because it can lead cells to adhere, migrate and proliferate in order to produce more matrix components and remodel it to attain the features of pristine ECM. The aim of the present study was to develop a carbon-doped silica (silicon oxycarbide) nanowires substrate, with higher carbon content than usual silica and to investigate the behaviour of L929 murine fibroblasts. Nanowires possess a very peculiar morphologic resemblance to natural ECM fibrils and due to their nanoranged size, are able to interact with cells in the dimension of receptors and molecules. Moreover, nanowires composition can be easily controlled during the synthesis process. SiO_xC_y was chosen because of its known biocompatibility and lack of toxicity, immunogenic activity and is therefore not constrained within the limits of natural biomaterials[5]. The CVD synthesis process previously reported allows to obtain silicon oxycarbide nanowires by using carbon monoxide as gaseous dopant precursor, a material which is a potential and attractive candidate for biomedical applications due to its higher elastic modulus, bending strength and hardness, and chemical durability[10]. In these regards, we investigate the biological response to nanowires structured biomaterial, following the ISO 10993 guidelines about the "Biological evaluation of medical devices" and especially its part 5 for in-vitro cytotoxicity testing. In fact, biocompatibility assessment is essential for pre-clinical testing of materials intended for use as implantable devices, due to the necessity of a biomaterial to be biocompatible both in the short term and in the long term when implanted *in vivo*. In particular, NWs could release toxic chemical species into the surrounding environment, thus potentially harmful for the surrounding tissues; also, silicon oxycarbide nanowires characteristics had to be studied and their compatibility with cells had to be assessed, as their shape, geometry or stiffness could be not attractive for cell ingrowth leading to the failure of the scaffold colonization. According to ISO 10993-5, in our study both, indirect and direct contact cytotoxicity assays were developed; ISO contact cytotoxicity assays assumes that a material is declared as biocompatible if cell viability is over 70%, and our results demonstrated that this criterion was met by the analysed NW structures, as mean cell viability was about 95% at the indirect assay and did not show sign of toxic agents release[13]. As well as indirect contact cytotoxicity assays, also direct contact assays provided interesting insights for biomedical applications, as showed by the fluorescence staining, where also the cell morphology underlined healthy cells, and its quantification. Based on viability and fluorescence assays, cells appeared initially more numerous on SiO_2 flat samples than on NWs; it could be argued

that quantitation of cell-covered area may not completely reflect cell number, when cells grow in clusters. Actually, cells on flat silica did tend to form clusters, however, the chemiluminescence-based proliferation assay confirmed our fluorescence data (unlike for indirect contact cytotoxicity assay, the use of a test as MTT, was not feasible, as this assay is based on redox reactions, and these substrates appeared to profoundly affect MTT). Moreover, it could seem that nanowires particular shape and size may make more difficult cell adhesion, because they offered little room for cells to attach on, but the interface between cells and nanowires appears more complex than imagined, in fact, as shown in Figure 7.10, there is an interplaying with nanowires passing under, over and sometimes through cell cytoplasm. This could appear as a point of weakness of nanowires substrates, but it is clear from the viability assay and fluorescence staining that L929 on nanowires rapidly caught up and outgrew at 96h, probably after starting to produce their own matrix on the material. Nevertheless, it cannot be said that the NWs 3D environment itself may have offered some advantages to later proliferation due to topographical or geometric cues, a very actual field of investigation due to the potential to bridge the gap between *in vitro* models and *in vivo* investigations by providing cell substrates that more closely mimic the architecture of natural tissues[14]. Very interesting is the ability of L929 to alter the profile of the nanowires bundle probably by pulling on nanowires through their actomyosin complexes. In fact, it is already known the capability of cells to generate an internal pre-stress tension with myosin and to pull the substrate on which they are growing on. The activation of myosin allows cells to change the substrate they are growing on and consequently to affect their own activity and differentiation due to the alteration by mechanical forces of the cytoskeletal conformation[15-17]; the relative substrate resistance activates various mechanical and intracellular pathways which direct cell fate. Our results show that L929 are for real capable to change the structure of the substrate, creating holes and pits in the nanowires matrix and colonizing that areas. The important key of the result is that the holes created by growing cells strictly resemble the porosity of some natural tissues, as for example the trabecular bone; it has been shown that scaffold parameters such as the presence of pores and pore size, fundamental characteristic of biomaterials, affects intra-cell force distribution and cell activity[18, 19]. No less than, cells appeared to grow even better in a such reorganized area, maybe due to a more close package of nanowires and the possibility for integrins to cluster more easily; fortunately, SiO_xC_y NWs scaffold could rely on an inherent plasticity that would enable them to adapt to the needs of the ingrowing cell population and provide a proper environment for matrix deposition. In addition, gene expression analysis results highlighted that in L929 cells cultured on nanowires substrates the level of transcript for the Cyclin D1, gene that controls the progression through the cell cycle, index that nanowires bundle did not impaired cell metabolic activity. Albeit non significantly, also the levels of mRNA for Collagen I and Alkaline phosphatase tended to be higher on nanowires bundle, probably due to the cytoskeleton stimulation and enhanced extracellular matrix production. The subsequent passage was the determination that nanowires could

provide a provisional matrix for incoming cells promoting the formation of such scaffold by triggering blood clotting. The data we obtained with SEM and immunoassay, showed that carbon-doped SiO_xC_y nanowires retain the platelet-activation properties of flat silicon, and that NW presence does not impair platelet activation, which is a pivotal event in wound healing, since platelet possess granules which store a large amount of bioactive compounds including the Platelet-Derived Growth Factor, which can act as a mitogen and stimulate the proliferation of precursors, that early event the whole fate of the regeneration approach ultimately depends on[20].

In conclusion, the cytotoxicity of silicon oxycarbide nanowires network, its effect on cell adhesion and proliferation, by indirect and direct contact tests according to ISO 10993-5 guidelines and on platelet activation has been evaluated. The results obtained *in vitro* with mouse fibroblasts cells showed that NWs did not release cytotoxic species and may represent a suitable platform for cell growth; moreover, we highlighted the capability of fibroblasts to reorganise the NWs network, adapting it to their own needs. Platelet activation assay and dynamic blood coagulation tests showed that nanowires can favour platelet activation and consequently active the metabolic cascade leading to tissue reparation. All the data together indicate that carbon-doped silicon oxycarbide nanowires are promising biomaterials for implantable scaffold in tissue engineering applications since they provide direct stimuli to cell growth and differentiation, activating the platelet and promoting the metabolic cascades.

References

1. Lagonegro, P.; Rossi, F.; Galli, C.; Smerieri, A.; Alinovi, R.; Pinelli, S.; Rimoldi, T.; Attolini, G.; Macaluso, G.; Macaluso, C.; Saddow, S. E.; Salviati, G., A cytotoxicity study of silicon oxycarbide nanowires as cell scaffold for biomedical applications. Mater Sci Eng C Mater Biol Appl 2017, 73, 465-471. DOI: 10.1016/j.msec.2016.12.096.

2. Colombo, P.; Bernardo, E.; Biasetto, L., Novel Microcellular Ceramics from a Silicone Resin. Journal of the American Ceramic Society 2004, 87 (1), 152-154. DOI: 10.1111/j.1551-2916.2004.00152.x.

3. Tamayo, A.; Rubio, J.; Rubio, F.; Oteo, J. L.; Riedel, R., Texture and micro-nanostructure of porous silicon oxycarbide glasses prepared from hybrid materials aged in different solvents. Journal of the European Ceramic Society 2011, 31 (9), 1791-1801. DOI: https://doi.org/10.1016/j.jeurceramsoc.2011.02.039.

4. Du P, W. X., Lin I K, Zhang X, Effects of composition and thermal annealing on the mechanical properties of silicon oxycarbide films. Sensors Actuators, A Phys. 176 90–8, 2012.

5. Zhuo, R.; Colombo, P.; Pantano, C.; Vogler, E. A., Silicon oxycarbide glasses for blood-contact applications. Acta Biomaterialia 2005, 1 (5), 583-589. DOI: https://doi.org/10.1016/j.actbio.2005.05.005.

6. Onclin, S.; Ravoo, B. J.; Reinhoudt, D. N., Engineering Silicon Oxide Surfaces Using Self-Assembled Monolayers. Angewandte Chemie International Edition 2005, 44 (39), 6282-6304. DOI: 10.1002/anie.200500633.

7. Rossi, F.; Bedogni, E.; Bigi, F.; Rimoldi, T.; Cristofolini, L.; Pinelli, S.; Alinovi, R.; Negri, M.; Dhanabalan, S. C.; Attolini, G.; Fabbri, F.; Goldoni, M.; Mutti, A.; Benecchi, G.; Ghetti, C.; Iannotta, S.; Salviati, G., Porphyrin conjugated SiC/SiOx nanowires for X-ray-excited photodynamic therapy. Sci Rep 2015, 5, 7606. DOI: 10.1038/srep07606.

8. Fabbri, F.; Rossi, F.; Melucci, M.; Manet, I.; Attolini, G.; Favaretto, L.; Zambianchi, M.; Salviati, G., Optical properties of hybrid T3Pyr/SiO2/3C-SiC nanowires. Nanoscale Res Lett 2012, 7 (1), 680. DOI: 10.1186/1556-276x-7-680.

9. Kuo, S. W.; Lin, H. I.; Ho, J. H.; Shih, Y. R.; Chen, H. F.; Yen, T. J.; Lee, O. K., Regulation of the fate of human mesenchymal stem cells by mechanical and stereo-topographical cues provided by silicon nanowires. Biomaterials 2012, 33 (20), 5013-22. DOI: 10.1016/j.biomaterials.2012.03.080.

10. Fabbri, F.; Rossi, F.; Negri, M.; Tatti, R.; Aversa, L.; Dhanabalan, S. C.; Verucchi, R.; Attolini, G.; Salviati, G., Carbon-doped SiO(x) nanowires with a large yield of white emission. Nanotechnology 2014, 25 (18), 185704. DOI: 10.1088/0957-4484/25/18/185704.

11. Rossi F, F. F., Attolini G, Bosi M, Watts B E, Salviati G, TEM and SEM-CL Studies of SiC Nanowires Mater. Sci. Forum 645-648 387–390 2010

12. Chen, G.; Dong, C.; Yang, L.; Lv, Y., 3D Scaffolds with Different Stiffness but the Same Microstructure for Bone Tissue Engineering. ACS Applied Materials & Interfaces 2015, 7 (29), 15790-15802. DOI: 10.1021/acsami.5b02662.

13. International Organization for Standardization - I.S.O. 10993, B. E. o. M., in 5-Tests for In Vitro Cytotoxicity., Geneva, Switzerland, 2009.

14. Knight, E.; Przyborski, S., Advances in 3D cell culture technologies enabling tissue-like structures to be created in vitro. Journal of Anatomy 2015, 227 (6), 746-756. DOI: 10.1111/joa.12257.

15. Engler, A. J.; Sen, S.; Sweeney, H. L.; Discher, D. E., Matrix Elasticity Directs Stem Cell Lineage Specification. Cell 2006, 126, 677.

16. Kilian, K. A.; Bugarija, B.; Lahn, B. T.; Mrksich, M., Geometric cues for directing the differentiation of mesenchymal stem cells. Proceedings of the National Academy of Sciences 2010, 107 (11), 4872. DOI: 10.1073/pnas.0903269107.

17. Ingber, D. E.; Wang, N.; Stamenović, D., Tensegrity, cellular biophysics, and the mechanics of living systems. Reports on Progress in Physics 2014, 77 (4), 046603. DOI: 10.1088/0034-4885/77/4/046603.

18. Reilly, G. C.; Engler, A. J., Intrinsic extracellular matrix properties regulate stem cell differentiation. Journal of Biomechanics 2010, 43 (1), 55-62. DOI: https://doi.org/10.1016/j.jbiomech.2009.09.009.

19. Galli, C.; Parisi, L.; Piergianni, M.; Smerieri, A.; Passeri, G.; Guizzardi, S.; Costa, F.; Lumetti, S.; Manfredi, E.; Macaluso, G. M., Improved scaffold biocompatibility through anti-Fibronectin aptamer functionalization. Acta Biomaterialia 2016, 42, 147-156. DOI: https://doi.org/10.1016/j.actbio.2016.07.035.

20. Schlessinger, J., How receptor tyrosine kinases activate Ras. Trends Biochem Sci 1993, 18 (8), 273-5. DOI: 10.1016/0968-0004(93)90031-h.

Chapter 8 - Osteoblasts adhesion and response mediated by terminal -SH group charge surface of SiO_xC_y nanowires

From: Osteoblast adhesion and response mediated by terminal -SH group charge surface of SiOxCy nanowires[1].
Published in Journal of Material Science: Materials in Medicine (2019) 30:43
DOI: 10.1007/s10856-019-6241-y

Abstract

To promote cell colonization of a scaffold and progenitors' differentiation, robust cell adhesion is fundamental. In this chapter is proposed the functionalization of oxycarbide (SiO_xC_y) nanowires with a molecule containing -SH terminal groups, 3-mercaptopropyltrimethoxysilane (MPTMS). The objective of this functionalization is to develop a -SH modified SiO_xC_y nanowires-surface (MPTMS-NWs) capable to adsorb proteins and promote cell adhesion, proliferation and differentiation. It was observed that functionalization affected in a remarkable way the adsorbed protein pattern as well as the *in vitro* proliferation of murine osteoblasts (MC3T3-E1), which was increased on functionalized nanowires if compared to pristine SiO_xC_y nanowires ($p<0,0001$). As confirmed by immunofluorescence images, cells showed a stronger adhesion on MPTMS-NWs than on control NWs, revealing a more homogeneous vinculin distribution in the cytoplasm. An upregulation of mRNA for Alkaline phosphatase and Collagen type I was also detected, putative markers of osteoblasts early differentiation phase.

These results suggest that 3-mercaptopropyltrimethoxysilane functionalization on a SiO_xC_y nanowires-substrate enhance cell growth, adhesion and the gene expression of osteoblastic phenotype, providing an interesting strategy to improve the biocompatibility and the cellular response of silicon-based nanomaterials for regenerative medicine applications.

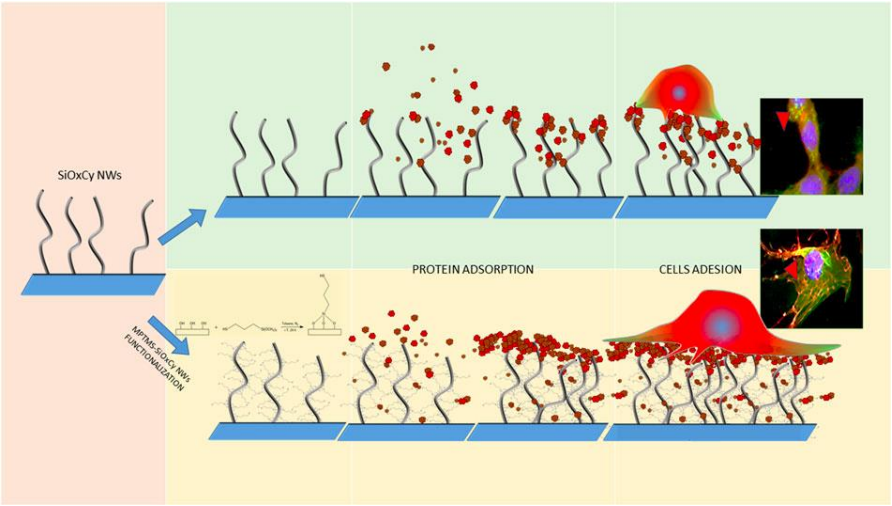

Figure 8.1: Graphical abstract of the chapter.

8.1 Introduction

Extracellular matrix encompasses micro and nanoscale aspects, acting as cues for cell, modulating their behavior and functionality. The ideal goal to create a suitable scaffold to promote tissue engineering and regeneration of tissues is based on the idea that the scaffold has to resemble the biomechanical properties of the targeted tissue and to serve as a host for either endogenous or implanted cells by supporting cell adhesion, migration, proliferation and differentiation. The emergence of nanotechnologies paves the way to numerous possibilities to comply with the nanoscale features of the human body, in the same dimensional range of cells, biomolecules, receptors and atoms[2-5]. Nowadays exist a large amount of implantable materials for a wide range of clinical applications, but many of them still requires improvement. In fact, since natural tissues and organs are structured in nanometric dimension, cells directly interact with ECM components; in this view, biomaterials chemical, physical and more than all topographical properties play a pivotal role in stimulating cell adhesion and proliferation. During cell response to a biomaterial, microscale structural aspects principally affect cell functionality (for example based on the shape of the material), while the nanoscale features predominantly trigger their effects through the plasmatic membrane components as it occurs for receptors or integrins. The information from extracellular environment are strictly associated to the input gave from integrin-based adhesion complexes, which are directly related to the actin cytoskeleton and regulates intracellular response and signaling cascade[6-10]. in the last few years nanotechnologies developed a number of materials with nano-patterned surfaces or with the possibility to modulate their surface to comply the nanoscaled environment of cells. In this arena, nanowires appear as suitable candidates for the design of biomimetic materials with a well-defined nanoscaled surface and useful for regenerative medicine applications. Nanowires substrates are composed by a disorganized three-dimensional meshwork whose spatial disposition strongly remember the organization of many human tissues (e.g. collagen I fibrils disposition or trabeculae of alveolar bone)[11]. Among all the material which can be used to produce nanowires, silicon is the one which shows more possibilities to be applied in clinical routine thanks to its interesting features; in particular, silicon oxycarbide presents high elastic modulus, strength and hardness, chemical stability and resistance in harsh environment; moreover, it has been seen to promote platelet activation, prompting rapid clot formation, essential in wound healing[12]. It is also known that proteins interact differently if the material possesses a nanometric dimension on the surface and that the layer of adsorbed proteins presents at the interface between biomaterial and cells in strongly influenced by the nanometric topography of the surface[4, 13, 14]. Silicon oxycarbide nanowires can as well be easily functionalized with a large number of molecules, to create a biomimetic material able to stimulate appropriate cell response[15].

To this purpose, Ghezzi et al. showed how functionalize silicon oxycarbide nanowires with 3-mercaptopropyltrimethoxysilane, a molecule containing silane groups able to interact with silicon oxide and that

presents free thiol groups able to retain and interact with plasma proteins through the formation of solid disulfide bridges. Besides, the silanization is a relatively fast method to tune the chemical properties of a surface and it has been demonstrated that in cells growth in an SH-modified environment it is stimulated osteogenesis *in vitro*, while other terminal groups allow the maintenance of mesenchymal stem cell phenotype[16]. In this regard, the hypothesis at the basis of our work is the possibility to ameliorate nanowires substrates through chemical functionalization in order to provide cells with a nanostructured surface able to support and foster cell proliferation and differentiation.

8.2 Materials and methods

Sample functionalization

SiO_xC_y NWs were grown on silicon substrate through an established CVD process (described in chapter 4), at a temperature of 1070°C, with CO as dopant precursor to obtain carbon-doped under-stoichiometric SiO_2 NWs. After SiO_xC_y NWs synthesis and characterization, the NWs substrate was functionalized with 3-mercaptopropyltrimethoxysilane (MPTMS) in order to develop a -SH modified SiO_xC_y nanowires-surface (MPTMS-NWs).

Functionalization of SiO_xC_y NWs with MPTMS occurred soaking the silicon surfaces with nanowires in 10ml of toluene solution and subsequently adding to the solution 15µl of 3mM 3-mercaptopropyltrimethoxysilane (MPTMS, 95% pure, Sigma-Aldrich). The mixture was then kept under N_2 constant flow for 24h, at room temperature (RT) and finally samples were rinsed in toluene and dried in vacuum.

Figure 8.2 shows the diagram of the functionalization strategy used to ameliorate NWs surface and to facilitate protein and cell binding to the material.

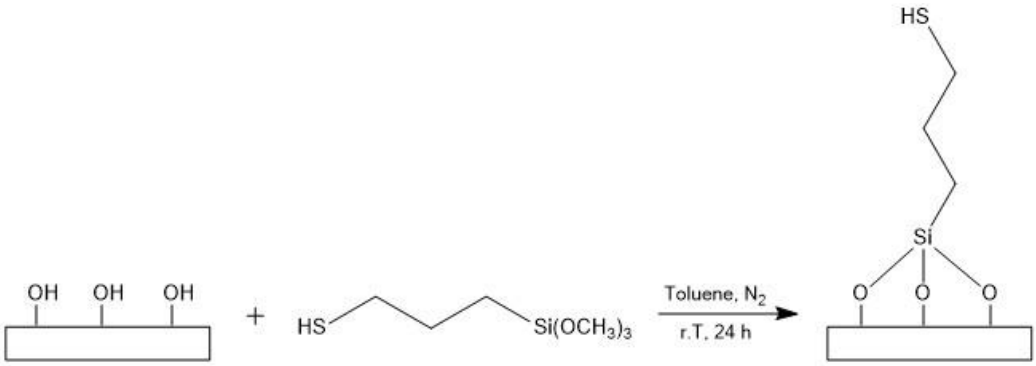

Figure 8.2: Scheme of the functionalization strategy. 3-mercaptopropyltrimethoxysilane was anchored to the SiO_xC_y NWs by binding to the -OH groups present on NWs surface; the final result is the presence of an additional free -thiol group available for protein binding.

Sample characterization

X-ray Photoelectron Spectroscopy – The presence of MPTMS was initially evaluated with X-ray Photoelectron Spectroscopy (XPS). XPS occurred with an X-ray photon source Mg-Kα emission at 1253.6 eV and a VSW HA100 hemispherical analyzer with a total energy resolution of 0.86eV was used to analyze the photoelectrons. The Au 4 f 7/2 peak at 84.0eV was used as reference for the calibration of the core level position, indicated by their binding energy (BE). The lineshape of all core levels (C1s, O1s, Si2p and S2p) were analyzed through a Voight function with

a Lorentzian-Gaussian fixed ratio of 0.3, following a Shirley background subtraction. The error related to the energy peak is ±0.05eV, while the precision for full width at half-maximum (FWHM) and for area evaluation was less than ±5% and ±2,5%, respectively.

Z-Potential analysis – To control if the functionalization had occurred, an analysis of surface electronegativity was done through measurement of the Z-Potential. Briefly, NWs were detached from the substrate by ultrasonicating with a Misonix, Ultrasonic Liquid Processor S-400 (New Highway, Farmingdale, NY 11735, USA). After NWs resuspension in phosphate buffer saline (PBS, Thermo Fisher Scientific, Waltham, MA, USA), they were sonicated 10 min to obtain a homogeneous suspension and subsequently diluted in culturing medium. An aliquot was then transferred to acrylic cuvettes and a measure of the Z-Potential was taken with a Zeta Potential Plus Analyzer (Brookhaven Instrument Corporation, NY, USA).

Protein adsorption studies

SDS PAGE – The quantification of serum protein adsorbed to MPTMS-NWs, an SDS-PAGE with Comassie staining was performed. In particular, samples were first incubated with 500µl of PBS supplemented with 2% Human Serum (HS, Sigma-Aldrich) for 1h at RT and subsequently washed twice in PBS to remove any unstable binded protein. Then samples were covered with 80µl of sample buffer 1X (Tris-HCl 62,5mM pH 6,8, SDS 1,5%w/v, DTT 100mM, with traces of Bromophenol Blue) and to obtain a complete recovery samples were freezed, thawed and sonicated for 15 min and finally boiled for 10 min. Standard and equal volume of samples were then loaded on 12% polyacrylamide gel (Acrylamide/BisAcrylamide 30%, Sigma-Aldrich and samples were separated at 180V for 1h. The obtained gels were exposed to Comassie solution (Comassie Brilliant Blue, Bio-Rad, USA) for protein staining.

Cell assays

Cell cultures – Cell assays were performed with murine osteoblastic cells (MC3T3-E1) obtained from the ATCC (LGC Standards srl, Milan, Italy). Cells were cultured in complete alpha-MEM (a-MEM, Thermo Fisher Scientific) supplemented with 10% FBS, 1% Penicillin and Streptomycin (PenStrep, Thermo Fisher Scientific) and 1% L-Glutamine (Thermo Fisher Scientific).

For cell culture experiments, cells were seeded on both SiO_xC_y NWs and MPTMS-NWs substrates (size 0,5cm x 0,5cm) at a final density of 20.000 cells/sample for viability assay, cell morphology observation and immunofluorescence, and of 40.000 cells/sample for gene expression analysis.

Cell viability assay – To quantify the amount of viable cells after 24h and 48h from plating on SiO_xC_y NWs and MPTMS-NWs substrates, a chemiluminescence assay (CellTiter-GLO, Promega, Madison, WI, USA) and a live/dead fluorescent staining were performed following manufacturer's instructions. Briefly, culture medium was discarded, samples were rinsed in PBS and a 50:50 solution of CellTiter-GLO Lysis Buffer and complete culture medium was added. Each sample was incubated for 2 min on an orbital shaker, the solution was collected, and luminescence was stabilized for 10 min in the dark. Samples were centrifuged for 30 sec to eliminate every bubble of the solution and subsequently luminescence was measured with a luminometer with double injectors (GLOMAX 20/20, Promega).

Scanning electron microscopy and Focused Ion Beam– To observe cell morphology and the interaction with the underlying substrate, scanning electron microscopy (SEM) morphological analysis was performed after 48h of culture. Cells were fixed with 2.5% glutaraldehyde (Sigma-Aldrich) solution in 0,1M Na-Cacodylate buffer for 30 min at RT, thus washed in Na-Cacodylate buffer for 5 min at RT and subsequently dehydrated in an ascendant series of ethanol (Sigma-Aldrich) at RT, for 10min each alcohol (EtOH 35%, 50%, 70%, 75%, 90%, 95%, 99%). Specimens were then coated with a nanometric gold layer through a SCD 040 coating device (Balzer Union, Wallruf, Germany) and studied using a dual beam Zeiss Auriga Compact system equipped with a GEMINI Field-Effect SEM column and a Gallium Focused Ion Beam (FIB) source (Zeiss). SEM analysis was performed at 5keV while cross-sectional analysis with FIB was performed with a Gallium Ion Beam at 30kV with a current of 10pA.

Immunofluorescence – Cytofluorescence was developed to observe the expression and distribution of focal adhesions, cell morphology and actin fibers organization. After 24h of culture, samples were rinsed in PBS and fixed in 4% paraformaldehyde solution (PFA, Sigma-Aldrich) for 10 min at RT. After two rinses in PBS, cells were permeabilized with 0.1% v/v TritonX-100 (Sigma-Aldrich) for 5 min at RT and washed twice in PBS. To block antibody aspecific binding sites, a 1% Bovine Serum Albumin solution (BSA, Sigma- Aldrich) was applied for 30min at RT and subsequently substituted with a solution of primary anti-Vinculin monoclonal antibody, clone 7F9 (1:100 dilution) (FAK100, Merk Millipore, Darmstadt, Germany) in BSA, for 1h at RT. After double rinse in PBS, to reveal the primary antibody, a secondary anti-mouse labeled with AlexaFluor ®488 chromophore (dilution 1:200) (Thermo Fisher Scientific), was co-incubated with a TRITC-conjugated phalloidin antibody (1:200 dilution) (FAK100, Merck Millipore), for 1h at RT. After three washes with PBS, nuclear counterstaining was performed by sample

incubation with DAPI (FAK100, Merck Millipore). Samples were then transferred on a microscope glass and a drop of mounting medium (DakoCytomation Fluorescence Mounting Medium, Dako, Carpinteria, CA, USA) was added before fluorescence microscope observation. Sample images were taken with a microscope equipped for fluorescence Zeiss Axio Imager A2 (Zeiss, Oberkochen, Germania).

Gene expression analysis – To observe if there were differences in terms of gene expression among the functionalized or not samples, after 96h of culture total RNA was extracted using TriZol (Thermo Fisher Scientific), according to manufacturer's indications. The purity of extracted RNA was measured through a NanoPhotometer™ P class (Implen GmbH, München, Germania) and subsequently RNA was retrotranscribed to cDNA with a High Capacity cDNA Reverse Transcription Kit (Thermo Fisher Scientific). TaqMan quantitative RT-PCR was performed on samples through a Real Time PCR machine (StepOne Plus, Life Technologies) and using the following primer probe sets from Life Technologies (Foster City, CA, USA): Alkaline Phosphatase (ALP, Mm00475834_m1); Collagen type I (COL1A1, Mm00801666_g1); Runt related transcription factor 2 (Runx2, Mm00501584_m1); Osteocalcin (OCN, for 5'-GCTGCGCTCTGTCTCTCTGA-3'; rev 5'-TGCTTGGACATGAAGGCTTTG-3';probe 5'-FAM-AAGCCCAGCGGCC-NFQ-3'); mouse glyceraldehyde-3-phosphate dehydrogenase (GAPDH) was used as housekeeping gene (Mm99999915_g1).

Statistical analysis – Data were analyzed using Prism6 (GraphPad, La Jolla, CA, USA). All the values are reported as the mean ± standard deviation of three repeated experiments. Differences among the groups were evaluated with either t-Test, one-way ANOVA or two-way ANOVA statistical tests and with the Tukey or Bonferroni post-test for multiple comparisons. Differences were considered significant when $p<0.05$.

8.3 Results

X-ray Photoelectron Spectroscopy analysis

XPS analysis was performed on control SiO_xC_y NWs and on MPTMS-NWs after functionalization to verify the success of the silanization process measuring the amount of sulphur present in the thiol groups characteristics of 3-mercaptopropyltrimethoxysilane.

In Figure 8.3 the main peak of core levels present in the samples are highlighted; it is notably from a first analysis of the spectrum that the mainly represented elements are carbon (C), silicon (Si) and oxygen (O), accordingly with the composition of our nanostructures. In MPTMS-NWs, two peaks at 400eV and 190eV are due to the grid and they were not taken into consideration.

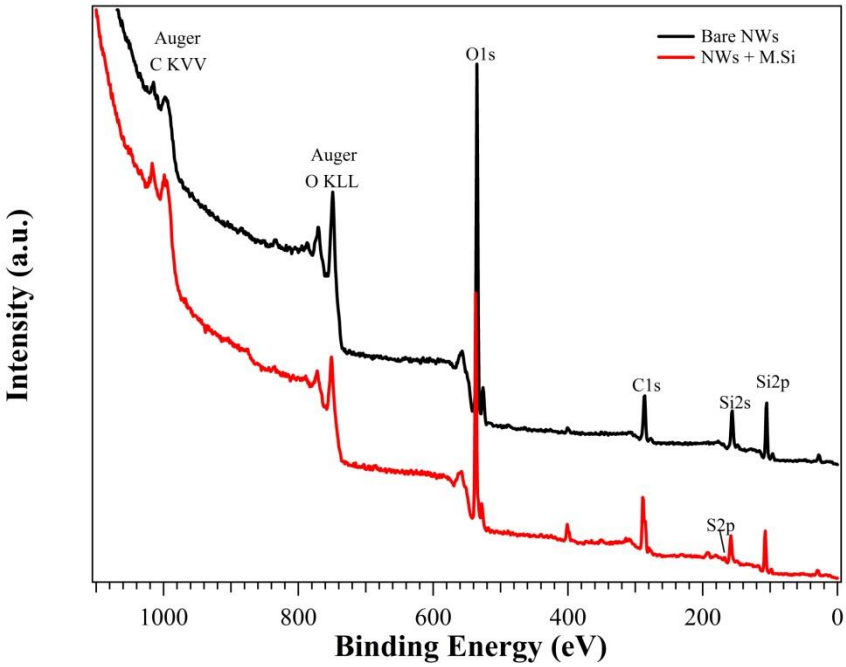

Figure 8.3: XPS spectra with high energy levels and evidences of the main peak of core levels present in the samples.

The presence of the sulphur peak at 180eV is evident only on MPTMS-NWs samples.

From the quantitative analysis of data, it has been possible to evaluate the atomic percentage of carbon, silicon, oxygen and sulphur. In particular, following the functionalization, the percentage of carbon increases, while the amount of oxygen and silicon decrease. Results are shown in Table 8.1.

Table 8.1: Chemical composition of SiO_xC_y NWs and MPTMS-NWs.

Chemical composition (%)				
	C	O	Si	S
SiO_xC_y NWs	25.0	42.6	32.4	0.0
MPTMS-NWs	40.8	32.5	26.1	0.6

XPS technique allows to define the chemical composition of samples in terms of surface atomic percentage and type of chemical bonds (C1s, O1s, Si2p and S2p). In particular, the initial carbon total atomic percentage of SiO_xC_y NWs surface was 25.0%, which increased up to 31.1% following the functionalization with MPTMS, with the consequent decrement of the oxygen and silicon content (from 42.6 and 32.4 % to 37.0 and 31.1 %, respectively). Sulphur in the MPTMS-NWs amounted to 0.8 % with respect the total composition of the material, while no sulphur was revealed on bare NWs.

Figure 8.4 shows the XPS core level spectra of the analyzed samples.

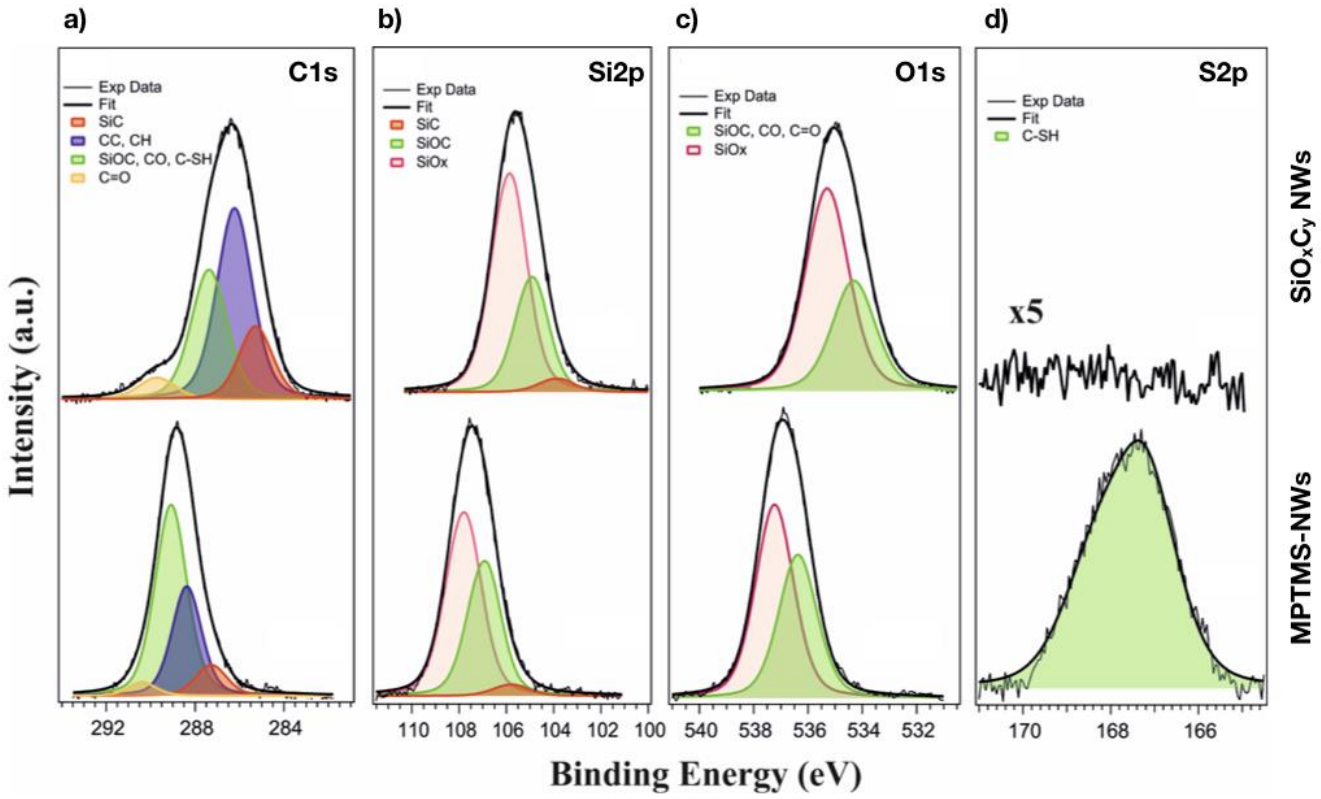

Figure 8.4: XPS core level spectra after background subtraction. a) C1s, b) O1s, c) Si2p, d) S2p signal. Graphs are relative to SiO_xC_y NWs in the upper panel and to MPTMS-NWs in the lower panel.

The C1s core level spectrum of NWs (Figure 8.4 a) was characterized by four components, associated to Si-C bond (285.27 eV), C-C bond (286.22 eV), oxycarbides such as SiOC, C-O (287.37 eV) and C=O groups (289.71 eV). The Si2p lineshape, in addition to the component related to the Si-C and SiOC bonds (103.69 and 104.74 eV), showed the typical contribution of SiO_x at 105.69 eV (Figure 8.4 c). The corresponding peak of the latter in the O1s core level was located at 535.29 eV. The O1s lineshape deconvolution was moreover characterized by another feature at 534.31 eV, related to SiOC, CO and C=O groups (showing similar BEs).

The analysis for all core levels were in agreement with studies previously reported in literature[17, 18]. All core levels were characterized by an energy shift of about 1 eV towards higher BE, with respect to the expected values, because of (not compensated) charging phenomena at the surface during the measurements. NWs functionalization, it was observed a higher energy shift (~3.0 eV), suggesting that MPTMS enhances the insulating character of the material[19]. Moreover, although having the same components, core levels in MPTMS-NWs showed different peak intensities. As a matter of fact, it is worthy to note that the intensity of the SiC, CC and C=O components (287.27, 288.37 and 290.37 eV) in C1s core level decreased, whereas an increase of the SiOC and CO contribution (289.08 eV) occurred (Figure 8.4 a). This trend was in line with the expected molecular structure of MPTMS, with SiOC and C-S groups enhancing the intensity of the peak at 289.08eV. At the same way, the corresponding components in Si2p (SiOC at 106.75 eV) and O1s (SiOC, CO and C=O at 536.37 eV) core levels (Figure 8.4 b-c) increased with respect to the contributions associated to SiO_x (537.23 and 107.62 eV, respectively) and SiC (105.62 eV). The S2p core level showed a single component at 167.22 eV, stemming from the C-S group in MPTMS (Figure 8.4 d).

The features of all the components for the C1s, O1s, Si2p and S2p core levels, in terms of BE, Full Width at Half Maximum (FWHM) and percentage calculated with respect the total area, are summarized in Table 8.2.

Table 8.2: Quantification of binding energy and percentage of the total core level area of the C1s, Si2p and S2p core levels of control SiO_xC_y NWs and MPTMS-NWs.

		SiO_xC_y NWs			MPTMS-NWs		
		BE [eV]	FWHM [eV]	%	BE [eV]	FWHM [eV]	%
C1s	SiC	285.27	1.80	16.8	287.27	1.64	8.9
	CC, CH	286.22	1.90	46.4	288.37	1.57	30.3
	SiOC, CO	287.37	1.90	31.4	289.08	1.70	57.3
	C=O	289.71	1.95	5.4	290.37	1.50	3.5
O1s	SiOC, CO, C=O	534.31	1.90	35.2	536.37	1.67	42.7
	SiOx	535.29	1.90	64.8	537.23	1.66	57.3
Si2p	SiC	103.69	1.60	3.9	105.62	1.60	3.5
	SiOC	104.74	1.50	31.8	106.75	1.50	39.4
	SiOx	105.69	1.62	64.3	107.62	1.62	57.1
S2p	C-SH	--	--	--	167.22	1.72	100

The presence of Sulphur and the change in percentage concentrations of the other elements related to MPTMS suggest that the functionalization occurred with success. Nevertheless, due to the complex structure and morphology of NWs substrates, it is only possible to suppose the presence of an inorganic layer of reasonable thickness of about 2nm (considering a value of 1-2nm for the inelastic mean free path of Si2p in the inorganic layer), which is the typical dimension of a single MPTMS monolayer.

Nanowires functionalization enhance surface electronegativity

To confirm XPS results about the presence of functionalization on NWs, their wettability was measured through a Z-Potential analysis. This test showed a change between control and functionalized NWs, confirming the presence of decorating molecules on the NWs surface.

As expected, MPTMS functionalization increased the electronegativity of nanowires if compared to control SiO_xC_y NWs, as shown in Table 8.3.

Table 8.3: Z-Potential results of control SiO_xC_y NWs and MPTMS-NWs.

SiO_xC_y NWs	MPTMS-NWs
-3,15 mV	-6,53 mV

Nanowires functionalization alters protein adsorption profile

The effects of MPTMS functionalization on serum protein adsorption pattern were investigated through SDS-PAGE and Comassie Blue staining (Figure 8.5).

Interestingly, on MPTMS-NWs the serum protein adsorption profile seemed altered if compared to the control SiO_xC_y NWs sample; in particular, both, control NWs and MPTMS-NWs did not show adsorbed proteins in the albumin region (about 65 kDa). Moreover, on modified NWs the group of proteins with molecular weight between 130 and 100 kDa seems disappeared; on the contrary, control NWs clearly show protein adsorption in this range. In addition, NWs surface modification seems to strongly reduce the amount of adsorbed proteins with molecular weight around 25kDa (very weak also in total serum samples) and to promote the adsorption of a group of proteins of molecular weight about 180kDa, detectable in total serum samples, but not in pristine NWs one.

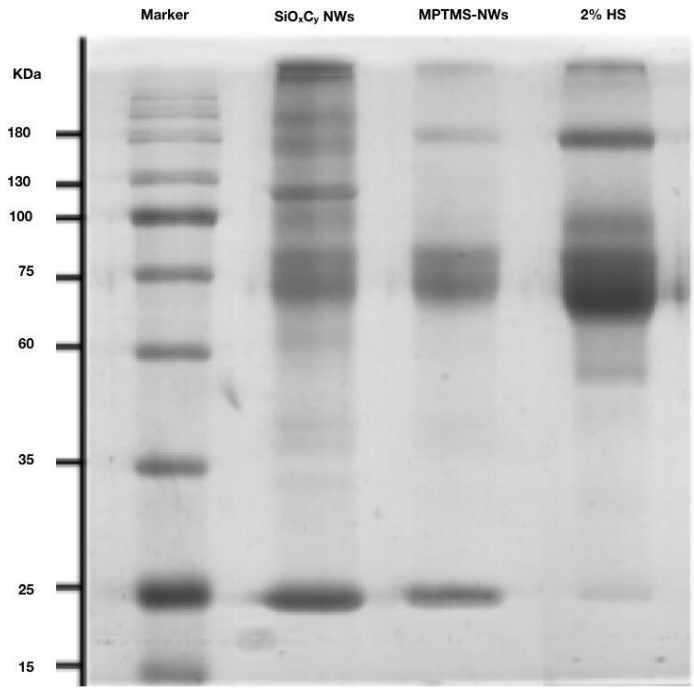

Figure 8.5: SDS-PAGE and Comassie Blue staining of protein adsorption on control SiO_xC_y NWs and functionalized MPTMS-NWs after incubation with 2% human serum in PBS.

Nanowires functionalization improves cell proliferation

To observe 3-mercaptopropyltrimethoxysilane effects on cell behavior, a chemiluminescence based viability assay was performed on MC3T3-E1 osteoblasts after 24 and 48h of culture. Luminescence data, shown in Figure 8.6, clearly demonstrate that NWs functionalization did not influence cell viability after 24h of culture, where no differences were detected between the groups. Interestingly, a highly significant increase of cell viability was observed after 48h of culture, suggesting that cells could grow more effectively in presence of the functionalization.

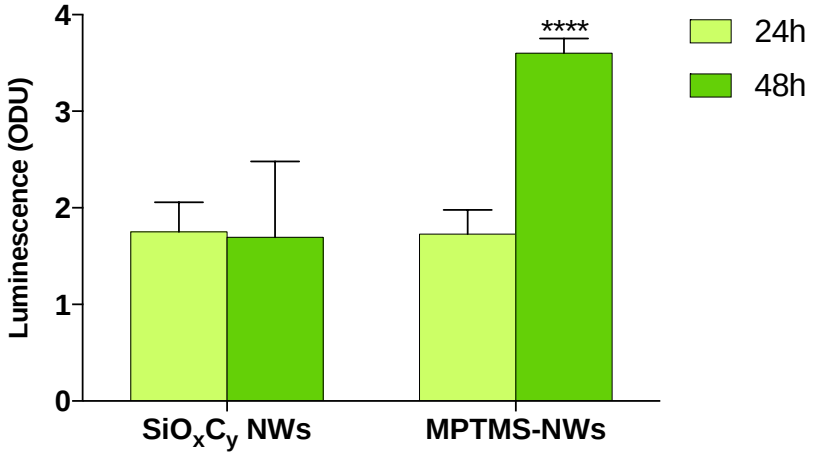

*Figure 8.6: Cell viability assay based on chemiluminescence measurement of MC3T3-E1 osteoblastic cells on control SiO_xC_y NWs and functionalized MPTMS-NWs after 24 and 48h of culture. ****p<0,0001.*

Nanowires functionalization affects cell morphology

Cell morphology on NWs was observed after culturing them on control and functionalized samples for 48h, because the alteration in protein adsorption profile could have strongly affected cell adhesion. On both samples, MC3T3-E1 osteoblasts appeared well adhered, with their typical polygonal shape (Figure 8.7 a-d), however, on MPTMS-NWs cells appeared larger and with several cytoplasmatic extroflections, maybe granting the cell body the adequate anchorage to the material (Figure 8.7 d-e). As highlighted in Figure 8.7 (b-e), NWs on both samples were able to cross the cell cytoplasm, which was surrounding NWs structures and sometimes was pierced by them.

Cell section obtained through FIB cutting (Figure 8.7 c-f) showed how osteoblasts were not able to penetrate the NWs meshwork, perhaps because the gaps between NWs were very tiny, but they were able to remain well anchored to the superficial layer of nanowires.

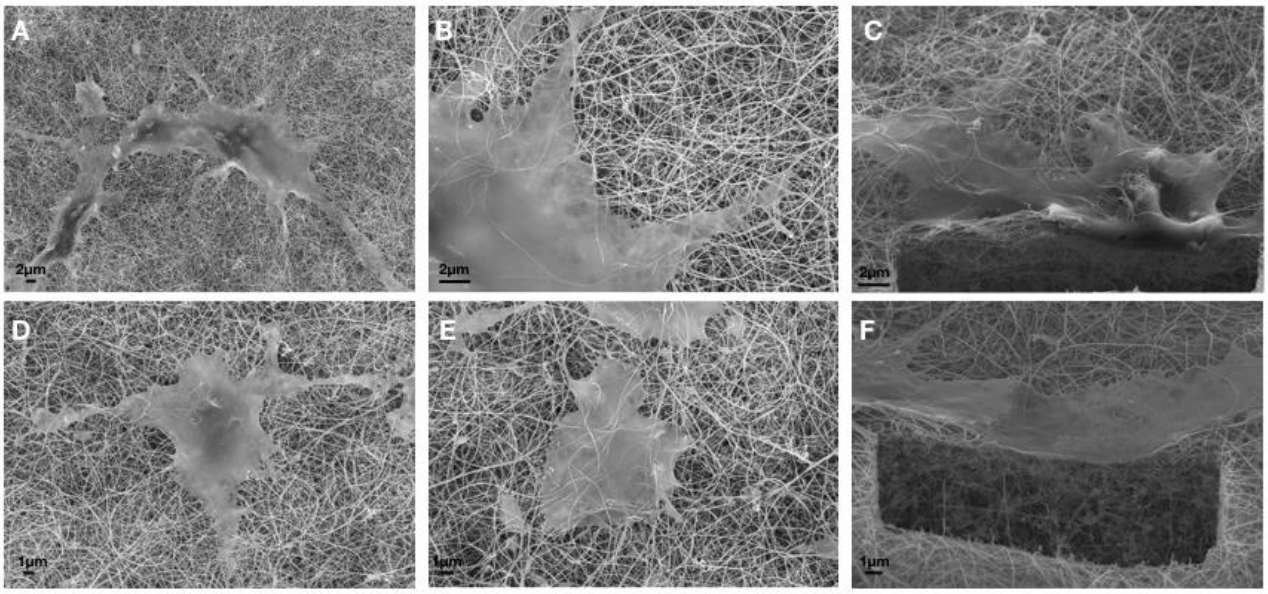

Figure 8.7: SEM images of MC3T3-E1 osteoblasts on control SiO_xC_y NWs (a-b) and functionalized MPTMS-NWs (d-e) after 48h of culture. Cells section obtained by FIB on control SiO_xC_y NWs (c) and functionalized MPTMS-NWs (f).

Nanowires functionalization improves focal adhesion

MC3T3-E1 osteoblasts were labeled for actin cytoskeleton, vinculin and DNA to investigate if the functionalized substrate acted as a better support for cell adhesion. In particular, cells were labeled with an anti-vinculin antibody, to detect a protein involved in the formation of focal adhesions (multi-proteic complexes involved in attaching cells to the substrate). As observed in SEM/FIB images, cells on MPTMS-NWs appeared larger (Figure 8.8). Moreover, they had more numerous small extroflections, perhaps filopodia, supported by visible and robust cytoskeleton apparatus. Vinculin appeared as discrete dot-like labels on control substrate (Figure 8.8 e), while on MPTMS-NWs vinculin appeared more diffused throughout the cytoplasm. In the first cate it suggests a discrete and small cell-substrate contact point formation, while in the second, cell seemed able to establish wider contact points, thus confirming SEM results. The improvement of cell adhesion was confirmed by the presence of more marked and thick actin filaments running along all the cell body and remarkably absent in control cells.

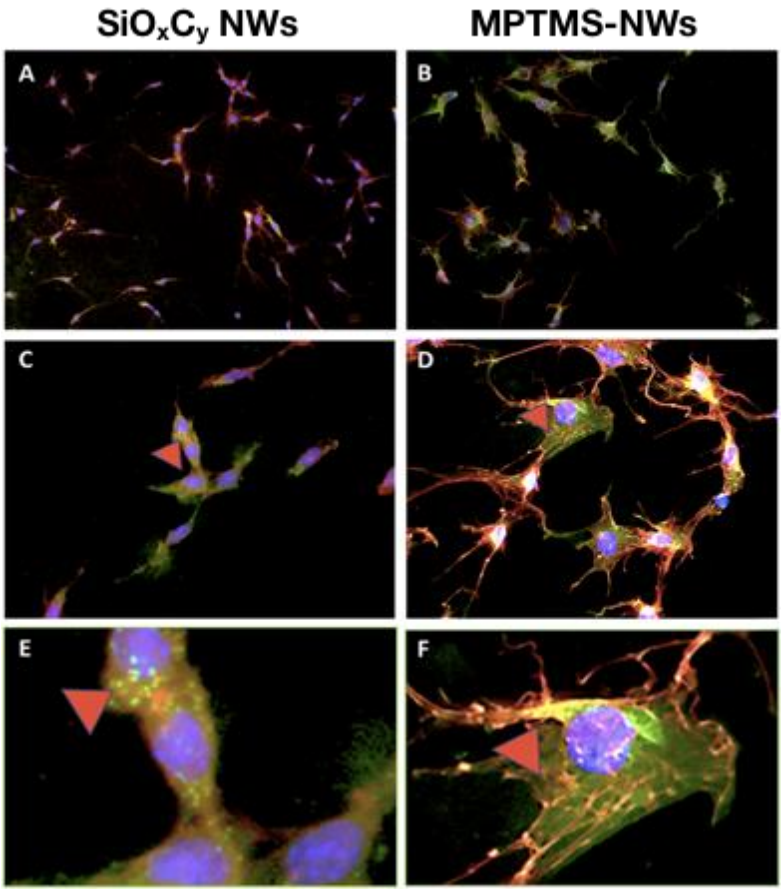

Figure 8.8: MC3T3-E1 osteoblasts marked after 48h of culture with immunofluorescence for vinculin of focal adhesions (green), actin (red) and nuclei (blue). Images a-c-e refer to cells on control SiO_xC_y NWs; b-d-f refer to cells on MPTMS-NWs. Magnification: a-b 20X, c-d 40X, e-f details of images c-d respectively.

Nanowires functionalization ameliorates gene expression

Finally, to confirm the support to cell differentiation given by the functionalization to osteoblasts, a gene expression analysis was done on cells growth on MPTMS-NWs and on control NWs. Specific osteoblasts related markers were took into consideration as Alkaline phosphatase (ALP), Runt related transcription factor 2 (Runx2), Osteocalcin (OCN) and Collagen type I (COL1A1). As shown in the graphs (Figure 8.9)there were found significantly higher levels of transcript for the early osteoblastic marker ALP and Collagen I, which could indicate that cells were prompted to produce new ECM. No differences were detected in the expression of the mature marker Osteocalcin and in RUNX2. However, the presence of significantly higher levels of early differentiation stage markers is promising and supports the idea that this substrates can afford a strong cell adhesion and can promote cell differentiation creating a suitable microenvironment able to promote cell commitment; moreover, it worth to say

that at 96h of culture is not possible to reach the complete osteoblastic differentiation, reason for the nonexistent differences in the mature marker.

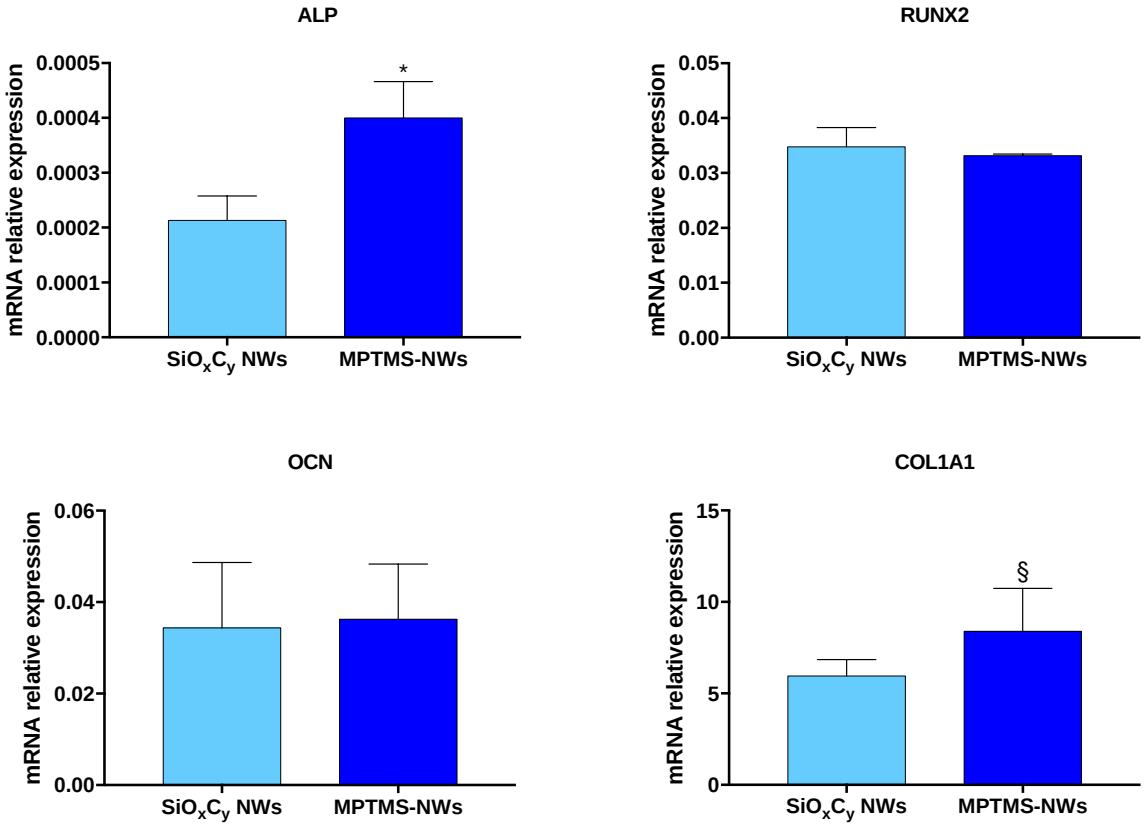

*Figure 8.9: Quantitative RT-PCR of mRNA from MC3T3-E1 osteoblasts cultured for 96h on control SiO_xC_y NWs and functionalized MPTMS-NWs. Gene of interest (Alkaline phosphatase, Runx2, Osteocalcin and Collagen I) values were normalized to GAPDH mRNA levels; values are reported as means ± standard deviation. *p=0,0286; §p=0,0411.*

8.4 Discussion

The introduction of nanostructured surfaces paved the way to the construction of biomimetic materials able to recreate the *in vivo* environment of cues and stimuli necessary for cell adhesion, proliferation, migration and differentiation, in order to regenerate a tissue. Moreover, the ability of nanosized material to resemble at least in dimension the components of extracellular matrix (e.g. collagen fibrils, hydroxyapatite, proteoglycans, cell receptors, etc.) can allow to the biomaterial to support cells and regulates their function by offering adhesion sites and a vast array of biochemical and physical cues that trigger or suppress cell activity or differentiation. In this arena, NWs strongly resemble the particular structure of ECM, constituted from fibrils of molecules such as collagen and proteoglycans, interspersed in water, and could be used to try to recreate this 3D structure as implantable scaffold[20-22]. A scaffold should not be only biocompatible (biocompatibility study about SiO_xC_y NWs has been deeply described in chapter 5), but it should also stimulate and improve cell adhesion and proliferation; for this reason, the functionalization with 3-mercaptopropyltrimethoxysilane could confer them a higher capability to bind proteins and subsequently cells[23]. In particular, 3-mercaptopropyltrimethoxysilane is a molecule rich in thiol groups, whose -SH terminal can easily react and bind other molecules (e.g. lateral chain of plasma proteins). Since the presence of a thin layer of proteins on the surface has been seen to be fundamental for cell adhesion and proliferation, the idea to bind plasma proteins through -SH groups could reveal a possible solution for the coating of an exogenous implantable biomaterial with a layer of firmly adsorbed proteins[23]. It is quite evident from protein adsorption studies that MPTMS functionalization completely changes the interaction between the material and serum proteins, in particular NWs become less adsorbent then pristine ones and at the same time more selective for a particular group of proteins of human serum including the 180kDa molecular weight, matching with fibronectin molecular weight. The enhanced amount of adsorbed fibronectin is fundamental because it has been seen as a key regulator of cell adhesion to biomaterials, and it is consistent with data showed by immunofluorescence and cell spreading[24, 25]. Moreover, it could represent a mechanism underlying the effect of biomaterials functionalization on cell behavior; in particular, MC3T3-E1 have been used because it is a well-established model for murine osteoblast differentiation, whose similarities with the clinical needs are more than those of a routinely cell line (e.g. L929). In particular, bone tissue is commonly grafted in routine practice and the need for a more effective implant material is increasing[26, 27]. The use of a 3-mercaptopropyltrimethoxysilane functionalization seems to ameliorate cell response to NWs; in fact, our previous works showed how NWs were cytocompatible, but L929 cells did not present a remarkable proliferation, instead it was stationary. In these regards, a MPTMS functionalization could appear as a promising solution to overcome problems encountered on not functionalized nanowires, due to the rapid proliferation of osteoblasts on MPTMS-NWs, which is an interesting

result for enhancing scaffold colonization. Cell morphology on functionalized nanowires was positively affected by 3-mercaptopropyltrimethoxysilane, cells showed a larger body, symptom of improved adhesion; it is worthy of note because cell adhesion on biomaterials is a key prerequisite for the successful incorporation of implants or the colonization of scaffolds in regenerative medicine. Moreover, cell adhesion to the substrate is a fundamental part of cell cycle, it is the base of the control of cell growth, proliferation and differentiation processes; cells can flatten out on a surface only after they have firmly adhered to it, their cytoskeleton can contract and cell body can spread becoming thinner and larger[28]. This mechanism of adhesion is mediated by peculiar structures characterized by multi-proteic complexes involved in the clustering of ligated trans membrane receptors integrins at the nanoscale. Literature showed many evidences that clustering of integrins requires a spacing between ligands of about 50-70nm, and that nanopatterned material with spacing >100nm could even inhibit cell proliferation[29, 30]. Obviously, a single nanowire offers a limited space to form focal adhesions, result corroborated by the immunofluorescence microphotographs, that show larger actin fibers (known as stress fibers) in the cytoplasm of cells growth on functionalized nanowires. Normally, stress fibers are arranged along the force vectors that are generated by actomyosin complexes within the fibers and they only form after solid adhesion of the cell to the substrate and the formation of focal adhesions occurred. Interestingly, stress fibers were only present on MPTMS-NWs and not on control SiO_xC_y NWs, and on the last type, focal adhesions appeared as little dots, probably due to the diameter of nanowires and the gap between them larger than 100nm; hence, as the formation of focal adhesion require a smaller distance, the functionalization could have provided a more favorable protein microenvironment and in this way promote cell adhesion mediating focal adhesion formation and clustering on nanowires[31]. Then cellular gene expression on nanowires was analyzed measuring specific osteoblastic and ECM genes; in particular, Alkaline phosphatase and Collagen I (markers of early stage osteoblastic differentiation[32] and ECM component, respectively) were upregulated on functionalized nanowires. Genes as Runx2 and Osteocalcin did not show any differences between MPTMS-NWs and control NWs, therefore even if functionalized nanowires cannot be proven to promote osteoblast differentiation, they could be interesting for the final goal of regenerative medicine. In fact, tissue regeneration initially requires the colonization of the scaffold by undifferentiated cells, whose proliferative potential is still high, in order to allow the complete colonization of the biomaterial. As cell differentiation is commonly associated to a decrease in proliferative activity, cells must not differentiate to early because it might compromise the colonization of the scaffold; only in the later phase cells should differentiate and promote tissue restoring.

In conclusion, the 3-mercaptopropyltrimethoxysilane functionalization of SiO_xC_y nanowires seems to be a viable strategy to improve cell response and the compatibility of silicon-based nanomaterials. As previously shown, nanowires functionalization leads to a different protein adsorption pattern if compared to pristine nanowires and

the cellular response in terms of cell proliferation was enhanced if nanowires were functionalized. Cell morphology observation showed almost the same healthy and polygonal shape in both nanowires, although on MPTMS-NWs cells showed several cytoplasmatic extroflections probably due to their better adhesion to the substrate. Focal adhesion staining and qRT-PCR analysis showed a higher amount of vinculin in the cytoplasm and an upregulation of specific osteoblastic genes (ALP, COL1A1) in cells growth of functionalized nanowires if compared to the control, confirming a better adhesion of cells and an induction through osteoblastic differentiation. Taken together, these data underly that 3-mercaptopropyltrimethoxysilane functionalization of SiO_xC_y nanowires enhance osteoblastic response, stimulating cell proliferation, adhesion as well as the initial differentiation, making MPTMS-NWs a suitable scaffold for biomedical applications.

References

1. Ghezzi, B.; Lagonegro, P.; Pece, R.; Parisi, L.; Bianchi, M.; Tatti, R.; Verucchi, R.; Attolini, G.; Quaretti, M.; Macaluso, G. M., Osteoblast adhesion and response mediated by terminal -SH group charge surface of SiOxCy nanowires. J Mater Sci Mater Med 2019, 30 (4), 43. DOI: 10.1007/s10856-019-6241-y.

2. Arnold, M.; Cavalcanti-Adam, E. A.; Glass, R.; Blummel, J.; Eck, W.; Kantlehner, M.; Kessler, H.; Spatz, J. P., Activation of integrin function by nanopatterned adhesive interfaces. Chemphyschem 2004, 5 (3), 383-8. DOI: 10.1002/cphc.200301014.

3. Cavalcanti-Adam, E. A.; Aydin, D.; Hirschfeld-Warneken, V. C.; Spatz, J. P., Cell adhesion and response to synthetic nanopatterned environments by steering receptor clustering and spatial location. Hfsp j 2008, 2 (5), 276-85. DOI: 10.2976/1.2976662.

4. Webster, T. J.; Schadler, L. S.; Siegel, R. W.; Bizios, R., Mechanisms of enhanced osteoblast adhesion on nanophase alumina involve vitronectin. Tissue Eng 2001, 7 (3), 291-301. DOI: 10.1089/10763270152044152.

5. Webster, T. J.; Ejiofor, J. U., Increased osteoblast adhesion on nanophase metals: Ti, Ti6Al4V, and CoCrMo. Biomaterials 2004, 25 (19), 4731-9. DOI: 10.1016/j.biomaterials.2003.12.002.

6. Born, A. K.; Rottmar, M.; Lischer, S.; Pleskova, M.; Bruinink, A.; Maniura-Weber, K., Correlating cell architecture with osteogenesis: first steps towards live single cell monitoring. Eur Cell Mater 2009, 18, 49-60, 61-2; discussion 60.

7. Unadkat, H. V.; Hulsman, M.; Cornelissen, K.; Papenburg, B. J.; Truckenmuller, R. K.; Carpenter, A. E.; Wessling, M.; Post, G. F.; Uetz, M.; Reinders, M. J.; Stamatialis, D.; van Blitterswijk, C. A.; de Boer, J., An algorithm-based topographical biomaterials library to instruct cell fate. Proc Natl Acad Sci U S A 2011, 108 (40), 16565-70. DOI: 10.1073/pnas.1109861108.

8. Hamilton, D. W.; Brunette, D. M., The effect of substratum topography on osteoblast adhesion mediated signal transduction and phosphorylation. Biomaterials 2007, 28 (10), 1806-19. DOI: 10.1016/j.biomaterials.2006.11.041.

9. Aznavoorian, S.; Stracke, M. L.; Krutzsch, H.; Schiffmann, E.; Liotta, L. A., Signal transduction for chemotaxis and haptotaxis by matrix molecules in tumor cells. J Cell Biol 1990, 110 (4), 1427-38. DOI: 10.1083/jcb.110.4.1427.

10. Lim, J. Y.; Donahue, H. J., Cell sensing and response to micro- and nanostructured surfaces produced by chemical and topographic patterning. Tissue Eng 2007, 13 (8), 1879-91. DOI: 10.1089/ten.2006.0154.

11. Kuo, S. W.; Lin, H. I.; Ho, J. H.; Shih, Y. R.; Chen, H. F.; Yen, T. J.; Lee, O. K., Regulation of the fate of human mesenchymal stem cells by mechanical and stereo-topographical cues provided by silicon nanowires. Biomaterials 2012, 33 (20), 5013-22. DOI: 10.1016/j.biomaterials.2012.03.080.

12. Tamayo A, R. J., Rubio F, Oteo J L, Riedel R, Texture and micro-nanostructure of porous silicon oxycarbide glasses prepared from hybrid materials aged in different solvents J. Eur. Ceram. Soc. 31 1791–1801 2011.

13. Webster, T. J.; Siegel, R. W.; Bizios, R., Osteoblast adhesion on nanophase ceramics. Biomaterials 1999, 20 (13), 1221-7.

14. Webster, T. J.; Ergun, C.; Doremus, R. H.; Siegel, R. W.; Bizios, R., Specific proteins mediate enhanced osteoblast adhesion on nanophase ceramics. J Biomed Mater Res 2000, 51 (3), 475-83.

15. Rossi, F.; Bedogni, E.; Bigi, F.; Rimoldi, T.; Cristofolini, L.; Pinelli, S.; Alinovi, R.; Negri, M.; Dhanabalan, S. C.; Attolini, G.; Fabbri, F.; Goldoni, M.; Mutti, A.; Benecchi, G.; Ghetti, C.; Iannotta, S.; Salviati, G., Porphyrin conjugated SiC/SiOx nanowires for X-ray-excited photodynamic therapy. Sci Rep 2015, 5, 7606. DOI: 10.1038/srep07606.

16. Curran, J. M.; Chen, R.; Hunt, J. A., The guidance of human mesenchymal stem cell differentiation in vitro by controlled modifications to the cell substrate. Biomaterials 2006, 27 (27), 4783-93. DOI: 10.1016/j.biomaterials.2006.05.001.

17. Negri M, D. S. C., Attolini G, Lagonegro P, Campanini M, Bosi M, Fabbri F, Salviati G, Tuning the radial structure of core-shell silicon carbide nanowires CrystEngComm, 2015; Vol. 17, pp 1258-1263

18. Fabbri, F.; Rossi, F.; Negri, M.; Tatti, R.; Aversa, L.; Dhanabalan, S. C.; Verucchi, R.; Attolini, G.; Salviati, G., Carbon-doped SiO(x) nanowires with a large yield of white emission. Nanotechnology 2014, 25 (18), 185704. DOI: 10.1088/0957-4484/25/18/185704.

19. Chastain J, M. J., King RC, Handbook of X-ray photoelectron spectroscopy: a reference book of standard spectra for identi fi cation and interpretation of XPS data. 1992.

20. Farrell, E.; O'Brien, F. J.; Doyle, P.; Fischer, J.; Yannas, I.; Harley, B. A.; O'Connell, B.; Prendergast, P. J.; Campbell, V. A., A collagen-glycosaminoglycan scaffold supports adult rat mesenchymal stem cell differentiation along osteogenic and chondrogenic routes. Tissue Eng 2006, 12 (3), 459-68. DOI: 10.1089/ten.2006.12.459.

21. Farrell, E.; Byrne, E. M.; Fischer, J.; O'Brien, F. J.; O'Connell, B. C.; Prendergast, P. J.; Campbell, V. A., A comparison of the osteogenic potential of adult rat mesenchymal stem cells cultured in 2-D and on 3-D collagen glycosaminoglycan scaffolds. Technol Health Care 2007, 15 (1), 19-31.

22. Yannas, I. V.; Lee, E.; Orgill, D. P.; Skrabut, E. M.; Murphy, G. F., Synthesis and characterization of a model extracellular matrix that induces partial regeneration of adult mammalian skin. Proc Natl Acad Sci U S A 1989, 86 (3), 933-7. DOI: 10.1073/pnas.86.3.933.

23. Capobianco, J. A.; Shih, W. Y.; Shih, W. H., 3-mercaptopropyltrimethoxysilane as insulating coating and surface for protein immobilization for piezoelectric microcantilever sensors. Rev Sci Instrum 2007, 78 (4), 046106. DOI: 10.1063/1.2727466.

24. Parisi, L.; Toffoli, A.; Ghiacci, G.; Macaluso, G. M., Tailoring the Interface of Biomaterials to Design Effective Scaffolds. J Funct Biomater 2018, 9 (3). DOI: 10.3390/jfb9030050.

25. Saccani, M.; Parisi, L.; Bergonzi, C.; Bianchera, A.; Galli, C.; Macaluso, G. M.; Bettini, R.; Elviri, L., Surface modification of chitosan films with a fibronectin fragment-DNA aptamer complex to enhance osteoblastic cell activity: A mass spectrometry approach probing evidence on protein behavior. Rapid Commun Mass Spectrom 2019, 33 (4), 336-342. DOI: 10.1002/rcm.8335.

26. Sudo, H.; Kodama, H. A.; Amagai, Y.; Yamamoto, S.; Kasai, S., In vitro differentiation and calcification in a new clonal osteogenic cell line derived from newborn mouse calvaria. J Cell Biol 1983, 96 (1), 191-8. DOI: 10.1083/jcb.96.1.191.

27. Wang, D.; Christensen, K.; Chawla, K.; Xiao, G.; Krebsbach, P. H.; Franceschi, R. T., Isolation and characterization of MC3T3-E1 preosteoblast subclones with distinct in vitro and in vivo differentiation/mineralization potential. J Bone Miner Res 1999, 14 (6), 893-903. DOI: 10.1359/jbmr.1999.14.6.893.

28. Hayashi, Y.; Furue, M. K.; Okamoto, T.; Ohnuma, K.; Myoishi, Y.; Fukuhara, Y.; Abe, T.; Sato, J. D.; Hata, R.; Asashima, M., Integrins regulate mouse embryonic stem cell self-renewal. Stem Cells 2007, 25 (12), 3005-15. DOI: 10.1634/stemcells.2007-0103.

29. Cavalcanti-Adam, E. A.; Micoulet, A.; Blummel, J.; Auernheimer, J.; Kessler, H.; Spatz, J. P., Lateral spacing of integrin ligands influences cell spreading and focal adhesion assembly. Eur J Cell Biol 2006, 85 (3-4), 219-24. DOI: 10.1016/j.ejcb.2005.09.011.

30. Cavalcanti-Adam, E. A.; Volberg, T.; Micoulet, A.; Kessler, H.; Geiger, B.; Spatz, J. P., Cell spreading and focal adhesion dynamics are regulated by spacing of integrin ligands. Biophys J 2007, 92 (8), 2964-74. DOI: 10.1529/biophysj.106.089730.

31. Tojkander, S.; Gateva, G.; Lappalainen, P., Actin stress fibers--assembly, dynamics and biological roles. J Cell Sci 2012, 125 (Pt 8), 1855-64. DOI: 10.1242/jcs.098087.

32. Farley, J. R.; Hall, S. L.; Tanner, M. A.; Wergedal, J. E., Specific activity of skeletal alkaline phosphatase in human osteoblast-line cells regulated by phosphate, phosphate esters, and phosphate analogs and release of alkaline phosphatase activity inversely regulated by calcium. J Bone Miner Res 1994, 9 (4), 497-508. DOI: 10.1002/jbmr.5650090409.

Chapter 9 – Titanium dioxide nanowires with improved *in vitro* osteogenic potential

From: Titanium dioxide nanowires grown on titanium disks create a nanostructured surface with improved *in vitro* osteogenic potential[1].
Published in Journal of Nanoscience and Nanotechnologies (2018) *19* (8), 4665-4670.
DOI: 10.1166/jnn.2019.16350.

Abstract

The study of nanomaterials and of their effects in biological environment is the focus of the current biomedical research. In particular, there is an increasing interest on titanium dioxide nanostructures for biomedical applications such as drug delivery or implant materials due to the optimal characteristics of the material, currently clinically used for orthopedic prostheses and dental implants. In this framework, a Chemical Vapour Deposition process to synthesize titanium dioxide nanowires (TiO_2 NWs) on a commercially pure titanium substrate and the testing of the material *in vitro* as a culture substrate for murine osteoblast-like MC3T3-E1 cells is presented. The inorganic samples were characterized physically, morphologically, structurally and optically by Electron Microscopy techniques and X-Ray Diffraction. Results showed that a mat of crystalline rutile TiO_2 NWs was obtained over the commercial substrate. Biological effects of the nanostructured surface were investigated *in vitro* through cell morphology analysis and gene expression study on murine MC3T3-E1 osteoblastic cells.

These experiments showed good cell adhesion to the nanostructured surface and a higher degree of early osteoblastic differentiation if compared to control titanium surfaces, indicating that the present nanostructured material. Therefore, TiO_2 NWs substrate shows good osteogenic potential for biomedical applications and provides a favorable template for bone cell growth and differentiation in order to improve bone-implant interface and design better dental and orthopedic implants.

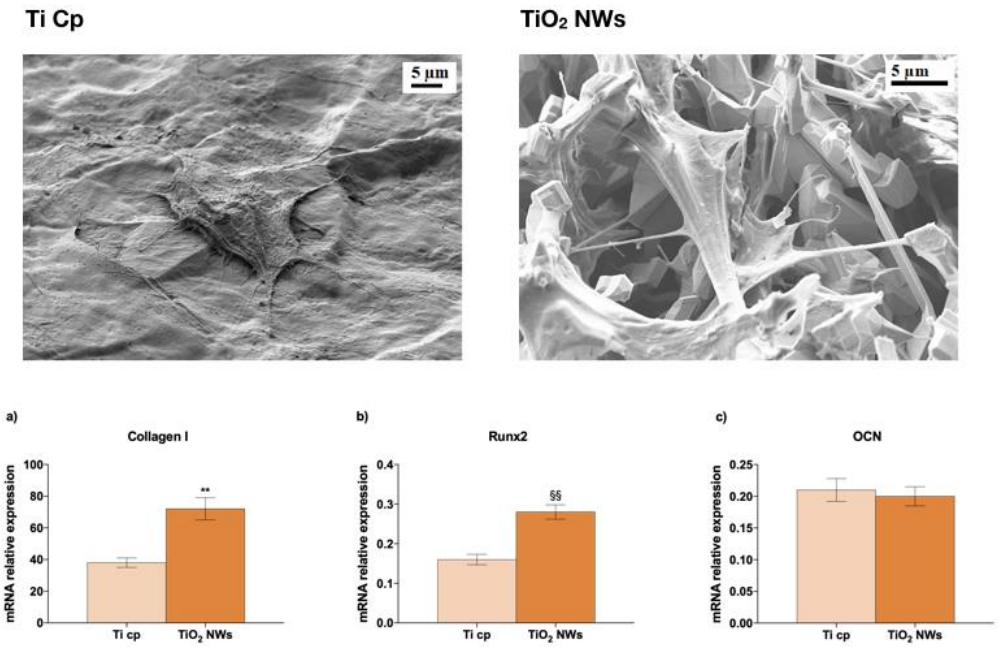

Figure 9.1: Graphical abstract of the chapter.

9.1 Introduction

Biomaterials are commonly used in regenerative medicine to restore the anatomy and function of damaged or missing tissues, with an increasing research interest in the field of endosseous implants, clinically employed to replace lost teeth or parts of the skeleton. Biomaterials suitable for such implants must integrate into bone, therefore a key requirement is their ability to promote the deposition of sound mineralized tissue along their surface, and their resistance to mechanical loads applied during function. In more detail, bone integration requires a medical device to be biocompatible and to provide the host organism with a microenvironment that resembles the extracellular matrix (ECM) of the original tissue, since the success of any clinical implant is directly related to cell-implant interaction, its effects, and implant integration within the surrounding tissue. Moreover, it is known the composition of extracellular environment (collagen, elastin, fibronectin, laminin, proteoglycans) and its localization in the nanometer scale, fundamentals to support the regeneration of the tissue[2]. Many attempts were made to mimic the natural ECM through the development of biomedical scaffolds with nanoscale features (spatial and geometrical) which may induce cell proliferation and differentiation. Starting from the evidence that ECM encompasses micro- and nano-scale aspects acting as cues for cells and modulating their behavior and functionality, several studies in the literature have analyzed how the physic-chemical characteristics of scaffolds, such as micro- and nano-structure, affect cell behavior and can dictate cell response to biomaterials[3]. In particular, titanium demonstrated excellent qualities in terms of biocompatibility and osteointegration at the bone-implant surface as a prerequisite for a successful clinical implantation and it is commonly used in the clinic after a surface treatment by sand blasting and acid etching to create rough surfaces for ameliorating bone integration. Moreover, according to many authors, the extent of osteointegration is strongly influenced by the surface properties and in particular by the nanotopography of the implant, underlying that osteoblasts adhesion and proliferation and in a larger view the osteointegration are significantly improved on nanostructured surfaces than on conventional metals substrate[4-9]. The constant improvement of nanotechnology research has resulted in the fabrication of various forms of titania nanostructure e.g. nanotubes, nanowires, nanorods and nanoribbons which attracted much interest in the biomedical field due to their peculiar characteristics of compatibility with the biological system and their ability to integrate functional moieties on the surface that can modulate biological response[10-12]. Research is more and more underlying the importance of TiO_2 nanostructures' morphology for biomedical applications such as drug delivery or implant materials, where interactions with small size proteins or molecules are primordial[11, 13, 14]. Bone response to nanostructured materials has been already tested, mainly with titanium nanotubes, *in vitro*, and the results showed that titanium nanostructures were providing a favorable template for bone cell growth and differentiation supporting cell adhesion and avoiding adverse immune response[10-13].

With these premises, the aim of the study was to address if a titanium dioxide nanowires surface could enhance osteoblast differentiation and osteointegration, investigating the physic-chemical characteristics of TiO_2 NWs grown on titanium disks by a simple Chemical Vapour Deposition process and their behavior in the biological environment, as a potential substrate for biomedical applications.

9.2 Materials and methods

Sample growth and characterization

Titanium dioxide nanowires (TiO_2 NWs) were grown on commercially pure polycrystalline titanium disks (Ti cp, 15mm diameter) through a CVD process with nickel nitrate as catalyst, for 20 min at 1120°C. As previously described in chapter 4, the process does not require the flow of a specific titanium precursor, because titanium is already provided by the substrate.

Substrates and nanowires morphology were characterized by Scanning Electron Microscopy (SEM) using a dual beam Zeiss Auriga Compact system equipped with a GEMINI Field-Emission SEM column operated at 10keV and the morphology of a single nanowire was observed through Transmission Electron Microscopy (TEM) in a JEOL 2200FS microscope operating at 200kV and working in conventional and scanning mode (STEM).

To observe the crystalline structure of the specimens, they were analyzed by X-Ray Diffraction (XRD) in a Siemens D-500 diffractometer with Cu Kα radiation.

Finally, cathodoluminescence (CL) was performed with a Gatan monocle system mounted on a S360 Cambridge Scanning Electron Microscope. The system is equipped with grating and a multi-alkali photomultiplier sensitive in the range 350/830 nm (3.6/1.5 eV). CL spectra were collected with a 10keV accelerating voltage and a 10nA electron beam current; they were subsequently deconvoluted using a standard Levenberg-Marquardt algorithm to minimize the Chi-Square. To avoid any possible artifacts, the full width of a maximum (w) was constraint to a value of 0.5eV, while the peak position (x_c)and the amplitude (A) were free fitting parameters. Their uncertainty was estimated to be about 5%.

Cell assays

Cell cultures – Cell assays were performed with murine osteoblastic cells (MC3T3-E1) obtained from the ATCC (LGC Standards srl, Milan, Italy), as established model for studying *in vitro* osteoblast differentiation. Cells were cultured in complete alpha-MEM (a-MEM, Thermo Fisher Scientific) supplemented with 10% FBS, 1% Penicillin and Streptomycin (PenStrep, Thermo Fisher Scientific) and 1% L-Glutamine (Thermo Fisher Scientific).

For cell culture experiments, cells were seeded on both, pristine commercially pure titanium disks and samples with nanowires (TiO_2 NWs) at a final density of 20.000 cells/sample for cell morphology study and of 40.000 cells/sample for gene expression analysis.

Scanning electron microscopy and Focused Ion Beam– To observe cell morphology and the interaction with the underlying titanium substrate, SEM morphological analysis was performed after 72h of culture. Briefly, cells were fixed with 2.5% glutaraldehyde (Sigma-Aldrich) solution in 0,1M Na-Cacodylate buffer for 30 min at RT, thus washed in Na-Cacodylate buffer for 5 min at RT and subsequently dehydrated in an ascendant series of ethanol (Sigma-Aldrich) at RT, for 10min each alcohol (EtOH 35%, 50%, 70%, 75%, 90%, 95%, 99%). Specimens were then coated with a nanometric gold layer through a SCD 040 coating device (Balzer Union, Wallruf, Germany). Microphotographs of cells distribution and morphology over Ti cp and TiO_2 NWs were taken in a dual beam Zeiss Auriga Compact system equipped with a GEMINI Field-Emission SEM column operated at 5keV.

Gene expression analysis – To observe if there were differences in terms of gene expression between nanowires and bare titanium disks, after 72h of culture total RNA was extracted using TriZol (Thermo Fisher Scientific), according to manufacturer's indications. The purity of extracted RNA was quantitated by spectrophotometry (Nanophotometer, Implen GmbH, München, Germany) and subsequently RNA was retrotranscribed to cDNA with a High Capacity cDNA Reverse Transcription Kit (Thermo Fisher Scientific). TaqMan quantitative RT-PCR was performed on samples through a Real Time PCR machine (StepOne Plus, Life Technologies) and using the following primer probe sets from Life Technologies (Foster City, CA, USA): Collagen type I (COL1A1, Mm00801666_g1); Runt related transcription factor 2 (Runx2, Mm00501584_m1); Osteocalcin (OCN, for 5'-GCTGCGCTCTGTCTCTCTGA-3'; rev 5'-TGCTTGGACATGAAGGCTTTG-3';probe 5'-FAM-AAGCCCAGCGGCC-NFQ-3'); mouse ribosomal protein S2 (ChoB) was used as housekeeping gene.

Statistical analysis – Data were analyzed using Prism7 (GraphPad, La Jolla, CA, USA). All the values are reported as the mean ± standard deviation of three repeated experiments. Differences among the groups were evaluated with either t-Test, one-way ANOVA or two-way ANOVA statistical tests and with the Tukey or Bonferroni post-test for multiple comparisons. Differences were considered significant when $p<0.05$.

9.3 Results

Material characterization

The surface of titanium with nanowires has been studied through SEM technique. The morphology of typical TiO_2 NWs surface is shown in Figure 9.2 (a) and a more enlarged view is shown in Figure 9.2 (b). NWs seem arranged as a dense needles bundle covering the entire substrate of the titanium disk.

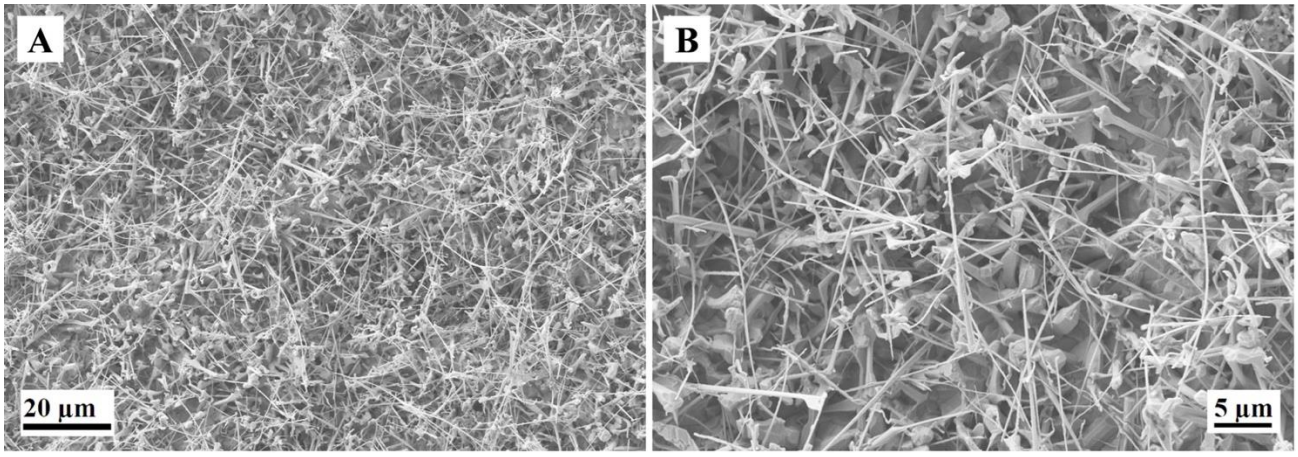

Figure 9.2: a) Typical SEM images of a wide area of titanium substrate with nanowires. b) Detail of the synthesized TiO_2 NWs.

The analysis of the crystallinity of NWs by X-Ray Diffraction (Figure 9.3) clearly demonstrate that NWs are crystalline and the 2θ position of the diffraction peaks identifies their phase as tetragonal rutile TiO_2.

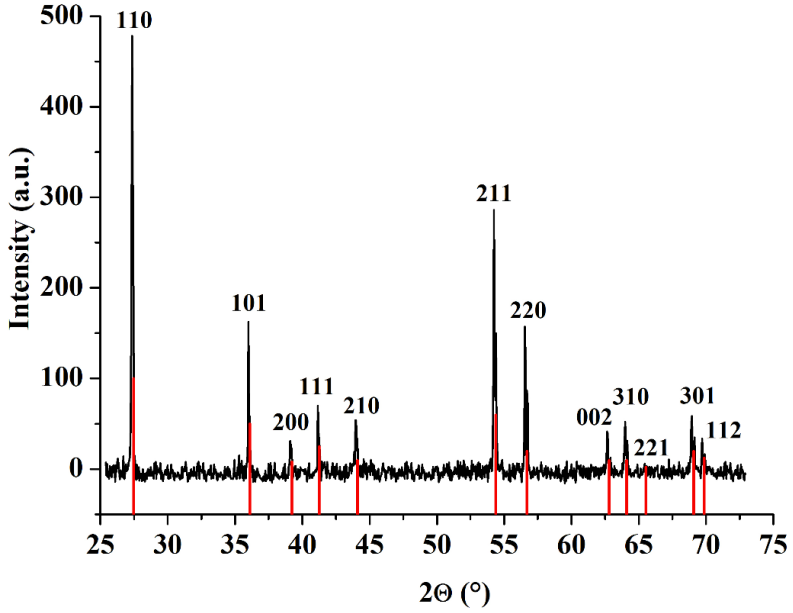

Figure 9.3: XRD profile. All the peaks can be indexed according to the TiO_2 rutile structure.

To better observe at nanoscale level a single nanowire, TEM technique was employed, in particular, a High Angle Annular Dark Field (STEM-HAADF) image of a nanowire segment is shown in Figure 9.4 a and the corresponding elemental maps of titanium and oxygen was obtained through X-Ray Spectroscopy (STEM-EDX). The contrast variation observed in both STEM-HAADF imaging and STEM-EDX mapping is due to the 3D faceted structure of the nanostructure. A detail of a single nanowire acquired by TEM is shown in Figure 9.4 b; NW appears as a stacking of interlocked nanocrystals. The higher magnification of High Resolution TEM imaging (HRTEM, Figure 9.4 c), shows that nanowire crystalline structure corresponds to perfect tetragonal rutile TiO_2 and no extended defects are observed. {010} and {110}-type facets are observed, as expected consistently with the Wulff construction and the calculated surface energies.

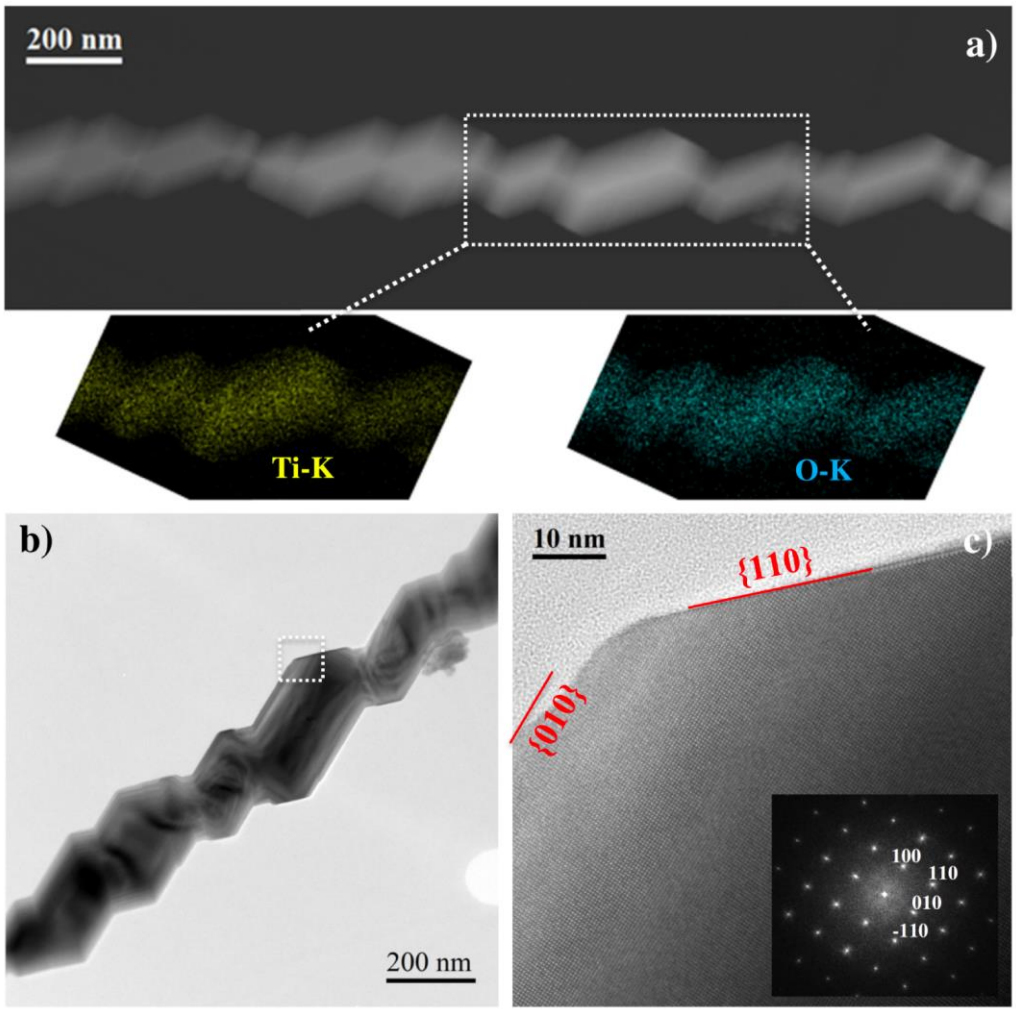

Figure 9.4: TEM characterization of the TiO_2 NWs. a) STEM-HAADF image of a single nanostructure, with corresponding elemental maps of titanium and oxygen acquired by STEM-EDX. b) TEM image showing an overview of a single nanostructure. c) HRTEM image of the region in the white box in b), with the corresponding Fast Fourier Transform in the inset. The crystalline structure corresponds to tetragonal rutile in zone-axis [001].

To evaluate the presence of radiative intra-gap centers and the light emission profile of rutile TiO_2 a cathodoluminescence spectroscopy analysis was performed and obtained CL spectrum are shown in Figure 9.5. The presence of three main light emissions set at 1.55 eV, 2.35 eV and 2.77 eV was extrapolated after a Gaussian deconvolution process and it is worth noting the presence of a high energy tail at 3.2 eV (Figure 9.5, black arrow). Since it is known the radiative centers of rutile TiO_2, this light emission can be attributed to particular point-defects; in particular, the infra-red emission at 1.55 eV can be related to the presence of titanium interstitials, while the two emissions in the visible range are attributed to different charge states of oxygen vacancies[15]. Moreover, it is known by literature that the (110) surfaces are more affected by the formation of titanium interstitials, giving rise to an intense infra-red emission, probably due to the excitonic recombination of rutile TiO_2[16, 17]. The presence of this excitonic emission is a benchmark for high quality material in terms of stoichiometry and crystalline structure.

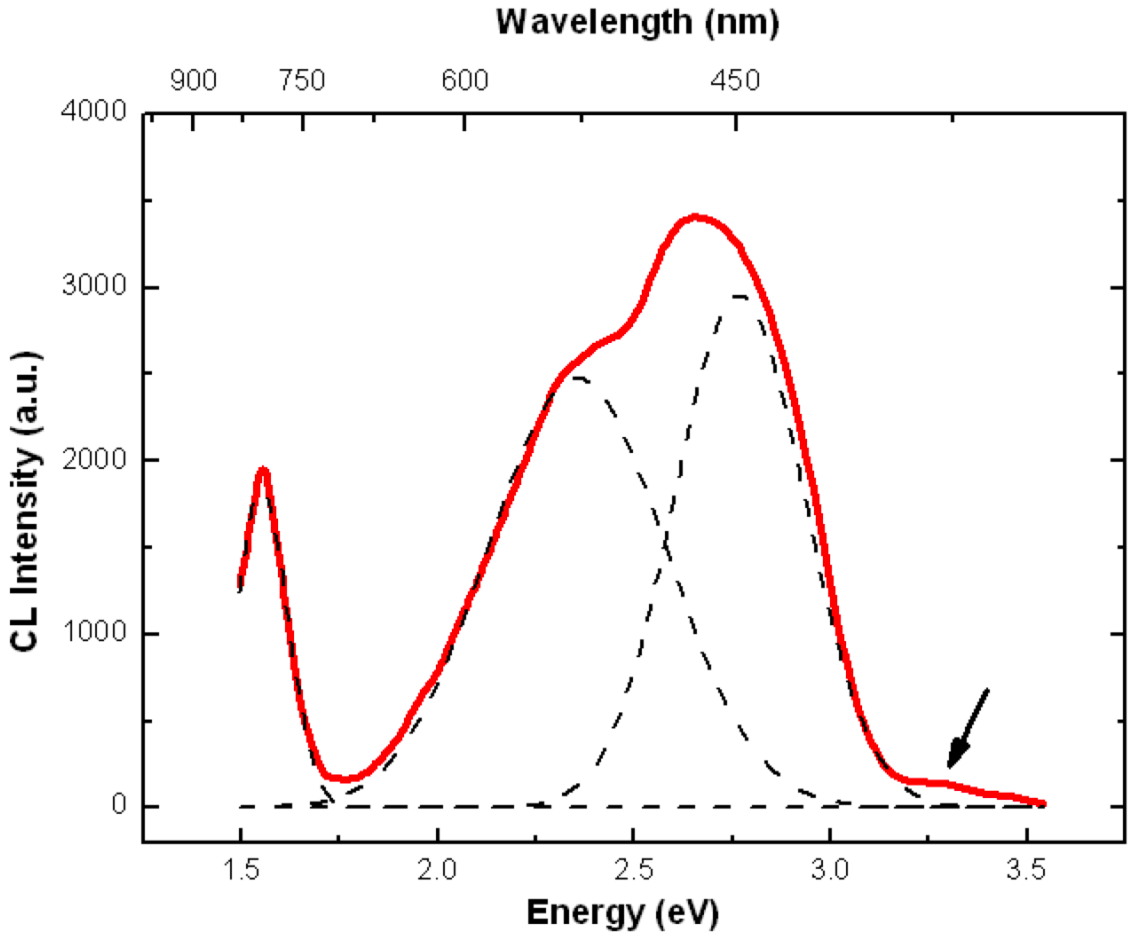

Figure 9.5: Typical room-temperature CL spectrum of the rutile TiO_2 nanostructures

Cellular assays

Murine osteoblasts (MC3T3-E1) behavior has been tested on nanowires sample and on control polycrystalline titanium disks, in view of potential medical applications. Firstly, cell shape and adhesion on the substrates were evaluated by SEM-FIB analysis. In Figure 9.6microphotographs of osteoblasts after 72h of culture on Ti cp or nanowires are reported.

All the cells show their typical healthy morphology, with intact cytoplasm, and polygonal shape with numerous small cellular extroflections. Cells seem strongly anchored on the NWs substrate as it occurs also on control titanium surface, where osteoblasts appear healthy and with rounded shape. In Figure 9.6 (a-b) MC3T3-E1 cells grown on flat titanium surface are shown in their typical well adherent shape; Figure 9.6 (d-e) shows the osteoblasts adherent to NWs, with healthy cells that often bridge on the wires. FIB cut allows to evaluate the interaction between cell and substrate; after the cut it appears evident that the osteoblasts follow the flat titanium topography (Figure 9.6c), while on nanowires (Figure 9.6 f-g) it seems trying to adapt the cytoskeleton to NWs morphology.

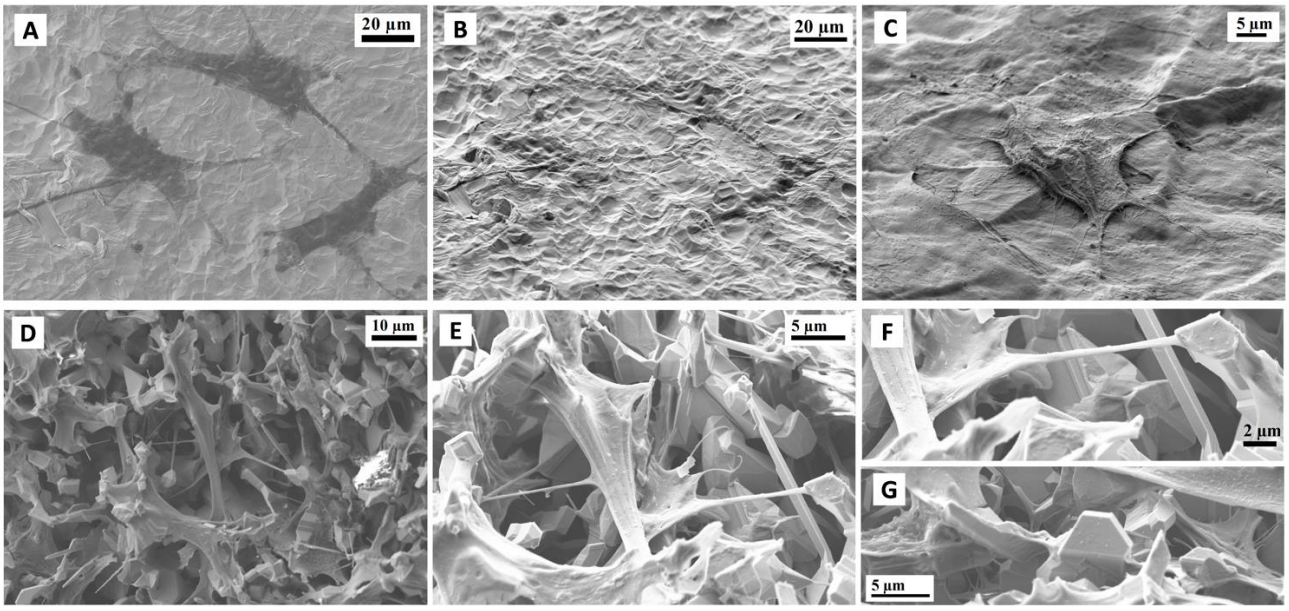

Figure 9.6: SEM images of osteoblastic MC3T3-E1 cells on control titanium (A-B) and on TiO_2 NWs (D-E). Images C and F represent osteoblasts after FIB cut, it is possible to observe the cell-material interaction.

The study of cell morphology was followed by an analysis of mRNA transcript related to osteoblastic lineage performed through qRT-PCR. The expression of one of the main components of extracellular matrix, Collagen type I (Col1A1) was studied together with two genes related to osteoblasts differentiation (Runx2 and OCN).

Interestingly, osteoblastic cells growing on TiO_2 NWs expressed higher levels of Collagen I if compared to control titanium disks (Figure 9.7 a), which suggests that these NWs may provide a favorable environment for cells to create an abundant extracellular matrix and act as a proper scaffold for tissue healing. Moreover, MC3T3-E1 cells on TiO_2 NWs expressed significantly higher levels of Runx2 (Figure 9.7 b), a transcription factor fundamental for osteoblastic differentiation; no statistically significant differences were observed in osteocalcin expression (Figure 9.7 c), although it must be considered that osteocalcin is a tardive gene related to MC3T3-E1 differentiation into mature osteoblasts and may occur in almost 21 days.

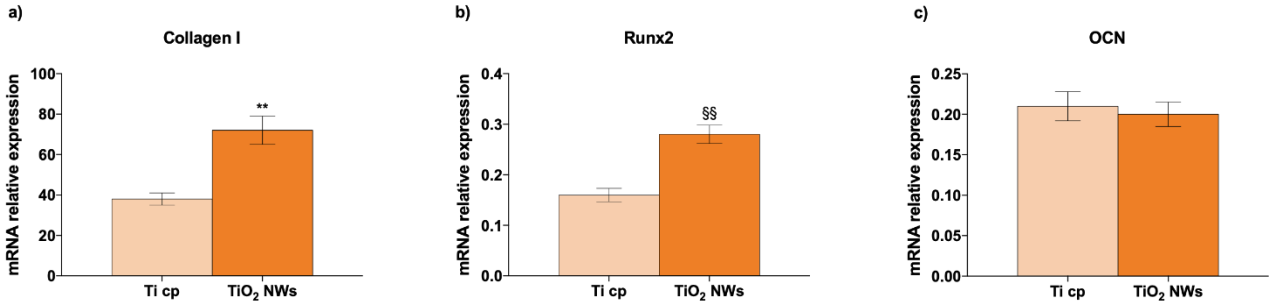

*Figure 9.7: mRNA relative expression of Col1A1 (a), Runx2 (b) and OCN (c) cultured for 72h on TiO_2 NWs or control titanium surface. **p=0,0015; §§p=0,0012.*

9.4 Discussion

The titanium implants, commonly used in orthopedic and dental surgery, risk failing due to the inappropriate integration at the bone-implant interface, leading to major clinical complications. In the last few years, the goal is to develop innovative biomaterials in order to improve the regeneration of tissues. The fundamental role of ECM in the stimulation and interaction with cells is a matter of fact and it occurs physiologically on a nanoscale level; bone is known for the presence of a hierarchical structure of matrix components which starts from the nanometer range (collagen, fibrin, laminin, etc.). Recent *in vivo* studies also revealed that nanofeatures on artificial surfaces can impact cell physiology in the same way as the natural ECM[18, 19]. In the general framework of nanomedicine, materials at the nanoscale have already been studied for many biomedical applications, such as cardiac, neural or dental applications[20-24]. An approach to realize such a nanotopography can be the growth of nanowire structures on conventional substrates.

Here we reported the synthesis and the characterization of TiO_2 crystalline rutile NWs on commercially pure titanium disks through a CVD established process. It is known from literature that for a successful osseointegration of an implant *in vivo*, cell adhesion to the material plays a critical role and that osteoblast activity can be significantly enhanced through the use of controlled nanotopographies[10]. Webster et al. provided a first reference of the better adhesion of bone forming cells to nanophase materials than to conventional ones, probably due to the increased nano-surface roughness and the higher surface area of nanostructures that provided many more sites for cell adhesion and protein deposition[8, 25]. Moreover, MC3T3-E1 osteoblasts have been seen to better adhere on vertical titanium nanotubes if compared to flat titanium surfaces, and it has been seen that incorporation of nanoarchitecture on implant surfaces will further facilitate long-term osseointegration[4, 10-12, 26-28]. In our study we demonstrate that TiO_2 NWs can support the *in vitro* culture of murine osteoblasts up to 72h; cells seemed strongly anchored on the NWs substrate, probably because a nanostructured material with high surface area provides available sites for protein adsorption and consequently enhances cell-biomaterial interaction. Gene expression analysis performed on osteoblasts growth on nanowires and on control titanium surfaces showed an increase in the transcription of genes related to the early osteoblastic differentiation (Col1A1 and Runx2) if compared to the control. This result indicates an earlier onset of cell differentiation due to the dimensions of the nanostructures. In fact, as shown by Brammer et al., titanium nanotubes with a diameter about 100nm induced cells to assume a very elongated morphology and to produce high levels of alkaline phosphatase, indicator of early osteoblastic differentiation[11].

Taken together, these data indicate that the deposition of a more abundant ECM on these NWs is coupled with a higher degree of osteoblastic maturation, a condition that is fundamental for the regeneration of bone and generally, for the use of implantable materials in regenerative medicine.

References

1. Lagonegro, P.; Ghezzi, B.; Fabbri, F.; Trevisi, G.; Nasi, L.; Galli, C.; Macaluso, G. M.; Rossi, F., Titanium Dioxide Nanowires Grown on Titanium Disks Create a Nanostructured Surface with Improved In Vitro Osteogenic Potential. J Nanosci Nanotechnol 2019, 19 (8), 4665-4670. DOI: 10.1166/jnn.2019.16350.

2. Yim, E. K.; Darling, E. M.; Kulangara, K.; Guilak, F.; Leong, K. W., Nanotopography-induced changes in focal adhesions, cytoskeletal organization, and mechanical properties of human mesenchymal stem cells. Biomaterials 2010, 31 (6), 1299-306. DOI: 10.1016/j.biomaterials.2009.10.037.

3. Anselme, K.; Davidson, P.; Popa, A. M.; Giazzon, M.; Liley, M.; Ploux, L., The interaction of cells and bacteria with surfaces structured at the nanometre scale. Acta Biomater 2010, 6 (10), 3824-46. DOI: 10.1016/j.actbio.2010.04.001.

4. Yu, W. Q.; Jiang, X. Q.; Zhang, F. Q.; Xu, L., The effect of anatase TiO2 nanotube layers on MC3T3-E1 preosteoblast adhesion, proliferation, and differentiation. J Biomed Mater Res A 2010, 94 (4), 1012-22. DOI: 10.1002/jbm.a.32687.

5. Wang, C. Y.; Zhao, B. H.; Ai, H. J.; Wang, Y. W., Comparison of biological characteristics of mesenchymal stem cells grown on two different titanium implant surfaces. Biomed Mater 2008, 3 (1), 015004. DOI: 10.1088/1748-6041/3/1/015004.

6. Zhang, E. W.; Wang, Y. B.; Shuai, K. G.; Gao, F.; Bai, Y. J.; Cheng, Y.; Xiong, X. L.; Zheng, Y. F.; Wei, S. C., In vitro and in vivo evaluation of SLA titanium surfaces with further alkali or hydrogen peroxide and heat treatment. Biomed Mater 2011, 6 (2), 025001. DOI: 10.1088/1748-6041/6/2/025001.

7. Webster, T. J.; Ergun, C.; Doremus, R. H.; Siegel, R. W.; Bizios, R., Enhanced functions of osteoblasts on nanophase ceramics. Biomaterials 2000, 21 (17), 1803-10.

8. Webster, T. J.; Ejiofor, J. U., Increased osteoblast adhesion on nanophase metals: Ti, Ti6Al4V, and CoCrMo. Biomaterials 2004, 25 (19), 4731-9. DOI: 10.1016/j.biomaterials.2003.12.002.

9. Zhang, L.; Hemraz, U. D.; Fenniri, H.; Webster, T. J., Tuning cell adhesion on titanium with osteogenic rosette nanotubes. J Biomed Mater Res A 2010, 95 (2), 550-63. DOI: 10.1002/jbm.a.32832.

10. Popat, K. C.; Leoni, L.; Grimes, C. A.; Desai, T. A., Influence of engineered titania nanotubular surfaces on bone cells. Biomaterials 2007, 28 (21), 3188-97. DOI: 10.1016/j.biomaterials.2007.03.020.

11. Brammer, K. S.; Oh, S.; Cobb, C. J.; Bjursten, L. M.; van der Heyde, H.; Jin, S., Improved bone-forming functionality on diameter-controlled TiO(2) nanotube surface. Acta Biomater 2009, 5 (8), 3215-23. DOI: 10.1016/j.actbio.2009.05.008.

12. Brammer, K. S.; Choi, C.; Frandsen, C. J.; Oh, S.; Johnston, G.; Jin, S., Comparative cell behavior on carbon-coated TiO2 nanotube surfaces for osteoblasts vs. osteo-progenitor cells. Acta Biomater 2011, 7 (6), 2697-703. DOI: 10.1016/j.actbio.2011.02.039.

13. Anselme, K.; Linez, P.; Bigerelle, M.; Le Maguer, D.; Le Maguer, A.; Hardouin, P.; Hildebrand, H. F.; Iost, A.; Leroy, J. M., The relative influence of the topography and chemistry of TiAl6V4 surfaces on osteoblastic cell behaviour. Biomaterials 2000, 21 (15), 1567-77. DOI: 10.1016/s0142-9612(00)00042-9.

14. Das, K.; Bose, S.; Bandyopadhyay, A., TiO2 nanotubes on Ti: Influence of nanoscale morphology on bone cell-materials interaction. J Biomed Mater Res A 2009, 90 (1), 225-37. DOI: 10.1002/jbm.a.32088.

15. Niculescu, M.; Budrugeac, P., Structural characterization of nickel oxide obtained by thermal decomposition of polynuclear coordination compound [Ni 2 (OH) 2 (H 3 CCH (OH) COO−) 2 (H 2 O) 2· 0.5 H 2 O] n. Revue Romaine de Chimie, 2013; Vol. 58 p381

16. Fernandez, I.; Cremades, A.; Piqueras, J., Cathodoluminescence study of defects in deformed (110) and (100) surfaces of TiO2single crystals. Semiconductor science and technology, 2005

Vol. 20, pp 239 -243.

17. Detto, F.; Armani, N.; Lazzarini, L.; Toccoli, T.; Verucchi, R.; Aversa, L.; Nardi, M. V.; Rossi, B.; Salviati, G.; Iannotta, S., Excitonic recombination in superstoichiometric nanocrystalline TiO2 grown by cluster precursors at room temperature. Phys Chem Chem Phys 2012, 14 (16), 5705-10. DOI: 10.1039/c2cp40120g.

18. Brammer, K. S.; Oh, S.; Gallagher, J. O.; Jin, S., Enhanced cellular mobility guided by TiO2 nanotube surfaces. Nano Lett 2008, 8 (3), 786-93. DOI: 10.1021/nl072572o.

19. McNamara, L. E.; McMurray, R. J.; Biggs, M. J.; Kantawong, F.; Oreffo, R. O.; Dalby, M. J., Nanotopographical control of stem cell differentiation. J Tissue Eng 2010, 2010, 120623. DOI: 10.4061/2010/120623.

20. Cohen-Karni, T.; Qing, Q.; Li, Q.; Fang, Y.; Lieber, C. M., Graphene and nanowire transistors for cellular interfaces and electrical recording. Nano Lett 2010, 10 (3), 1098-102. DOI: 10.1021/nl1002608.

21. Qing, Q.; Pal, S. K.; Tian, B.; Duan, X.; Timko, B. P.; Cohen-Karni, T.; Murthy, V. N.; Lieber, C. M., Nanowire transistor arrays for mapping neural circuits in acute brain slices. Proc Natl Acad Sci U S A 2010, 107 (5), 1882-7. DOI: 10.1073/pnas.0914737107.

22. Patolsky, F. a. T. B. a. Y. G. a. F. Y. a. G. A. a. Z. G. a. L. C., Patolsky, F., Timko, B. P., Yu, G. H., Fang, Y., Greytak, A. B., Zhang, G. F. & Lieber, C. M. Detection, stimulation, and inhibition of neuronal signals with high-density nanowire transistor arrays. Science 313, 1100-1104. Science (New York, N.Y.) 2006, 313, 1100-4. DOI: 10.1126/science.1128640.

23. Espinosa, H. D.; Soler-Crespo, R., Materials science: Lessons from tooth enamel. In Nature, England, 2017; Vol. 543, pp 42-43. DOI: 10.1038/543042a.

24. Ramos-Tonello, C. M.; Lisboa-Filho, P. N.; Arruda, L. B.; Tokuhara, C. K.; Oliveira, R. C.; Furuse, A. Y.; Rubo, J. H.; Borges, A. F. S., Titanium dioxide nanotubes addition to self-adhesive resin cement: Effect on physical and biological properties. Dent Mater 2017, 33 (7), 866-875. DOI: 10.1016/j.dental.2017.04.022.

25. Webster, T. J.; Siegel, R. W.; Bizios, R., Osteoblast adhesion on nanophase ceramics. Biomaterials 1999, 20 (13), 1221-7.

26. Oh, S.; Daraio, C.; Chen, L. H.; Pisanic, T. R.; Finones, R. R.; Jin, S., Significantly accelerated osteoblast cell growth on aligned TiO2 nanotubes. J Biomed Mater Res A 2006, 78 (1), 97-103. DOI: 10.1002/jbm.a.30722.

27. Yu, W. Q.; Zhang, Y. L.; Jiang, X. Q.; Zhang, F. Q., In vitro behavior of MC3T3-E1 preosteoblast with different annealing temperature titania nanotubes. Oral Dis 2010, 16 (7), 624-30. DOI: 10.1111/j.1601-0825.2009.01643.x.

28. Park, J.; Bauer, S.; Schlegel, K. A.; Neukam, F. W.; von der Mark, K.; Schmuki, P., TiO2 nanotube surfaces: 15 nm--an optimal length scale of surface topography for cell adhesion and differentiation. Small 2009, 5 (6), 666-71. DOI: 10.1002/smll.200801476.

Chapter 10 – Conclusions

Nanomedicine is a new branch of medicine, that offers new opportunities in fields as diagnostic imaging, drug delivery, therapy techniques and tissue engineering; moreover, nanotechnologies reached the dentistry world in multiple manner, from the preventive to the therapeutic dentistry. The aim of the design of biomimetic material is to develop a three-dimensional scaffold that is able to support cell functions and the regeneration of the targeted tissue, avoiding toxic reaction and host immune response.

In the view of the average size of cells, it has been recognized the importance of the cell/material contact and of the nano-topographical organization of extracellular signals; in fact, cells firstly attach, adhere and finally spread. It is known that osteoblastic response, and the consequent quality of the adhesion, is different according to surface roughness (in terms of micro- and nano-topography), suggesting some type of topography-dependent transduction of the signal. Thereafter the quality of adhesion will influence cellular morphology and capacity of proliferation and differentiation. In this regard, the goal of biomedical engineering nowadays is to find the perfect micro- and nano-pattern to favor cell attachment, proliferation and differentiation, in order to obtain a good quality *ex novo* ECM.

In this thesis we examined the concept of nanomedicine, starting from the definition up to applications with the main aim to develop a suitable nanomaterial for bone tissue regeneration, opening the way to new promising application in biomedical field.

We focused on 1D nanostructures and we showed the CVD technique improved to allow the growth of silicon oxycarbide and titanium dioxide nanowires, then we evaluated their biological potentiality. As we showed, silicon oxycarbide nanowires are biocompatible and suitable for nano-tailoring with biological devices; the possibility to combine silicon with oxygen and carbon permitted to obtain different characteristics and properties, which make the material suitable for applications in bone tissue regeneration. Furthermore, the dimensions of NWs, comparable with extracellular matrix features as receptors or molecules, can morphologically resemble the extracellular environment of the biological systems promoting the direct interaction of nanowires with cells and the faster integration of the scaffold whit the tissue.

All the cytocompatibility study of silicon oxycarbide nanowires were performed following the ISO 10993-5 guidelines, while the blood-materials interaction study was performed following the ISO 10993-4.

The experiments demonstrated that the SiO_xC_y NWs were not cytotoxic and the kinetics of adhesion and proliferation were slow in the first 48h, but increased after 96 h. After this time, the SEM observation showed that

cells can colonize the platform and reorganize the substrate to create a better environment to grow, promoting the formation of stable focal adhesions. The blood compounds interactions were evaluated by platelets activation which was triggered by SiO_xC_y NWs. These characteristics are very interesting because demonstrate that SiO_xC_y NWs are suitable nanomaterials to develop scaffold for bone tissue engineering and regenerative medicine, since they provide direct stimuli to cell differentiation and platelet activation.

Then, in chapter 8 we experimented if it could be possible to ameliorate the initial scarce adhesion of cells on the surface with a 3-mercaptopropyltrimethoxysilane functionalization. The silanization is a process that allows to have free thiol groups on the surface of the material, leading to an easier reaction and binding of other molecules (e.g. lateral chain of plasma proteins) and an encouraged protein adsorption, which plays a pivotal role in the subsequent host reactions, implant integration and consequent tissue regeneration. After the testing for the occurred functionalization, we observed the response of osteoblastic cells and we showed that 3-mercaptopropyltrimethoxysilane consented an increase in proliferation at 48h, a better cellular adhesion at 24h, a greater formation of focal adhesions and the transcription of genes related to the early differentiation stage of osteoblasts (ALP, COL1A1). In this optic, 3-mercaptopropyltrimethoxysilane functionalization may appear as a promising solution to allow a rapid scaffold colonization and to overcome the problems of slow osteoblast proliferation encountered on SiO_xC_y NWs.

In the last part of this thesis we analyzed *in vitro* the osteoblastic response to titanium dioxide nanowires. Titanium is one of the most common implantable materials, both in orthopedic and dental fields, it is accepted for its high biocompatibility and resistance during the time, but its implant risk the failure due to the inappropriate integration at the bone-implant interface. The idea to develop titanium-based nanowires is linked to the possibility to ameliorate implants nano- and micro-topography to favor the initial osseointegration of dental implants. Our data showed a good degree of osteoblasts proliferation up to 72h; osteoblastic genes transcription was higher, and cells appeared to have a better anchorage to the material on nanowires substrates compared to the flat material. Thus, to confirm the idea that on nanostructured surfaces the ECM deposition and the osteoblastic maturation, fundamental condition for the regeneration of bone, are strongly enhanced.

In conclusion, we can assert that both, silicon oxycarbide and titanium dioxide nanowires may be promising tools for ameliorating the surface features of implantable materials and for a viable approach to nanodentistry advancement.